Electrospraying of Polymers with Therapeutic Molecules: State of the Art

N. Bock[1,2,3,], T. R. Dargaville[2], M. A. Woodruff[1]*

Institute of Health and Biomedical Innovation, Queensland University of Technology
60 Musk Avenue
Kelvin Grove, QLD 4059, Australia

[1]Biomaterials and Tissue Morphology group, [2]Tissue Regeneration and Repair group
[3]Regenerative Medicine group

*Corresponding author.
E-mail address: n.bock@qut.edu.au (N. Bock).

Abstract

The encapsulation and release of bioactive molecules from polymeric vehicles represents the holy grail of drug and growth factor delivery therapies, whereby sustained and controlled release is crucial in eliciting a positive therapeutic effect. To this end, electrospraying is rapidly emerging as a popular technology for the production of polymeric particles containing bioactive molecules. Compared with traditional emulsion fabrication techniques, electrospraying has the potential to reduce denaturation of protein drugs and affords tighter regulation over particle size distribution and morphology. In this article, we review the importance of the electrospraying parameters that enable reproducible tailoring of the particles' physical and *in vitro* drug release characteristics, along with discussion of existing *in vivo* data. Controlled morphology and monodispersity of particles can be achieved with electrospraying, with high encapsulation efficiencies and without unfavorable denaturation of bioactive molecules throughout the process. Finally, the combination of electrospraying with electrospun scaffolds, with an emphasis on tissue regeneration is reviewed, depicting a technique in its relative infancy but holding great promise for the future of regenerative medicine.

Keywords

Electrospraying
Microparticles
Encapsulation
Drug delivery
Controlled release
Electrospinning

Table of Contents

1. Introduction
2. The technique of electrospraying
    2.1. Electrospraying principles
    2.2. Fabrication techniques
        2.2.1. Electrospraying apparatus
        2.2.2. Encapsulation of biomolecules
3. Control of particle characteristics with electrospraying parameters
    3.1. Importance of electrospraying parameters
        3.1.1. Polymers
            3.1.1.1. Polymer types
            3.1.1.2. Solvents
            3.1.1.3. Polymer solutions
        3.1.2. Processing parameters
            3.1.2.1. Spraying modes
            3.1.2.2. Electrical conductivity
            3.1.2.3. Flow rate
            3.1.2.4. Other parameters
    3.2. Tailoring of electrosprayed particle characteristics
        3.2.1. Morphology
        3.2.2. Size
4. Electrospraying and drug release characteristics
    4.1. Choice of molecules
    4.2. Loading and encapsulation
        4.2.1. Definitions and methods
        4.2.2. Influence of parameters on loading and encapsulation
            4.2.2.1. Loading capacities
            4.2.2.2. Encapsulation efficiencies
    4.3. Molecule dispersion
    4.4. Release kinetics
    4.5. Denaturation
    4.6. Bioactivity
    4.7. *In vivo* performance
5. The use of electrosprayed particles in electrospun scaffolds
    5.1. Electrospun nanofibers and drug delivery
    5.2. Electrospun nanofibers and particles for drug delivery
        5.2.1. Loaded particles in electrospun nanofibers
        5.2.2. Multiple electrospraying/electrospinning
            5.2.2.1. Concept
            5.2.2.2. Multiple electrospinning
            5.2.2.3. Applications of multiple electrospraying/electrospinning
                5.2.2.3.1. Drug delivery
                5.2.2.3.2. Other applications
6. Conclusions

Abbreviations

ALP, alkaline phosphatase;
API, active pharmaceutical ingredient;
AV, applied voltage;
BDNF, brain-derived neurotrophic factor;
BDP, beclomethasone dipropionate;
BSA, bovine serum albumin;
C6, coumarin-6;
CD, circular dichroism;
C_{ent}, critical entanglement concentration;
Chi, chitosan;
CLSM, confocal laser scanning microscopy;
C_{ov}, critical chain overlap concentration;
CS, chondroitin sulphate;
DCM, dichloromethane;
DDPS, drug delivery particulate systems;
DMF, N,N-dimethylformamide;
DMSO, dimethyl sulfoxide;
DOX, doxorubicin;
DSC, differential scanning calorimetry;
DTAB, didodecyltrimethylammonium bromide;
EBM-20, endothelial media;
EE, encapsulation efficiency;
EGF, epidermal growth factor;
ELP, elastin-like polypeptides;
FBS, fetal bovine serum;
FDA, food and drug administration;
FITC, fluorescein isothiocyanate;
FR, flow rate;
FTIR, Fourier transform infrared;
GF, growth factor;
H&E, hematoxylin and eosin;
HA, hydroxyapatite;
HUVEC, human umbilical vein endothelial;
HyA, hyaluronic acid;
ID, internal diameter;
IGF-1, insulin-like growth factor-1;
K_{OW}, octanol/water partition coefficient;
LC, loading capacity;
LF, lung fibroblasts;
M_e, average entanglement molecular weight;
$MgCO_3$, magnesium carbonate;
$Mg(OH)_2$, magnesium hydroxide;
MPHB, methylparahydroxybenzoate;
MSC, mesenchymal stem cell;
MW, molecular weight;
MWD, molecular weight distribution;
NGF, nerve growth factor;
NHEF, human epidermal fibroblasts;
NHEK, human epidermal keratinocytes;

o/o/w, oil-in-oil-in-water;
PAAC, poly(amidoamines)-cholesterol;
PCL, polycaprolactone;
PDGF, platelet-derived growth factor;
PEG, polyethylene glycol;
PEO, polyethylene oxide;
PEUU, poly(ester urethane) urea;
PLA, polylactide;
PLACL, poly(L-lactic acid)-co-polycaprolactone;
PLGA, poly(lactic-co-glycolic acid);
PLL, poly(ε-carbobenzoxy-L-lysine);
PLLA, poly-L-lactide;
PMMA, poly(methyl methacrylate);
PPE-EA, polyamino ethyl ethylene phosphate;
PSU, polysulfone;
PU, polyurethane;
PUU, polyurethaneurea;
PVA, poly(vinyl alcohol);
PVC, poly(vinyl chloride);
R_g, radius of gyration;
RHO_B, rhodamine B;
RHO_{BOEP}, rhodamine B octadecyl ester perchlorate;
SD, standard deviation;
SDS-PAGE, dodecyl sulphate-polyacrylamide gel electrophoresis;
SEM, scanning electron microscopy;
SMC, smooth muscle cell;
SS, salbutamol-sulfate;
TE, tissue engineering;
TEC, tissue-engineered construct;
TET, tetracycline hydrochloride;
TFE, 2,2,2-trifluoroethanol;
TGF- β1, transforming growth factor beta-1;
TPP, tripolyphosphate;
TTC, tip-to-collector;
UV, ultraviolet;
VEGF, vascular endothelial growth factor;
vWF, von Willebrand factor;
w/o, water-in-oil;
w/o/w, water-in-oil-in-water;
XPS, X-ray photoelectron spectroscopy;
XRD, X-ray diffractometry.

1. Introduction

The need for controlled delivery of therapeutic molecules has prompted the investigation of polymeric particles as biodegradable reservoirs which are designed to degrade at a determined rate, thereby releasing their encapsulated molecules for sustained and site-specific delivery [1-2]. This approach could potentially overcome the limitations of bolus delivery and has drawn much research attention in the last decades, particularly in the fields of cancer therapies, hormonal treatments, asthma delivery, and tissue engineering, for which tailored and multiple-molecule delivery is necessary for therapeutic effect [3]. Many techniques exist for producing these drug delivery particulate systems (DDPS) with emulsion/evaporation-based methods being the most extensively used [4]. In this context, the term "drug" refers to any type of molecule that has a therapeutic effect. Coacervation, spray-drying, nanoprecipitation and microfluidics are additional techniques each presenting their own specific advantages and they are broadly described in the literature [5-8]. However, to date, very few of the DDPS generated using these techniques have been effectively translated to the clinic, with few devices being commercialized each year. This lack of translational research is mainly attributed to several shortfalls associated with these production methods [9]. For instance, there are issues surrounding molecule degradation (such as denaturation of proteins) and instability during the processes. In emulsion techniques, the aqueous/organic interface and shear stresses are the first source of limitation [10]. Moreover, entrapped molecules differ in terms of therapeutic function and physicochemical properties, demonstrating a different degree of stability and sensitivity to stress. In other techniques, prolonged exposure to organic solvents and residual traces of solvents or other processing agents in the final DDPS are of concern. Such factors can affect the nature and stability of the encapsulated therapeutic molecules, limiting their performance both *in vitro* and *in vivo,* and thus limiting their clinical use. Furthermore, different applications require different therapeutic molecule release profiles matching the need of a specific treated tissue, and ideally mimicking the *in vivo* release profiles generated by the cells from such tissues. For this to happen, it is critical to have a thorough grasp of the complex interplay of fabrication parameters which govern the resultant particle characteristics. Particle size and morphology for example ultimately dictate the degradation, and hence release profiles from DDPS, although it should be noted that tight control is currently limited in the traditional fabrication techniques.

One approach to overcome these drawbacks is the technique of electrospraying. Although electrospraying is a well-established technique in the field of mass spectrometry and ink-jet printing, it has only been applied to the loading of therapeutic molecules in the last 20 years and its understanding and optimization are still in their relative infancy with respect to biological loading [11-13]. Briefly, in electrospraying, a high voltage is applied to a liquid infused through a capillary nozzle. The electric charge generated on the droplet competes with the surface tension of the droplet, causing the droplet to break up in nano- to micro-droplets, which undergo solvent evaporation. The resulting dried particles can then be collected [14]. Therapeutic molecules can be incorporated into the polymer solution prior to electrospraying resulting in loaded particles. There are numerous advantages to electrospraying including the following: the use of an emulsion is optional but not required; there is no use of high temperature such as in spray-drying; there is no further drying step required since particles are instantaneously dried during the process; and there is an enhanced control over the size distribution of particles with the possibility of producing quasi-monodisperse particles [15]. The latter is particularly desirable in drug delivery since monodispersity provides more controlled, and hence reproducible release profiles, which may in turn be more easily customized for a desired application [16]. Furthermore, in the specific case of nanoparticles, size affects cellular uptake and thus uncontrolled size distribution may

lead to different biological responses [17-18]. Control of size is thus of paramount importance when producing loaded polymeric particles and electrospraying is a technique which can provide such control over and above that achieved with traditional techniques, when appropriate parameters are used [19].

Electrospraying also holds potential to reduce denaturation by limiting exposure to organic solvents and is highly versatile in terms of the choice of polymers, apparatus, and therapeutic molecules. For instance, if the therapeutic molecule is highly sensitive to solvents, such as enzymes and DNA molecules, coaxial electrospraying may be employed. In this way, core-shell capsules are formed and the protein resides in the core of the capsule in an aqueous solution while the polymer matrix composes the shell of the capsule [20]. Finally, although electrospraying through one nozzle has a low throughput, the flexibility of the technique would enable the use of several nozzles in parallel for a multiplexed system, ideal for scale-up [21-22]. To date, therapeutic molecules such as antibiotics (ampicillin [23], rifampicin [24]), anti-cancer agents (paclitaxel [25-32], doxorubicin [33], suramin [30], cisplatin [34]), inhalation drugs (beclomethasone dipropionate (BDP) [35], salbutamol-sulfate (SS) [36]), anti-inflammatory drugs (celecoxib [37], budesonide [38], naproxen [39]), drugs for hormonal treatments (β-oestradiol [40], tamoxifen [41-42]), model proteins (bovine serum albumin (BSA) [43-46]) and growth factors (insulin-like growth factor-1 (IGF-1) [47], vascular endothelial growth factor (VEGF) and platelet-derived growth factor (PDGF) [48]) have been loaded in electrosprayed particles and these studies will be discussed hereafter.

Here we present a comprehensive review of the current state of the art in electrospraying technology for the controlled release of therapeutic molecules from polymeric particles. We review the methods used for producing electrosprayed particles and encapsulating therapeutic molecules, including important considerations to enable both the physical properties and *in vitro* drug release profiles of the particles to be tailored and optimized. The focus of the review is on *in vitro* data since very little in vivo data is available yet in the literature, although discussion of existing *in vivo* data is also provided. The various applications of electrospraying with electrospinning technologies, with an emphasis on tissue engineering, are also reviewed, for a portrayal of the latest techniques used to produce scaffolds in the diverse and fascinating field of regenerative medicine.

2. The technique of electrospraying

2.1. Electrospraying principles

Electrospraying is a method of liquid atomization, also known as electrohydrodynamic atomization. The principle of electrospraying is based on the theory of charged droplets; stating that an electric field applied to a liquid droplet exiting a capillary is able to deform the interface of the droplet [12]. The electric charge generates an electrostatic force inside the droplet which competes with the surface tension of the droplet, forming the *Taylor cone*, characteristic of a charged droplet. Eventually, the electrostatic force, generated by the use of high voltage on the capillary, is able to overcome the surface tension of the droplet. The excess charge then needs to be dissipated and smaller charged droplets on the micro to nano-scale are ejected from the primary droplet, thus reducing its charge without significantly reducing its mass. Due to Coulomb repulsion of the charges, the droplets disperse well and do not coalesce during their flight towards the collector [15]. Several spraying modes can occur during electrospraying; the most desired being the single cone-jet mode, due to its stability and reproducibility [14].

The various theories of electrospraying physics have been summarized elsewhere with reviews on the recent advances and applications of the technology [11-12] however limited literature exists pertaining to theoretical and practical inclusion of bioactive molecules in this

process. Briefly, the two major parameters that characterize the electrosprayed aerosol are the size of droplets and electric charge. The latter is difficult to determine, due to parasitic electrical discharge, although the maximum surface charge of a droplet, q, has been identified as a function of the surface tension, γ, and radius of droplet, R, expressed in Equation (1) [49]. From the surface charge, the Rayleigh limit, L_R, can be identified, which determines the charge leading to droplet break-up (fission) and is expressed in Equation (2) where ε is the permittivity of the surrounding medium. Droplets produced by electrospraying are highly charged, usually close to half of the Rayleigh limit [12].

$$q = 8\pi\sqrt{\varepsilon_0 \gamma R^3} \qquad (1)$$

$$L_R = q(64\pi^2 \varepsilon \gamma R^3) \qquad (2)$$

Similarly, the jet break-up mechanism is shown to be dependent on the ratio of the electrical normal stress over the surface tension stress. It is dependent on the viscosity and surface charge as in the Rayleigh limit (Equation (2)), but also on the acceleration of the jet. With increasing flow rate, the current increases and the stress ratio of the jet increases, above a threshold value whereby the jet starts to whip, leading to the production of heterogonous sized droplets. Ideally, a sufficient stress ratio value must be employed to allow for jet break-up, but still a minimal value must be obtained for production of monodisperse and homogeneous particles [14].

2.2. Fabrication techniques

The electrospraying setup can be simple and cheap: a polymer solution is loaded into a syringe fitted with a conductive nozzle, and infused at a desired rate generally implemented by a syringe pump. The nozzle is subjected to high voltage (in the order of kilovolts and mostly positive) and various types of collectors, often grounded or more rarely negatively charged, are placed at a distance ranging from a few centimeters to several tens of centimeters from the nozzle. Once the droplets are ejected from the Taylor cone according to the theory of charged droplets, solvent evaporation leads to the progressive contraction and solidification of droplets resulting in solid polymeric particles impacting onto the collector. While particles are generally assumed to be dry or proven to contain residual solvent falling within the limit of safety standards [50], many studies also use subsequent vacuum treatment to ensure all residual solvent is removed. In the context of loading, the biologically active molecule (biomolecule) is generally mixed into the polymer solution before electrospraying; this approach is covered in section 2.2.2, Encapsulation of biomolecules.

2.2.1. Electrospraying apparatus

Electrospraying and drug loading characteristics can be tailored by changes in the choice and configuration of the equipment. One type of apparatus involves the use of nozzle-ring devices (Fig. 1A) which are placed inside glass chambers and subjected to a stream of air/nitrogen (Fig. 1B). This setup is sometimes referred as the “Delft type” (from the Technical University of Delft, The Netherlands) [32]. A potential difference is generated between the nozzle and a ring placed around the nozzle [27, 31-32, 43]. Usually the high voltage is applied on the nozzle and the lower voltage on the ring, respectively. The use of a ring stabilizes the electrospraying process [32], enabling better control over the desired spraying pattern [31]. For instance, in the single cone-jet mode, more uniform particles are produced [28]. The use of a ring is recommended when using water as the solvent since a

stable cone-jet mode is harder to achieve with water [33]. A corona discharge is generated by a grounded needle placed opposite the charged nozzle in order to discharge the highly charged droplets. Particles can be collected through filters, transported by an air/nitrogen flow applied in the chamber [31], or collected around the grounded needle in a Petri dish [43]. The use of a chamber reduces solvent evaporation rate and smaller particles may be produced [28], however, yield is lowered in this configuration due to deposition of particles in the glass wells of the chamber (where up to 30% can be deposited) before collection in the filter [31, 45]. Consequently, this setup is not recommended for loading of molecules where losses cannot be afforded. However it can be optimized by improving vacuum aspiration and efficient discharging of particles [31] to reach up to 80% yield. Furthermore, the reduction of solvent evaporation rate generated by using an enclosed chamber can lead to smoother microparticle morphologies due to enhanced polymer relaxation and thus better organization of polymer chains within the evaporating droplet [51], which, in turn, allow more homogenous particle degradation and release.

An alternative method for collection involves electrospraying loaded droplets into a liquid, within a beaker containing an immersed grounded collector [44-45, 52] or a wire wrapped around the beaker [36] (Fig. 1C-D). Collection media include distilled water [44-45], ice-water/methanol [53], anhydrous ethanol [30], or 70% ethanol supplemented with surfactants (such as 0.01% to 0.1% (v/v) Polysorbate 80 (Tween 80) [36]), to lower the surface tension of the solution and prevent the aggregation or coalescence of particles [7]. However, it should be noted that high surfactant concentrations (such as >0.1% of Tween 80) have been shown to broaden the size distribution of particles which reduces consistency between batches [36]. Stronger solvents such as acetone may also be used, in order to neutralize residual solvent from the spraying solution [52]. After collection in the liquid, particles can be further filtered and dried. The major disadvantage of this collection technique is the loss of surface-adsorbed drugs which may be desorbed into the media. There is, therefore, no burst release of biomolecules (from the surface of electrosprayed particles) seen with these systems, and a proportional amount of molecules is lost, which again is a concern for loading efficiency and cost. An alternative is to use a collection media in which the particles have poor solubility, as seen for polylactide (PLA) particles electrosprayed into 70% ethanol, preventing the leakage of the drug [36]. The use of additives in the collection media has also been utilized for cross-linking of bovine serum albumin-loaded chitosan capsules electrosprayed into an aqueous tripolyphosphate solution, to improve the mechanical properties of capsules [44]. Agglomeration in solution is a potential issue with hydrophobic polymers when electrospraying in aqueous solutions. Coating is one approach to enable better stabilization of individual particles as seen for poly(lactic-co-glycolic acid) (PLGA) particles electrosprayed into a poly(vinyl alcohol) (PVA) solution [22].

When solid matrices, such as hydrogels, have been used to entrap particles, as seen in cancer treatment where the containment of particles may be necessary, loaded electrosprayed microspheres could be electrosprayed for a second time, from an aqueous solution containing alginate, directly into a calcium chloride, $CaCl_2$, solution. The instantaneous gelation resulted in calcium-cross-linked hydrogel macrobeads that held the microspheres within the matrix. Low voltages were used in this context so that the dripping mode of electrospraying occurred, generating macrobeads with millimeter sizes. This mode is usually unwanted when electrospraying nano/microparticles due to the macro-size outcome, but it does present an interesting alternative for generating larger particles such as hydrogel macrobeads that act as holding matrices. Again, the use of a surfactant such as Tween 80 in the alginate solution is recommended so that the highly hydrophobic microspheres stay uniformly suspended during dripping. According to gelation time, $CaCl_2$ concentration and microsphere loading, different release kinetics may be obtained with this setup [25].

The most common collector for electrospraying polymers solutions containing biomolecules remains a conductive and grounded collector such as an aluminum or copper substrate [23-24, 33, 35, 51] (Fig. 1E). The use of a conductive substrate restricts the deposition of particles to the charged area, limiting losses and does not require any subsequent washing or filtering step.

In practice, despite electrospraying enabling better control over size and morphology of particles compared to the traditional fabrication techniques, it is not without associated drawbacks, including the low-throughput of the technique and yields in the order of milligrams/hour [12]. This can be overcome with multiple electrospray sources as seen in Fig. 1E. An extractor is essential in this type of setup to minimize interference between sources and to localize the electric field. Morphology and size of microparticles were similar to that of the single setup and particle production could be increased from milligrams to grams per hour using 19 parallel nozzles [21].

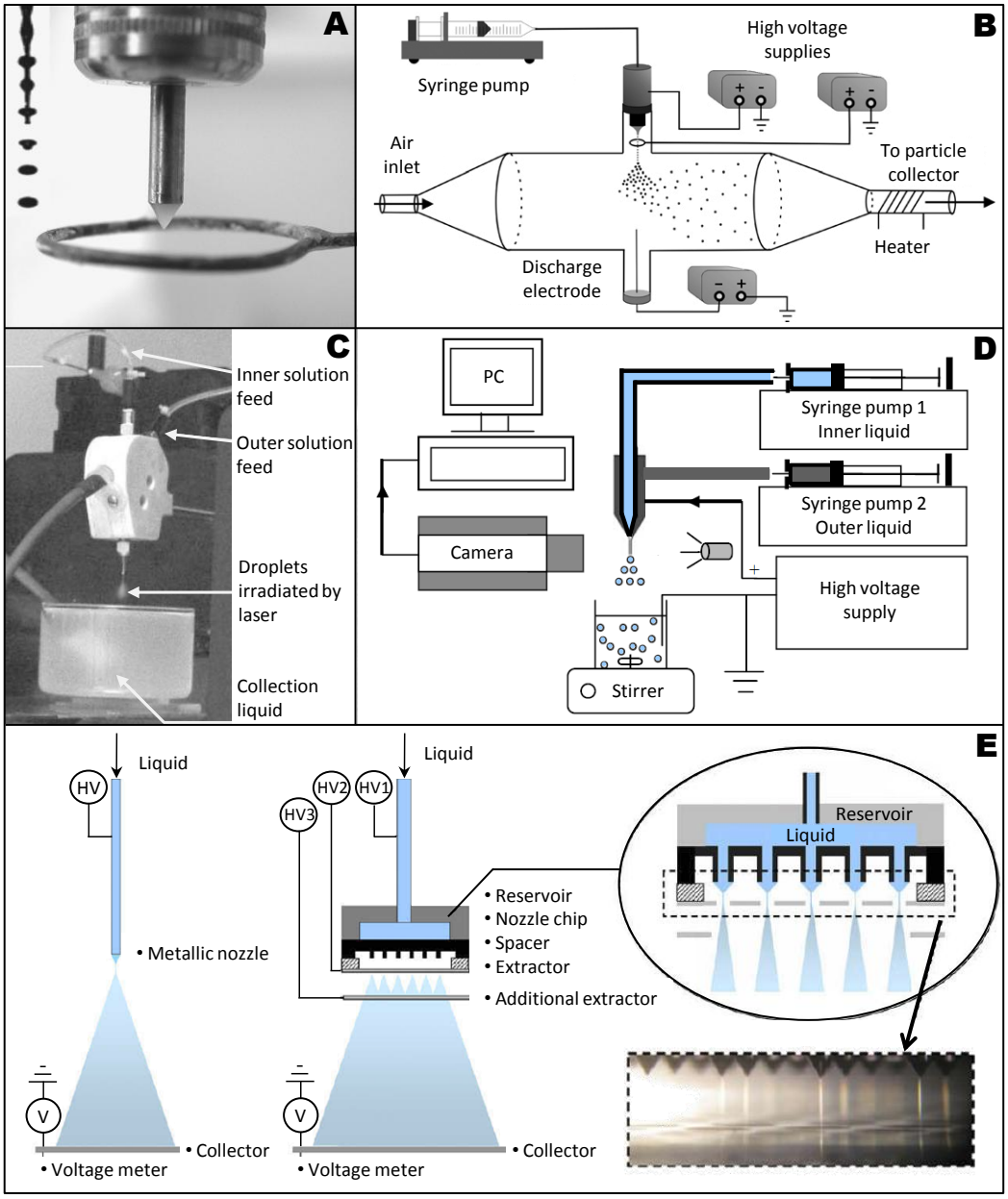

Fig. 1. Electrospraying apparatus. (A) Formation of the Taylor cone in a nozzle-ring setup. (B) Electrospraying via a nozzle-ring setup inside a glass chamber under air flow [32]. (C,D) Coaxial electrospraying in a solution with size measurement by laser optical spectrometer

[52]. (E) Single and multiplexed electrospray setup on grounded collectors [21]. *Adapted from [21, 32, 52] with permission. 2006, 2010 Elsevier Science Ltd. [21, 32]; 2006 Royal Society [52]*.

2.2.2. Encapsulation of biomolecules

Conventional medication via oral or bolus administration typically does not provide spatially or temporally controlled release of therapeutic molecules. The short half-lives in solution of most of these molecules also imply that they lose their bioactivity quickly following implantation, or are rapidly cleared by metabolism in the body [9]. Such shortfalls require high doses of therapeutic molecules to be used, resulting in increased cost and possible complications due to levels potentially toxic for cells and tissues [54].

In recent years, the encapsulation of therapeutic molecules has become a powerful tool for delivering controlled amounts to target cell populations and tissue sites, with minimal signal propagation to non-targeted cells and tissues. Encapsulation can be obtained by the processing of biodegradable polymers which maintain integrity and relative long-term biological activity of therapeutic molecules. Polymeric devices can finally provide an exposure for extended periods ranging from hours to months by gradual polymer degradation allowing a specific release pattern of biomolecules for treatment [55].

Several methods can be employed for the encapsulation of biomolecules (also referred as drugs) into electrosprayed polymeric particles, as shown in Fig. 2. The resultant particles may be categorized into two distinct groups:

- Particulate systems, where the drug is intimately distributed within the polymer structure;
- Capsules, where the shell is made of the polymer while the aqueous drug solution is located in the core.

Capsules may be obtained by coaxial electrospraying shown in Fig. 2 RHS, where the aqueous core solution and organic shell solution are extruded independently through two concentric nozzles leading to the electrospraying of particles with a distinct core-shell structure. The bi-component syringe may be connected via tubing to separate syringes with independent flow using two syringe pumps [12, 20].

Particulate systems may be obtained by monoaxial electrospraying where the drug is mixed with the polymer solution before electrospraying commences, shown in Fig. 2 LHS. In the course of electrospraying the solvent evaporates from the droplet and the drug remains entrapped within the polymer structure, ideally randomly distributed. The drug can be mixed in its solid state, where it is directly dispersed in the polymer solution and vortexed before electrospraying. The drug may also be dissolved in an aqueous solution before mixing with the polymer solution, by emulsification or nanoprecipitation as shown in Fig. 2. Emulsions are widely used in traditional encapsulation methods with the water-in-oil-in-water (w/o/w) double emulsion being the most common used, since it provides access to a wide range of particle sizes by adjusting the conditions of the process. For electrospraying, a single water-in-oil emulsion (w/o) may be performed where hydrophilic molecules are first dissolved in water before encapsulation. Different surfactants may be added to tailor the encapsulation efficiency (EE) and release profiles [43]. However, the interface between the organic and aqueous phases may result in protein denaturation and aggregation, which is the main drawback of all emulsion-based methods [10, 51]. Nanoprecipitation, on the other hand, avoids the denaturation problem since high shearing rates and interfaces are absent. However it can lead to agglomeration and is not suitable for hydrophilic biomolecules due to leakage in the aqueous phase [8]. Solid dispersion may thus remain the most attractive option in monoaxial electrospraying, with no or limited denaturation and high versatility of drugs that may be incorporated (both hydrophilic and hydrophobic, small molecule and protein drug types).

Advantages of coaxial electrospraying include high drug encapsulation efficiencies within the capsules and the assurance that the drug has minimum contact with the organic solvent from the polymer solution, meaning less risk of drug degradation. Nevertheless, the biomolecules remain in aqueous solution within the capsules before delivery, which happen when the shell starts to degrade and channels open for release. This is an issue since the stability of some biomolecules in the aqueous state is known to be lower compared to its dry state, which may consequently result in loss of bioactivity [43]. Nevertheless coaxial electrospraying supposedly allows better control over release kinetics due to an increased number of variable parameters [20, 56-57].

More complex devices such as tri-needle coaxial devices can allow for more drugs to be loaded within separated layers of the capsule for sequential and multiple release [53, 58]. This can also be achieved with normal coaxial electrospraying with loading of a second drug in the polymer core. However it was previously shown that the hydrophilic nature of the drug is of importance and capsules that contain a hydrophobic drug in the core and a hydrophilic drug in the shell can easily be made, whereas the opposite configuration is more difficult to achieve [30].

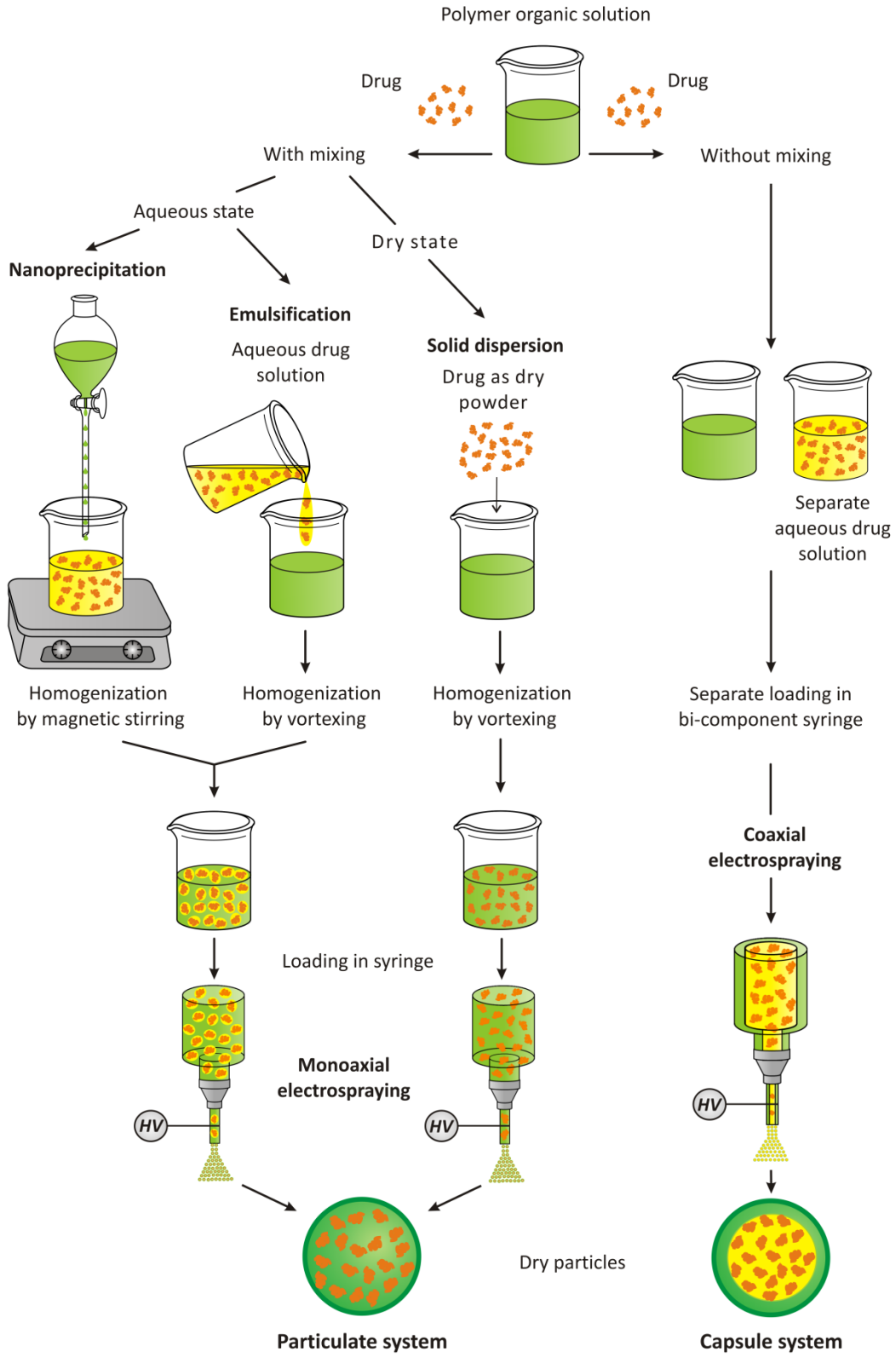

Fig. 2. Different methods of drug incorporation within polymeric particles through *monoaxial electrospraying* (by aqueous nanoprecipitation, emulsification, and solid dispersion) for production of particulate systems (LHS), and *coaxial electrospraying* for production of capsule systems (RHS), respectively.

3. Control of particle characteristics with electrospraying parameters

3.1. Importance of electrospraying parameters

Although electrospraying is accepted as a technique which can produce particles with monodisperse size distributions and reproducible morphologies by controlling the electrospraying parameters [21, 59], producing particles with very specific requirements remains challenging due to the large number of variables involved in the process and their complex inter-dependence. The primary pre-requisite for reproducible electrospraying and monodisperse size production is the stable cone-jet mode, for which the working window can be found by tailoring the field strength, conductivity and flow rate of the polymer solution. Morphology and size can be further controlled by adjusting additional parameters, such as the polymer concentration and molecular weight, the solvent vapor pressure, the flow rate, the electrospraying distance and chamber environment.

3.1.1. Polymers

3.1.1.1. Polymer types

Currently, the most common synthetic biodegradable polymer used in the field of drug delivery and also most commonly used in electrospraying is poly(lactic-co-glycolic acid) (PLGA). This aliphatic polyester is approved by the food and drug administration (FDA) and it is widely used in several medical devices (sutures, grafts, prostheses) and drug delivery devices [55]. PLGA degrades mainly through hydrolysis, which distinguishes it from natural biodegradable materials such as fibrin and collagen which are actively degraded enzymatically in the presence of cells. The natural products arising from degradation (lactic and glycolic acid) are then cleared by metabolic pathways [60]. In contrast, the degradation of PLGA via hydrolysis results in the generation of acidic species which can provoke inflammation of tissues and generate problems for long-term stability when encapsulating bioactive molecules. For instance, *in vitro* simulations of the polymer microclimate of PLGA microparticles produced using traditional methods revealed a highly acidic environment (pH<3), further triggering unfolding of encapsulated bovine serum albumin, resulting in peptide bond hydrolysis and non-covalent aggregation [61]. Anti-acid excipients such as magnesium carbonate ($MgCO_3$) or magnesium hydroxide ($Mg(OH)_2$) can be used in the microparticle fabrication process to buffer the pH [62]. BSA structural losses and aggregation were indeed prevented for over one month with $Mg(OH)_2$ from PLGA microparticles and this strategy was further employed for delivering angiogenic basic fibroblast growth factor and bone-regenerating morphogenetic protein-2 [61]. However no studies so far have tested these anti-acids in electrosprayed particles, where microclimate pH was mentioned but not addressed [43], although PLGA remains the most utilized polymer for electrosprayed particles [24-31, 43].

Polylactides (PLAs) have similar properties to PLGAs but they afford a more crystalline structure responsible for a slower degradation [30]. Select studies have chosen pure PLAs over the PLGA copolymers for monoaxially electrosprayed particles [32, 36, 45-46], or simultaneously in coaxial electrospraying with PLA as the core and PLGA as the shell to ensure that the drug in the core was not released prematurely by choosing a core of slower degrading material than the shell [30, 63]. Very different molecular weights (MW), such as 2 kDa [36] and 175 kDa [45], have been chosen when electrospraying PLAs. MW has a great influence on degradation and thus subsequent release of encapsulated biomolecules; PLA 2 kDa degrades quicker *in vivo* and is more soluble than higher MW PLAs [36].

The biodegradable polyester polycaprolactone (PCL) is an interesting candidate for drug delivery and has also been used in electrospraying [27, 31, 38, 40, 43]. Compared to PLGA

and PLA, PCL is semi-crystalline with a melting temperature of approximately 60°C and a glass transition temperature around -60°C (compared to 40 to 65°C for PLGA/PLA) conferring superior viscoelastic properties and easy formability [64-65]. PCL is also FDA-approved and various drugs have been encapsulated in PCL microspheres and nanospheres since PCL is highly permeable to small drug molecules. Due to its crystallinity and lower ester concentration, PCL presents the advantage of a less acidic environment being generated during degradation as compared to PLGA-based polymers [40, 66]. Nevertheless, the high hydrophobicity of PCL remains a concern for encapsulation of hydrophilic substances such as peptides, enzymes and other proteins [2].

Although all the aforementioned biodegradable polyesters, PLGA, PLA and PCL, have generated considerable interest in the last decades as potential matrices for drug delivery, overall concerns remain, particularly with regard to slow degradation and hydrophobicity (in the case of PCL) and acidic environment generation (in the case of PLGA and PLA) leading to possible instability, aggregation and structural changes of the loaded drug/protein. The introduction of functional groups can provide these polymers with tunable crystallinity and enhanced hydrophilicity. The description of such functional polymers and use so far in the field of drug delivery has been recently summarized in the review by the group of Hennink [67].

An elegant approach to improve the utility of PCL is to copolymerize with a more hydrophilic commoner. For example, PCL has been functionalized with hydrophilic components such as polyamino ethyl ethylene phosphate (PPE-EA), in order to improve hydrophobicity. The amphiphilic block copolymer, PCL-PPE-EA, was indeed shown to encapsulate BSA more efficiently than PCL alone [68]. During the w/o emulsion procedure, when the protein is introduced into the polymer solution, micelles are formed around the protein with the hydrophilic part of the polymer (PPE-EA) in contact with the protein. Such micelle-derived electrosprayed particles encapsulating BSA were 3 μm in diameter on average and exhibited a linear release profile for 20 days whereas no protein was released from PCL only particles. Unfortunately, the formulation and processing parameters of PCL particles loaded with BSA were not described in the study and the release data was not normalized to the amount of loaded protein, rendering the assessment of the system delicate [68].

Natural polymers have also been electrosprayed, including elastin-like polypeptides (ELP) [33, 69], a bioresponsive biopolymer that can be dissolved in water, an advantage compared to polyester based polymers that require organic solvents to dissolve them. ELP are inspired by the amino acid sequence of natural elastin and can be synthesized by recombinant DNA methods, allowing for a control over the ELP sequence and thus over its biofunctionality [70]. Chitosan is another natural polymer that has been electrosprayed in the past. Chitosan comes from the alkaline deacetylation of chitin and its main advantage is that it is hydrophilic, which improves facilitation of drug-polymer interactions compared to hydrophobic synthetic polymers [44]. Its performance as a drug delivery system is affected mainly by its molecular weight and degree of deacetylation, while its cationic nature allows for ionic cross-linking for improved material properties [23, 44]. Compared to synthetic polymers, the degradation products of chitosan are amino sugars, which are easily metabolized by the body [23], therefore there is no concern of an acidic microclimate being generated by chitosan particles. So far, the use of chitosan in electrospraying has been used limited to the use of encapsulating BSA [44], ampicillin [23], an antibiotic to treat bacterial infections, doxorubicin [71], an anti-cancer agent, and insulin [72]. In the case of BSA and doxorubicin, the microparticles were sprayed in a tripolyphosphate (TPP) solution, a non-toxic biocompatible cross-linking agent ideal for chitosan [44, 71].

Miscellaneous polymers that have also seen use in electrospraying applications include poly(amidoamines)-cholesterol (PAAC) conjugates, for encapsulation of Tamoxifen [42].

Along with their amphiphilic character – due to the presence of cholesterol, and low molecular weight (13 kg/mol), they are likely to produce nanosized particles with a low degree of polymer chain entanglements, thus providing rapid drug release rates (within hours). Polyvinylpyrrolidone, a water soluble polymer, has also been used for self-assembly of nanoparticles including tristearin, a lipophilic excipient and naproxen, an anti-inflammatory drug [39]. Although the versatility of electrospraying allows the use of many types of polymers, only a restricted number of polymers have been tested so far for encapsulation of biomolecules. Many more polymers remain to be investigated, for providing a higher degree of diversity in terms of physical and drug release characteristics of particles, as well as possibly enhanced drug-polymer interactions.

3.1.1.2. Solvents

Organic solvents are required to solubilize polymers prior to electrospraying. The most widely used solvent for electrospraying particles loaded with drugs is dichloromethane (DCM), a chlorohydrocarbon with the lowest boiling temperature (40°C) of the common solvents used in electrospraying. Other solvents include (by increasing boiling temperatures): acetone [46], chloroform [24], ethanol [36], acetonitrile [27], 1,2-dichloroethane [45-46], acetic acid [23, 44], and N,N-dimethylformamide (DMF) [46], which may be used alone or in combination. The boiling temperature of a solvent is the temperature at which the vapor pressure equals the ambient atmospheric pressure and it is representative of the solvent's volatility. Solvents with low vapor pressure (high boiling temperatures) are vaporized less easily than solvents with high vapor pressure (low boiling temperatures) and are thus less volatile.

This means that polymer diffusion is reduced in electrosprayed droplets from solvents with high vapor pressures, where solvent evaporation occurs at a higher rate. This effects the size and morphology of particles and it was previously shown that an increase in boiling point, corresponding to a decrease in volatility, correlated with a decrease in particle size with smoother surfaces generated for solvents with boiling temperatures above 140°C (such as DMF, 146°C) [73]. A greater particle size and more textured surfaces can be seen with solvents with low boiling temperatures such as chloroform (61°C) [59] and dichloromethane (40°C) [74]. This is due to fast solvent evaporation, where less time is available for polymer chains to contract and re-arrange within the evaporating droplet exposed to electric field. Faster evaporation can also result in the formation of pores [70] and even hollow particles [32, 75].

Importantly it was shown that a decrease in vapor pressure weakens the forces of polymer chain entanglements [76]. Therefore, the Coulombic repulsion is able to overcome the surface tension of evaporating droplets, leading to the ejection of small and highly charged offspring droplets. This was seen with PLGA particles where the addition of 30% DMF to chloroform reduced the vapor pressure from 21 kPa to 15 kPa and induced a bimodal size distribution. The use of a co-solvent with low vapor pressure is thus not recommended to obtain monodisperse particles [76].

It must also be noted that different polymers have different interactions with solvents, affecting polymer chain entanglements and final morphology of particles and both concentration and molecular weight greatly dictate these interactions [77].

3.1.1.3. Polymer solutions

When electrospraying polymer solutions, electrosprayed droplets undergo solvent evaporation and polymer diffusion simultaneously. Chain entanglements occur during these processes and are responsible for the final morphology of particles. In electrospraying, uniform microparticles and smaller droplets are favored by limiting chain entanglements [78]. The number of entanglements per chain in solution, $(n_e)_{sol}$, can be expressed with the polymer

volume fraction φ, the average molecular weight M_w and the average entanglement molecular weight M_e according to Equation (3):

$$(n_e)_{sol} = \frac{\varphi M_W}{M_e} \qquad (3)$$

It was previously shown that electrospraying occurred for 1 entanglement per chain ($(n_e)_{sol}$ = 2) whereas 2.5 entanglements per polymer chain ($(n_e)_{sol}$ = 3.5) would lead to formation of fibers; a process known as electro*spinning* [78]. Beaded fibers can form for intermediate values of $(n_e)_{sol}$. M_e is primarily a function of chain geometry and corresponds to the average molecular weight between entanglement junctions. M_e is readily available for more than 70 polymers but in the absence of experimental values, it can be theoretically estimated by employing the entanglement constraint model used by Shenoy *et al.* [78].

Polymer concentration plays an important role in the entanglement regime which dictates particle or fiber formation and is an essential parameter to control in order to optimize the process. The critical chain overlap concentration, C_{ov}, is known as the point when solution concentration is equal to the concentration inside the radius of gyration of every single macromolecular chain and is inversely proportional to the intrinsic viscosity [η], as shown in Equation (4) [79]:

$$C_{ov} \propto \frac{1}{[\eta]} \qquad (4)$$

When the concentration C is below C_{ov}, there are no chain entanglements and the regime is known as the *dilute regime* (Fig. 3A). Above C_{ov}, the concentration is large enough for chains to overlap but not sufficient to generate a significant degree of entanglement. The regime is the *semi-dilute unentangled regime*, and some entanglement is observed (Fig. 3B) although not desirable since particles have the ability to deform during evaporation, leading to inferior, non-reproducible morphology. Such a regime can be used for the production of electrosprayed films, another type of delivery device useful in some therapies such as chemotherapy. Multi layers of polymers encapsulating various drugs can thus be made by electrospraying in either the *dilute* or *semi-dilute unentangled regime*, allowing for a controlled release of therapeutic molecules tailored by the thickness of the films [29].

For electrospraying of particles, the regime of choice is the *semi-dilute moderately entangled regime*. It happens for C_{ent}, the crossover from the *semi-dilute unentangled regime* to the *semi-dilute moderately entangled regime*, where a significant degree of entanglement is observed and dense, solid and reproducible particles can be produced (Fig. 3C). However for C/C_{ov}>3, molecular cohesion is generally too high for electrospraying and beaded fibers or fibers are electrospun, corresponding to the *semi-dilute highly entangled regime* (Fig. 3D). For optimal particle electrospraying, it is thus essential to work above C_{ent} but not overcome C/C_{ov}>3. The molecular weight (MW) and molecular weight distribution (MWD) do affect C_{ov} due to differences in intrinsic viscosity, and it was demonstrated that an increase in MW reduces the C/C_{ov} ratio, narrowing the working window of the *semi-dilute moderately entangled regime*, thus narrowing the range of appropriate concentrations for reproducible electrospraying. On the other hand, for broader MWD, the ratio C/C_{ov} required to obtain the *semi-dilute highly entangled regime* was shown to be higher than 3, broadening the working window of the *semi-dilute moderately entangled regime* where reproducible electrospraying can be obtained [79].

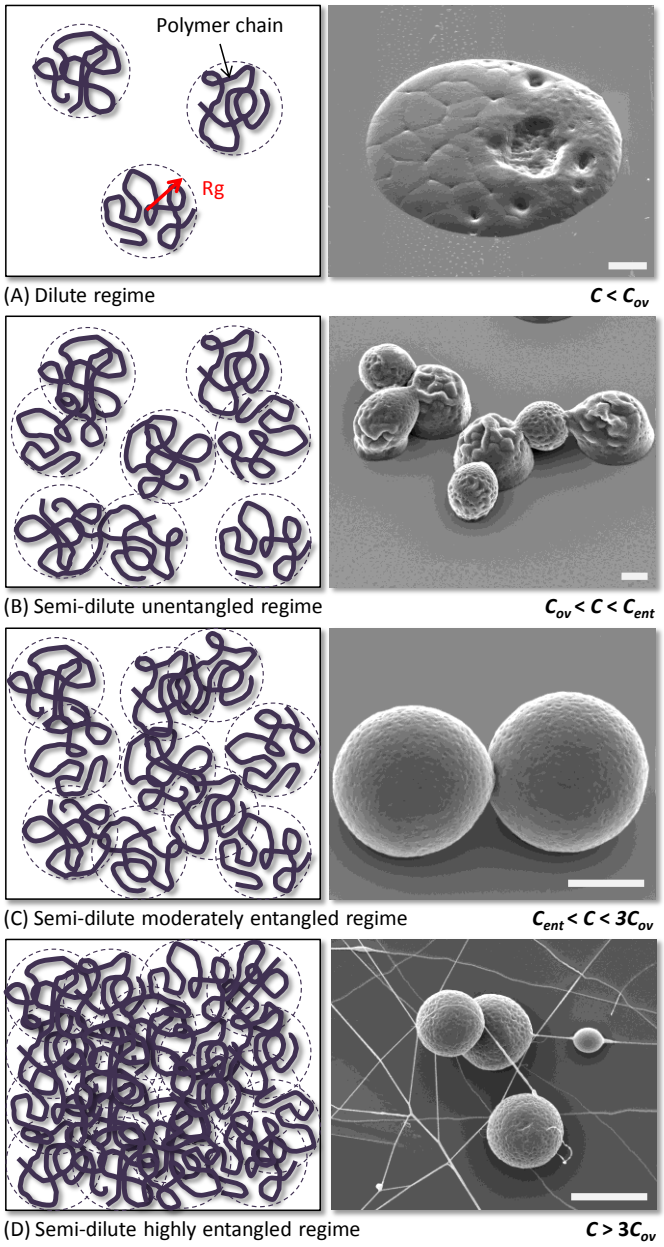

Fig. 3. Left column: Physical representation at the molecular level of various entanglement regimes obtained for different polymer concentrations. *Rg* is referred as the radius of gyration). *Adapted from [79] with permission. 2005 Elsevier Science Ltd.* Right column: Examples of corresponding scanning electron micrographs of dried PCL microparticles. PCL concentration in chloroform was: (A) 5%, (B) 7.4%, (C) 8.7%, (D) 9.6% w/v. Electrospraying conditions were 26 G for needle gauge, 20-25 cm for tip-to-collector distance, 0.5 mL/h for flow rate and 10 kV for voltage. The molecular weight of PCL on average was 130 kg/mol with a polydispersity index of 1.45. Scale bar is 10 µm.

3.1.2. Processing parameters

3.1.2.1. Spraying modes

Different spraying modes can take place in the course of electrospraying and they vary according to the field strength and flow rate of the polymer solution. The magnitude of the field strength is a key to reproducible spraying patterns [31] and its variation leads to different spraying modes, starting from the dripping mode and moving to cone-jet modes with increasing applied voltage [12]. When sufficient voltage is applied to the droplet to form the

Taylor cone (corresponding to the change-over from dripping to cone-jet modes), the ejection of small and highly charged droplets assumes the form of a cone which proportionally increases with an increase in the tip-to-collector distance. This single cone-jet mode seen for moderate field strengths is stable and fairly consistent from one replicate to the next [40]. Conversely, when increasing the field strengths, multiple cone-jets are formed, which are unstable and unpredictable, and importantly can vary throughout the course of electrospraying [31]. Such modes can be found in all types of electrospraying setups and are also observed for the nozzle-ring setup when increasing the potential difference between the nozzle and ring [27]. The multiple cone-jet mode needs to be avoided so that only targeted areas are sprayed, in order to ensure a high yield of particles. This is especially important when loading expensive molecules, where minimal loss is desired.

One strategy to obtain the single cone-jet mode is to lower the electrical conductivity and surface tension of the solution [40]. When incorporating therapeutic molecules to the polymer solution, the stable mode can be maintained by decreasing the protein concentration and the loading since the electrical conductivity increases with increasing protein concentration, as has been shown for BSA [46, 80]. As a result, the stable single cone-jet mode region shrinks and shifts to a lower flow rate for higher protein concentration (Fig. 4A-B). On the other hand, increasing the viscosity of solutions (by increasing polymer concentration for instance) results in a shift of the cone-jet mode to higher voltages, as seen in Fig. 4C. This is because of the lower conductivity of more viscous solutions: a stronger electric field should be applied to overcome the surface tension and liquid viscosity to form the cone-jet [40].

It is very important to keep in mind that only in the stable cone-jet mode is the production of monodisperse particles possible. Only then can the size and morphology of particles be controlled by carefully changing other parameters.

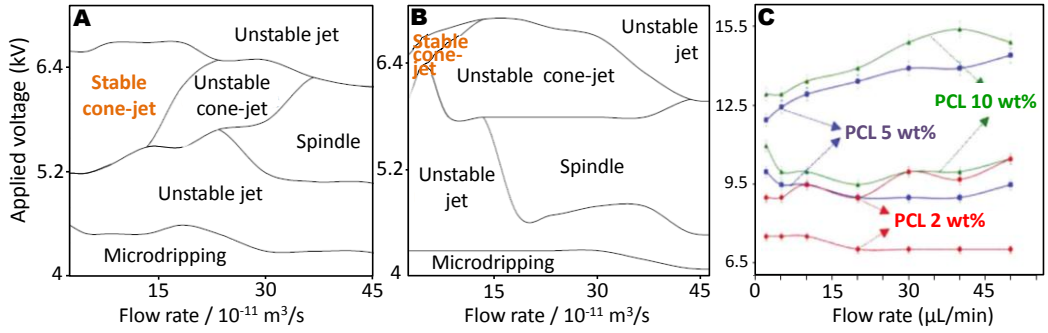

Fig. 4. Mode selections maps to obtain different electrospraying modes, for (A) 5.5 mg/mL and (B) 20 mg/mL as-prepared BSA solution. In the case of an unstable jet, a clear mode classification was not possible. Microdripping and spindle both refer to undesirable electrospraying modes [80]. (C) Cone-jet mode maps for different PCL solutions [40]. *Adapted from [40, 80] with permission. 2005 Springer [80]; 2010 Royal Society [40].*

3.1.2.2. Electrical conductivity

Since electrospraying depends on the electrostatic attraction of charged particles to a grounded or oppositely charged collector, the electrical conductivity, *K*, of the polymer and solvent is an important parameter when optimizing the process. Along with flow rate, electrical conductivity provides a powerful means to control the electrosprayed particle size, as demonstrated by the scaling laws from Gañan-Calvo, where a higher conductivity leads to a decrease in size [81].

An increased conductivity of a solution implies that more charge is carried by the electrospraying jet. In general, a low electrical conductivity is preferred to obtain quasi-monodisperse particles [76] since a higher conductivity may favor elongated particles or even

fibers if the polymer concentration is high enough [82]. Correlating with viscosity, stable electrospraying is known to be achieved only when viscosity is high or conductivity is low [83]. Changes in electrical conductivity can be obtained by changing the electrospraying solvent or using co-solvents, although this latter case may be detrimental to size distribution and morphology of particles [46, 76]. Organic solvents are generally less conductive than aqueous solvents and their conductivity can be increased by the addition of electrolytes, such didodecyltrimethylammonium bromide (DTAB) [28] or ammonium hydroxide [36], which can increase conductivity by orders of magnitude. For instance the conductivity of a 5% (w/v) PLGA solution in acetonitrile containing 10% (w/w) paclitaxel was shown to increase from 0.51 µS/cm to 116.5 µS/cm by the addition of 2 mM DTAB. This led to a particle size decrease from around 1.2 µm to 355 nm [28]. Compared to pure solvents, it must be kept in mind that the addition of a polymer will most likely decrease the electrical conductivity, although remaining in the same order of magnitude [84].

When the electrical conductivity of the solution is lower than 0.01 µS/m, it is likely that insufficient current can flow, and the liquid cannot be electrosprayed, although too a high conductivity value leads to unstable electrospraying [31]. The bending instability of the jet becomes more important when more charges are present due to increased conductivity, leading to a wider deposition of particles on the collector. With higher electrical conductivity, the Coulombic repulsion forces are higher and compete with the viscoelastic forces of the solution, disentangling more easily the polymer network which is being formed during electrospraying. In other words, increasing conductivity makes it easier for the solution to be broken up into smaller droplets. Therefore for the same polymer dissolved at the same concentration in a higher conductive solvent (or the same solvent but supplemented with organic salts), less chain entanglements take place during electrospraying, in turn reducing the final particle size. However, if the Coulombic repulsion forces are sufficiently high to overcome the entanglement forces, then Coulomb fission occurs before strong entanglements can form, and smaller offsprings are ejected from the primary droplet. This will provide a bimodal size distribution, with particles presenting various types of morphologies, mostly unwanted and further discussed in the section 3.2. Low electrical conductivity may thus be more favorable for electrospraying of quasi-monodispere microparticles.

When nanoparticles are required, increasing conductivity may be a good means of reducing particle size, although sufficient viscosity needs to be ensured so that entanglement forces remain higher than Coulomb forces, and the ejection of offspring droplets is avoided. Higher flow rates can also be used to produce nanoparticles if higher salt concentration is used to increase solution conductivity [28]. In the context of electrospraying emulsions, the organic/aqueous volume ratio is another significant factor influencing the electrical conductivity whereby addition of water to the organic phase significantly increases the electrical conductivity of the resulting emulsions [45].

3.1.2.3. Flow rate

After the selection of polymer solutions, flow rate is arguably the second most important parameter in electrospraying and together with the solution parameters (polymer MW, concentration, solvent, and conductivity) can control polymer entanglements and Coulomb fission [21]. Flow rate thus has consequences for both the morphology and size of particles and must be judiciously chosen since both these characteristics will influence the drug dispersion within the polymer matrix, ultimately affecting drug release.

Firstly, it is essential to use a flow rate that allows for complete solvent evaporation, which is not possible with high flow rates. Particles are partially solvated when they impact the collector leading to a deformed and non-consistent morphology [27, 59]. Furthermore, higher flow rates can trigger the formation of secondary and satellite droplets that confer a bimodal or polydisperse character to the size of electrosprayed particles. This is explained by the

processes involved in solvent evaporation from the charged droplet, based on φ_{Ray}, the polymer volume fraction in a droplet at the Rayleigh limit, and expressed in Equation (5). *Q* is the liquid flow rate ($m^3.s^{-1}$), *I* the current, ε_{air} the permittivity of air, γ the surface tension of solution in ambient air, and *d* the initial droplet diameter. *I/Q* and *d* can be determined as a function of *Q* and the polymer solution properties.

$$\varphi_{Ray} = \varphi \frac{288\ \varepsilon_{air}\ \varepsilon\ \gamma}{\left(\frac{I}{Q}\right)^2 d^3} \quad (5)$$

Considering φ_{ent} as the critical entanglement polymer volume fraction and φ_{ov} as the critical chain overlap polymer volume fraction, it was shown by Almería *et al.* that for $\varphi_{ov}<\varphi_{Ray}<\varphi_{ent}$ in the *semi-dilute unentangled regime* mentioned previously, the polymer network can preserve some droplet integrity, but is not strong enough to preserve the particle from deforming via stretching during the fission process, while droplets are stabilized from such rupture when $\varphi_{Ray}>\varphi_{ent}$ [21]. For $\varphi_{Ray}<\varphi_{ov}$, the droplets behave like a pure liquid and there are no entanglements, leading to the ejection of offspring droplets from the primary droplet; a consequence of Coulomb fission. In order to obtain a spherical morphology and monodispersity, it is important that sufficient entanglements are present before the Rayleigh limit is reached so that the droplet cannot be disrupted by Coulomb fission, ensuring that $\varphi_{Ray}>\varphi_{ent}$. According to Equation (5), flow rate has a significant influence on φ_{Ray} and it was shown for the morphology of PLGA particles that larger flow rates lead to smaller φ_{Ray}, and thus non-spherical morphology and formation of satellite and primary droplets, while higher polymer concentrations would preserve particle sphericity at higher flow rates [21].

In practice, the formation of satellite and primary droplets can be explained by the phenomena occurring when the droplets are ejected from the Taylor cone. Initially, a filament unites 2 droplets, but it is further broken up by the charge. Once broken from the farthest droplet, the filament flows back to the nearest droplet from the cone, and monodisperse particles can be achieved. This is seen for relatively low flow rates enabling $\varphi_{Ray}>\varphi_{ent}$. At increased rates, φ_{Ray} becomes smaller, eventually falling in the case where $\varphi_{ov}<\varphi_{Ray}<\varphi_{ent}$ where entanglements are not strong enough to preserve the droplet integrity. Thus the filament cannot reach the former droplet anymore and instead it breaks, forming a secondary smaller droplet. At even higher flow rates, a filament between primary and secondary can form, which, being unable to reach back to the primary droplet, turns into a satellite droplet (even smaller than secondary droplets) [14]. If the solvent has a high evaporation rate, it is even possible that the filament remains frozen, leading not only to polydisperse sizes but also leading to elongated particles [21].

The same rules apply for coaxial electrospraying where the inner and outer flow rates may strongly affect the properties of electrosprayed capsules. Usually the flow rate of the core solution is much lower than the shell solution [51], resulting in uniform sizes. In contrast, for a shell flow rate slower or equal to that of the core flow rate, irregular morphologies are obtained, while for increasing ratios of shell:core flow rates, the shell becomes thicker [56]. This presents a useful tool for the tailoring of release kinetics.

3.1.2.4. Other parameters

Effect of gauge

The diameter of a needle is commonly expressed in gauge (G), each gauge size arbitrarily correlating to multiples of 0.001 inches [85]. For the electrospraying of particles loaded with bioactive molecules, these diameters range from 18 G (internal diameter (ID) of 1.27 mm) [45-46] to 29 G (ID of 0.33 mm) [28]. Prior to electrospraying, beveled needles are typically shortened and given a flat end for homogeneous spraying, although characterization of the needle tip, while important, is often overlooked. The effect of gauge has little effect on

morphology or size of particles. For instance when comparing the size of PCL particles made with 21 G versus 26 G, the average size was equivalent for both gauges, however the size distribution was slightly broader for the bigger gauge (21 G) with standard deviation (SD) of 3.42 while SD was 2.40 for 26 G, suggesting that a smaller gauge can produce a narrower size distribution [59]. A similar result was observed in the 20 to 26 G range when electrospraying ampicillin-loaded chitosan nanoparticles, where the use of the 20 G led to sputtering only, 22 G led to a mixture of particles and sputtering, while 24 and 26 G led to spherical particles with no sputtering and with reduced polydispersity for the smallest gauge (26 G) [23].

Effect of voltage

The main incidence of voltage is on spraying modes as described previously in section 3.1.2.2, Spraying modes. Within the single cone-jet mode, size is not significantly affected by voltage where only a slight decrease in size is observed when voltage is increased [24]. Morphology however will be changed as stated by Shenoy *et al.*, since as the voltage is increased, the morphology changes from spherical particles to elongated particles or beaded fibers to eventually only fibers if concentration is sufficiently high [78]. This is due to more charge acting on droplets with increased voltage, leading to stretching and elongation of droplets. It is therefore recommended to use moderate voltages that allow for the single cone-jet mode to take place while maintaining the spherical morphology of particles.

Effect of tip-to-collector (TTC) distance

The lower limit of distance is determined by electric discharge. A small TTC distance can impair full solvent evaporation and consequently, wet microspheres impact the collector, leading to collapsing, coalescence and broad size distributions [23]. Increasing the distance leads to more spherical morphologies since polymer chains have sufficient time to diffuse within the droplet [59] and thus also reduced polydispersity. At constant voltage, a decrease in the TTC distance leads to an increase in the strength of the electric field, thus leading to a decrease in particle size [84]. Depending on the type of solvent used, an increase in TTC distance may also be detrimental for morphology as shown with polyacrylonitrile microspheres in DMF where at 10 cm, the evaporation rate of DMF allowed round spheres to be formed, while at 20 cm, the round spheres collapsed into half-hollow spheres and the authors stated that the evaporation rate was excessive. However this result was not clearly evident in the images shown by the authors, and no explanation was proposed [86].

3.2. Tailoring of electrosprayed particle characteristics

3.2.1. Morphology

The morphology of electrosprayed particles is controlled by solvent evaporation and polymer diffusion [21]. The polymer solution thus plays a determinant role in these mechanisms, where the nature of polymer (solubility, molecular weight, concentration) and solvent (vapor pressure, miscibility, conductivity of solution) coupled with the solution flow rate form the levers of morphology tailoring [59]. As explained previously in the section 3.1.1.3, regarding polymer solutions, concentration and molecular weight can dictate the entanglement regime taking place, leading to reproducible and solid electrosprayed particles, when a certain degree of chain entanglement is obtained. Therefore in most studies, morphology is initially linked to polymer concentration and molecular weight, where a decrease in concentration or an increase in molecular weight induces non-spherical morphologies such as shell-like, wrinkled, hollow particles, beaded fibers or particles with tails (Fig. 5A-B).

As seen in the section 3.1.2, flow rate also has a significant influence on morphology through φ_{Ray}, the polymer volume fraction in a droplet at the Rayleigh limit (expressed in Equation (5)), where it was shown that φ_{Ray} needs to be greater than $\varphi_{ent.}$ In this case,

electrosprayed droplets are stabilized against rupture, leading to a desirable spherical morphology. For lower flow rates, we may fall in the regime where $\varphi_{ov}<\varphi_{Ray}<\varphi_{ent}$ where entanglements are not strong enough to preserve the particle from deforming via stretching during the fission process, leading to a deformed morphology.

These theories were confirmed for BSA-loaded PLGA microparticles when polymer concentration (in DCM) was decreased from 10 to 6%, and wrinkled particles were obtained instead of dense and spherical particles [43]. Similarly, this trend was observed in paclitaxel-loaded PLGA microparticles where the morphology changed from spherical to shell-like shapes when decreasing polymer concentration from 8 to 6% [27], while a decrease from 2 to 1% in ampicillin-loaded chitosan gave abnormal shapes instead of spherical particles seen for 2% [23]. Hollow particles were seen when decreasing the concentration of aqueous elastin-like polypeptides from 1 to 0.5% while spherical spheres were initially obtained at higher concentrations [33]. All these results are a consequence of high solvent concentration, hindering complete solvent evaporation by the time the particles reach the collector, which in turn resulted in deformed morphology. The effect of polymer concentration was also considered with MW where a higher MW (70,200 g/mol versus 17,800 g/mol) provided tailed structures or beaded fibers instead of spherical particles for both concentrations [33]. As explained previously, this is a consequence of φ_{Ray} being reached before strong entanglements are present within the droplet. This leads to the stretching of the primary droplet ($\varphi_{Ray}<\varphi_{ent}$) since an increase in MW leads to a decrease in surface tension and thus a decrease of φ_{Ray} in accordance to Equation (5).

In coaxial electrospraying, flow rates of both core and shell solutions are determinant for reproducible morphology and size of capsules, where inner flow rates are required to be lower than outer feed rates. Decreasing the inner flow rates led to a thicker capsule shell and reduced particle size (Fig. 5E) [56]. When loading paclitaxel and suramin in the PLGA shell and poly-L-lactide (PLLA) core of microcapsules, respectively, it was concluded that a Q_{core} ranging between 1.0 and 2.0 mL/h and a constant Q_{shell} of 2.0 mL/h may maintain a stable cone-spraying mode and consequently result in uniform and smooth microspheres with varied core sizes [30, 63].

In electrospraying of emulsions, a decrease in the organic/aqueous phase volume ratio (from 20:1 to 6.7:1) led to a degeneration of the spherical shape of particles with a more wrinkled surface. This was tentatively explained by a corresponding decrease in viscosity which would hinder the shrinkage of droplets during evaporation [45].

Similarly, loading of biomolecules into the particles affects the morphology and wrinkled particles were observed for a 30% - and above - loading of rifampicin in PLGA particles [24]. This is a consequence of the difference in molecule types: PLGA is a linear macromolecule whereas rifampicin is a small organic molecule. It was stated that the addition of rifampicin decreased the diffusion coefficient of solutes and weakened the intermolecular entanglements of PLGA. When the concentration of the drug is higher than a critical value, diffusion is slower than solvent evaporation, resulting in the increase of drug concentration near the front of the droplets. Drug molecules accumulate and form a layer of semi-solidified skin on the surface. With further evaporation of solvent, the intermolecular polymer entanglements in the droplet skin predominate, forcing the semi-solidified skin to collapse, leading to wrinkles [24].

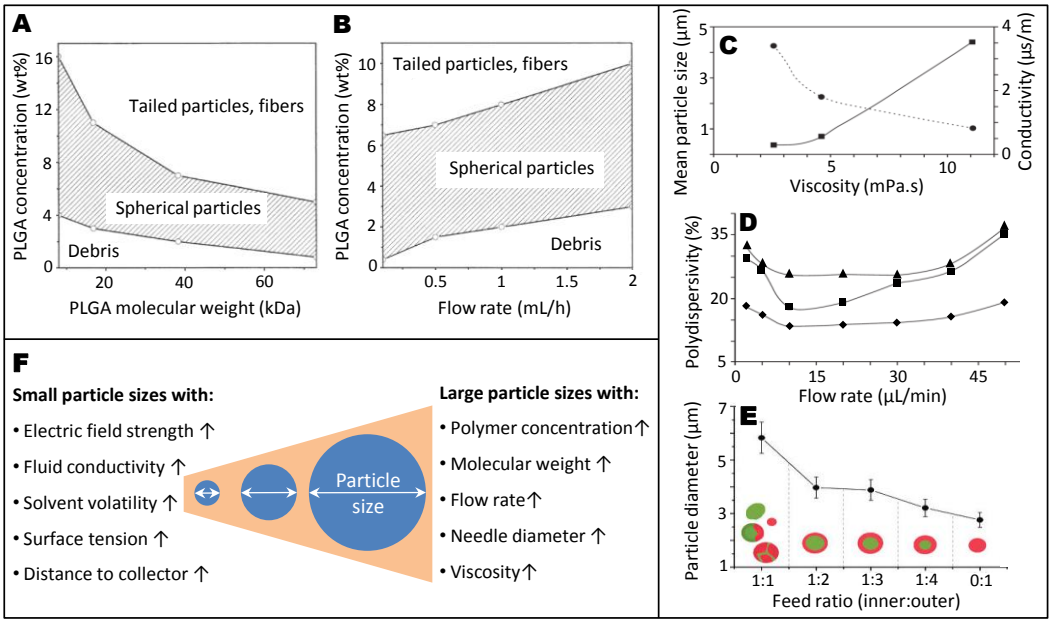

Fig. 5. Importance of electrospraying parameters. (A-B) Effect of various parameters on morphology of PLGA particles: (A) Effect of concentration and molecular weight (FR=1mL/h and AV=10kV). (B) Effect of concentration and liquid flow rate (MW=38kDa and AV=10kV) [76]. (C) Relationship between mean particle size, electrical conductivity and viscosity of PCL solutions (FR=10µl/min, AV=10kV). Square with solid line: mean size; circle with dotted line: conductivity. (D) Polydispersivity index of PCL particles produced in the cone-jet region as a function of flow rate (AV=10kV). Square line: PCL 2wt% (viscosity: 2.6 mPa.s); triangle line, PCL 5wt% (viscosity: 4.6 mPa.s); diamond line: PCL 10wt% (viscosity: 11.1 mPa.s) [40]. (E) Dependence of the size and shape of microcapsules made by coaxial electrospraying on the feed ratio between outer and inner solutions [56]. (F) Diagram depicting the influence of parameters on particle diameter (↑: increase) [20]. *Adapted from [20, 40, 56, 76] with permission. 2009 John Wiley and Sons [76]; 2010 Royal Society [40]; 2008 American Chemical Society [56]; 2009 Elsevier Science Ltd. [20].*

3.2.2. Size

The size of polymeric particles that contain bioactive molecules significantly influences their therapeutic capabilities. For instance, the release rate increases with a larger surface to volume ratio of the particles [28] and is dependent on surface diffusion and degradation. Control of size is therefore essential for tailoring release properties. The electrospraying technique can produce particles with sizes varying from tens of micrometers to tens of nanometers [35] and by choosing the right parameters, low polydispersity can be obtained with relative standard deviations (RSD) within 2 to 27% of the average size [34, 43]. This is advantageous in drug delivery since drug distribution within the matrix can be controlled more precisely with a single known particle size, allowing degradation rates and diffusion of drugs to be better tailored to fit a desired application [16]. However, this is a constant issue when microparticles are made from double emulsion fabrication methods where broad distributions are obtained, ranging from 49 to 110% RSD [22, 36].

When nanoparticles are considered, the control of size and polydispersity becomes even more important since they can greatly affect cell response mechanisms where particles are internalized by cells. This involves particles lower than 500 nm for uptake by epithelia cells for example [18], and lower than 100 nm for applications such as tumor targeting by the enhanced permeability and retention (EPR) effect. However, although the electrospraying

technique allows the generation of nanoparticles such as pharmaceutical nanoparticles (APIs) or non-organic nanoparticles (for coating for instance), when polymeric carriers were used to encapsulate drugs, the resulting electrosprayed particles were mainly found to be on the micron to submicron size. The minimum size reported so far is 116.1 nm with budesonide-loaded PCL particles [38] and very few studies are found in the 100 to 500 nm range [28, 33, 36, 42, 71]. This is likely due to polymer chains used in electrospraying of polymers with drugs since a significant molecular weight and polymer concentration are needed in order to efficiently encapsulate a drug within the polymeric matrix. The nanosize of electrosprayed polymer/drug systems is thus less likely and most systems actually produce micrometric sizes as seen in Table 1.

Table 1. Size and polydispersity (expressed as the relative standard deviation to the average particle size (RSD) in %) achieved by electrosprayed polymeric particles loaded with various types of therapeutic molecules.

Size domain	Size range studied	Size with lowest polydispersity	RSD (%)	Polymer	Loaded Molecule	Ref.
Below 500 nm	116.1 - 165 nm	165 nm	11.5	PCL	Budesonide	[38]
	-	247 nm	7.2	PAA-cholesterol	Tamoxifen	[42]
	304.9 - 569 nm	304.9 nm	6	TPP-Chitosan	Doxorubicin	[71]
	255 - 355 nm	335 nm	18.2	PLGA	Paclitaxel	[28]
	-	370 nm	6.8	Elastin-like polypeptides	Doxorubicin	[33]
	250 - 500 nm	470 nm	2.1	PLA	BDP/SS	[36]
500 nm - 1 µm	510 - 630 nm	630 nm	11.1	PLA	BDP/SS	[36]
	-	840 nm	21.4	PLA	BSA	[45]
	580 - 910 nm	910 nm	12	PLGA	Rhodamine	[22]
1 - 5 µm	1.12 - 1.34 µm	1.12 µm	10	PLGA	Rhodamine	[22]
		1.34 µm	10	PLGA	Doxorubicin	[22]
	1.64 - 4.77 µm	3.95 µm	12.9	PLA	BSA	[46]
	-	4.13 µm	26.9	PLA	Cisplatin	[34]
	2.3 - 4.4 µm	4.4 µm	7.4	PLGA	Celecoxib	[37]
Above 5 µm	5 - 5.31 µm	5 µm	15.0	PLA/PLGA (30/70)	Cisplatin	[34]
	5.4 - 5.7 µm	5.4 µm	16.7	PLGA	IGF-1	[47]
	6.51 - 12.8 µm	7.5 µm	6.8	PCL	Paclitaxel	[31]
	7.9 - 10.4 µm	8 and 10 µm	15	PLGA	BSA	[51]
	5.67 - 9.78 µm	9.39 µm	3	TPP-Chitosan	BSA	[44]
	-	11.4 µm	7.9	PCL	Paclitaxel	[27]
	-	11.76 µm	23.7	PLGA	Paclitaxel	[25]
	-	15 µm	11.3	PLGA	Paclitaxel	[26]
	14.2 - 15.2 µm	15.1 µm	4.6	PLGA	Paclitaxel	[27]
	-	20 µm	15.5	PCL	BSA	[43]
	20.3 - 22.1 µm	21.2 µm	7.1	PLGA	BSA	[43]

Monodispersity remains a very important factor for micron sizes, especially for release properties and Table 1 shows a non-exhaustive summary of the various polydispersities (expressed as the relative standard deviation to the average size of one formulation) that have

been achieved so far by loaded electrosprayed polymer particles, per size domain. It can be seen that several similar sizes can provide very different polydispersivities according to the processing parameters and also depend case by case on the polymer/drug/solvent selection. It is thus possible to obtain very low polydispersivity with electrospraying (as low as 2.1% [36, 43]), by tailoring electrospraying parameters, but this is a complex undertaking. Monodispersity is obtained with reduced flow rates, increased polymer concentrations (higher viscosities), reduced conductivity of the electrosprayed solutions and reduced applied voltages [40, 87]. This applies for the stable-cone jet mode known to be the only one able to produce monodisperse particles and when parameters such as flow rate are used in the central cone-jet region. Indeed, when flow rate is used close to the upper and lower limit of the cone-jet region, the polydispersivity index of particles increases, as seen in Fig. 5D [40].

The size of electrosprayed polymer particles is greatly influenced by flow rate and polymer concentration, where increased particle sizes are most significantly obtained with an increase in flow rate and polymer concentration and a decrease in conductivity (Fig. 5C) [59]. However, at increasing flow rates, the size distribution also becomes broader [35] and formation of secondary and satellite droplets can take place if the polymer network is not entangled enough ($\varphi_{ov}<\varphi_{Ray}<\varphi_{ent}$). This leads to a bimodal size distribution which is quite common in electrospraying and sometimes unavoidable [12, 24, 31, 59]. Some strategies have been suggested to separate the two size populations by using a steel plate with a 3 cm circular hole as the grounded electrode, which serves to collect only the primary droplet population. Often a spatial separation occurs after the droplet break-up where two regions of electrospray can be seen during the stable cone-jet mode, since satellite/secondary droplets have a larger surface charge density but less mass than primary droplets. Therefore primary droplets can be found in the inner core of the spraying cone, while satellite/secondary droplets get ejected at the periphery of the cone [24]. By using a plate with a circular hole as a screen on top of the collector, satellite/secondary droplets thus are left behind and only primary droplets are recovered ensuring monodispersity, although reduced yield may be of concern. Hartman *et al.* measured very small currents (31-57 nA) during electrospraying and found that another way to reduce the frequency of satellite droplets is to lower the current by lowering the applied voltage or flow rate [14]. However satellite/secondary droplets remain difficult to eliminate completely [24].

These findings are explained by the relationship between size and electrospraying variables depicted by Hartman *et al.* in the stable single cone-jet mode and shown in Equations (6) and (7) [14]. The droplet diameter, *d*, can be modeled using various equations generated by De La Mora and Loscertales [88] in 1994, Gañan-Calvo *et al.* in 1997 [81] and Hartmann in 2000 [14] (Equations (6) and (7)) for the single cone-jet mode. They are functions of the liquid flow rate, *Q*, the solution density, ρ, the current, *I*, the surface tension in ambient air, γ, and the liquid conductivity, *K* (α is a constant).

$$d = \alpha \left(\frac{\rho \varepsilon_0 Q^4}{I^2}\right)^{\frac{1}{6}} \qquad (6)$$

$$I \propto (\gamma K Q)^{\frac{1}{2}} \qquad (7)$$

Particle size is directly proportional to droplet size, where an increase in size is obtained with increasing flow rate and decreasing surface tension, and is shown to correspond to an increase in polymer content [86]. However as stated earlier, an increase in flow rate is also responsible for broader size distributions [35], thus a compromise needs to be made between particle size and dispersity. This is explained in section 3.1.2.1, where higher flow rates lead to smaller φ_{Ray}, eventually falling in the case where $\varphi_{ov}<\varphi_{Ray}<\varphi_{ent}$ where polymer

entanglements are not strong enough to preserve the droplet integrity during electrospraying. This unwanted regime will lead to the ejection of offspring, secondary and satellite droplets from the primary droplets and broaden the resultant size distribution considerably. The first pre-requisite of monodispersity of electrosprayed particles is thus the use of a flow rate that ensures $\varphi_{Ray}>\varphi_{ent}$, where primary droplets cannot be disrupted by Coulomb fission. As stated by Almeria *et al.*, if increasing particle size is highly desired, while maintaining monodispersity, increased flow rates could be coupled with higher polymer concentrations so that the $\varphi_{Ray}>\varphi_{ent}$ is still validated [21].

When involving the polymer concentration parameter, particle size has been shown to increase compared to the theoretical calculations for PLGA microparticles containing paclitaxel made from low polymer concentrations (4, 6 and 8% in acetonitrile), while it was in good agreement for 10%. This was attributed to the non-spherical shape and high porosity of particles made from lower concentrations [28]. The increase in particle size as a function of the square root of flow rate was also shown to be sharper for higher polymer concentrations. An increase in concentration from 5% to 10% PCL in DCM, however, led only to a slight increase in size, for paclitaxel-loaded particles from around 9 to 13 µm [31], suggesting that rate is more determinant than polymer concentration for directing the size of loaded particles. Indeed, increasing the flow rate from 4 to 8 mL/h when electrospraying chitosan solutions significantly increased the size of microparticles at each chitosan concentration [44]. However the size did not increase significantly with an increase in concentration from 1 to 2%. In a similar study, an increase in polymer concentration from 4 to 8% (PLGA 50:50 in acetonitrile) resulted in a limited change in the particle size while for 10%, the sizes were considerably larger. This was explained by the low diffusion rate of PLGA chains where a shell of solid PLGA would form on the surface of the droplets. For lower polymer concentrations in the 4-8% range, the shell would be thinner but a similar overall size would be obtained, while for concentrations higher than 8% a high polymer concentration was established on the surface of the droplet with less solvent evaporation, resulting in a larger final particle size [28]. All these results underline the strong effect and inter-dependence of flow rate coupled with concentration on particle size.

Drug loading was also shown to affect microparticle size; loading from 0% to 15.8% of the anti-cancer drug paclitaxel increased PLGA particle size from around 13 to 15 µm although the number of particles analyzed (*n*) or the technique for size measurement was not described in the study [27]. The link between loading and size is however less evident than previous variables. In the case of electrospraying of emulsions, the size was shown to first decrease and then increase as the BSA:PLA weight ratio decreased from 1:2 to 1:6. This was tentatively explained by a decrease in viscosity from less solid mass in the emulsion causing the initial decrease in size, and the lower conductivity causing the subsequent increase [45].

As explained in section 3.1.2.2, the electrical conductivity is indeed a potent parameter for controlling particle size where the scaling laws from Gañan-Calvo show that a decrease in particle size can be obtained with an increase in conductivity, according to Equation (8) [81]:

$$d = \left(\frac{1}{K}\right)^{1/6} \qquad (8)$$

The use of a solvent with a higher conductivity can thus decrease particle size as seen when comparing PLGA particles made using acetonitrile and dichloromethane as the solvents [84] or when adding acetone to a PLA solution of 1,2-dichloroethane (1:1) [46] where conductivity was increased from 0.058 to 0.412 µS.cm^{-1} and particles decreased in size from 4.8 to 1.6 µm. However, it was shown that the use of co-solvent with increased conductivity broadened the size distribution with a bimodal character and reduced the spherical morphology of PLGA particles [76] and PLA particles [46], respectively. The use of organic

salts is more effective to increase conductivity without causing a concomitant deterioration in the initial morphology of particles as seen with 2 mM of didodecyltrimethylammonium bromide (DTAB) added to an acetonitrile solution of PLGA and paclitaxel [28]. In this case, particle size was decreased from 1.2 µm to 355 nm. Other possible electrolytes include ammonium hydroxide (0.02 to 0.2% (v/v)) [36]. Although conductivity is pivotal in size tailoring, it must be kept in mind that an increase in conductivity reduces the region of the stable cone-jet mode and hence standard deviation tends to increase, broadening the size distribution [35]. Again this is due to a consequent decrease in φ_{Ray} which may eventually be smaller than φ_{ent} where the ejection of offspring, secondary and satellite droplets from the primary droplets is possible. Such broadening was also observed with increasing surfactant concentration, thus conductivity of the solution, as seen for 2-16% Pluronic F127 in PLGA solution in acetonitrile, although it did not appreciably reduce the average particle size [28]. However, for budesonide-loaded PCL particles, a decrease of Tween 20 from 0.005 to 0.001% led to a decrease from 884 to 116.1 nm under optimal electrospraying conditions [38].

Emulsions comprising organic/aqueous and protein/polymer phases also have significant impact on particle size [45]. Particle size increased with organic/aqueous volume phase ratio. This was due to a corresponding increase in viscosity and decrease in electrical conductivity which makes it more difficult for the solution to be broken up into smaller droplets in the course of electrospraying, thus increasing particle size. Such correlation between size, viscosity and electrical conductivity was also seen for β-oestradiol-loaded PCL particles where an increase of PCL concentration from 2 to 10 wt% led to a change in viscosity and electrical conductivity of the PCL solutions from 2.6 to 11 mPa.s and from 3.4 to 0.8 µS/m, respectively. This resulted in a mean particle size increase from 0.3 to 4.5 µm [40].

4. Electrospraying and drug release characteristics

4.1. Choice of molecules

Most pharmaceutical drugs and proteins are expensive. For this reason the majority of drug delivery studies are first undertaken with model drugs or model proteins, to enable optimization of parameters and characteristics of particles in the first instance, before loading fragile and expensive drugs/proteins. A non-exhaustive summary of various drugs and proteins that have been loaded so far in electrosprayed particles is presented in Fig. 6.

As far as proteins are concerned, bovine serum albumin (BSA) has been widely used for this ‘model’ purpose in traditional encapsulation techniques [89], and to some extent in electrospraying [43-46, 51, 53, 68, 90]. BSA is readily available and it offers high stability and low cost, which is advantageous in the early stages of optimization. The molecular mass of BSA is 66.4 kg/mol, which is similar in size to some growth factors (GFs) used for tissue regeneration, providing a more suitable choice than smaller model molecules. Serum albumins are also extensively used as an excipient, i.e. as an inactive substance used as carrier for the molecules of interest, since they have the ability to bind a wide variety of biological molecules, e.g. cationic, anionic, hydrophilic, hydrophobic substances. Many drugs, such as anti-coagulants and anesthetics, are also transported in blood while bound to albumin [80]. Serum albumins have no adverse effect in most biochemical reactions and they have been shown to assist decreasing the initial burst release occurring in most particulate systems [91], and stabilize and protect the bioactivity of molecules during the harsh conditions of encapsulation [92].

Due to its combined advantages, BSA has often been selected as a model protein to be encapsulated in electrosprayed particles, in studies focusing on release of proteins or drugs. Unfortunately, only a handful of studies can be found where electrosprayed particles have

been loaded with the actual protein of interest other than BSA, in part due to their high cost. It would be valuable for more studies to progress towards using therapeutic proteins in place of these model systems. Some examples of studies who do encapsulate therapeutic molecules include growth factors such as insulin-like growth factor-1 (IGF-1) [47], vascular endothelial growth factor (VEGF) and platelet-derived growth factor (PDGF) [48]. Growth factors (GFs) are essential actors during natural tissue formation. These polypeptides are produced *in-situ* by cells and transmit signals to modulate cellular activities [9, 93]. During tissue growth a complex and orchestrated delivery of several types of GFs occurs and tissue growth is dependent on this delivery. Thanks to the current technologies, GFs can now be recombinantly produced, albeit at very high cost, and have thus attracted a lot of interest among tissue engineers. Many DDPS have attempted to encapsulate and release GFs in a sustained manner, mimicking the normal *in vivo* production. For GFs that were encapsulated in electrosprayed particles, we find IGF-1, PDGF and VEGF, which are mostly involved in angiogenesis. It must be noted that their molecular mass ranges from around 7 (IGF-1) to 45 kg/mol (VEGF) and are therefore lower than BSA (66.4 kg/mol). Compared to small drugs, proteins are also prone to denaturation, which is often an issue in DDPS production where organic solvents are used. The technique of electrospraying however, offers a reduced contact of proteins with solvents and most importantly does not require the emulsion step present in the traditional fabrication processes. The aqueous/organic interface is thus avoided along with its respective shear stresses, mainly responsible for protein denaturation [10]. Electrospraying may thus prove to be superior to traditional techniques for loading of proteins, sensitive to denaturation. This is further discussed in section 4.5 and 4.6.

As far as small molecules are concerned, various drugs have been loaded in electrosprayed particles, finding applications in the fields of inhalation therapies, antibiotic delivery, cancer treatments and hormonal treatments. In inhalation therapies, the control and monodispersity of particle sizes obtained with electrospraying allow for more efficient administration of drugs by a reduction of the required dose and higher drug availability for treatment. The major drugs that have been utilized to date by direct electrospraying of the drug solutions or by encapsulation in PLA particles, are beclomethasone dipropionate (BDP) [35-36] and salbutamol-sulfate (SS) [36], which is delivered through a bronchodilatator and is commercially known as ventolin. These small molecules (both less than 1 kg/mol) are used in the treatment of asthma and other chronic obstructive lung diseases and need to be inhaled for direct effect on bronchial smooth muscle [35]. BDP and SS have very different properties; for one they are hydrophobic and hydrophilic, respectively. For this reason electrospraying represents a superior alternative to traditional techniques since it does not require for the experimental parameters or setup to be changed, being renowned as a method suited to molecules that do not process well (such as those with different solubilities) [36]. Methylparahydroxybenzoate (MPHB) is a model drug that can be used for mimicking BDP and it has been demonstrated that the electrospraying of both drug solutions were similar, validating its use as a model molecule [35].

Antibiotics have also been encapsulated in electrosprayed particles, such as rifampicin, an anti-tuberculosis drug, [24] and ampicillin [23] which function to treat bacterial infections (Fig. 6). Similarly to inhalation drugs, ampicillin and rifampicin have a small molecular mass of 350 g/mol and 823 g/mol, respectively, an important contrast with the mass of polymer chains used in electrospraying, ranging up to hundreds of kg/mol.

Anti-cancer drugs remain the most frequently tested drugs in electrospraying. Encaspulated anti-cancer drugs include cisplatin [34], paclitaxel (sold commercially as Taxol®) [25-32, 63], a hydrophobic molecule, suramin [30, 63], and doxorubicin [22, 33, 71], both hydrophilic and shown in Fig. 6. In cancer therapies, multiple and temporal drug delivery is generally required for treatment. However, previous methods to obtain double-walled microspheres such as the oil-in-oil-in-water (o/o/w) emulsion require several hours of

rapid stirring to create an emulsion, which is detrimental to the drug, limiting loading, with possible degradation issues and difficulties in controlling the drug distribution [30]. Coaxial electrospraying is thus advantageous in this instance since it allows: encapsulation of different types of drugs in different compartments in one single step; encapsulation of both hydrophobic and hydrophilic drugs; and tailoring of release (sequential or coupled) with the tailoring of electrospraying parameters and physical disposition of drugs within the core and shell [30, 63].

Less commonly in the field of hormonal treatments, sex hormones or drugs have also been encapsulated in electrosprayed particles. β-oestradiol, a contraceptive and hypocholesteraemic drug of low molecular weight (272 g/mol) was for instance encapsulated in PCL particles [40], while tamoxifen (371.5 g/mol), a drug that blocks the effects of oestrogen in breast tissue was encapsulated in lipid-based particles [41-42].

Miscellaneous drugs that have been encapsulated in electrosprayed particles include α-lipoic acid, an agent shown to be effective in treating various diseases (diabetes, atherogenesis) [57]. Anti-inflammatory drugs, such as celecoxib, budesonide and naproxen have also been encapsulated in chitosan, PCL, and PVP particles, respectively [37-39]. Celecoxib is widely used in the treatment of osteoarthritis but has undesirable properties such as high cohesiveness and low solubility. The use of electrospraying for encapsulating celecoxib in PLGA microparticles allowed an increase in celecoxib dissolution rate, which is desired to improve oral bioavailability [37].

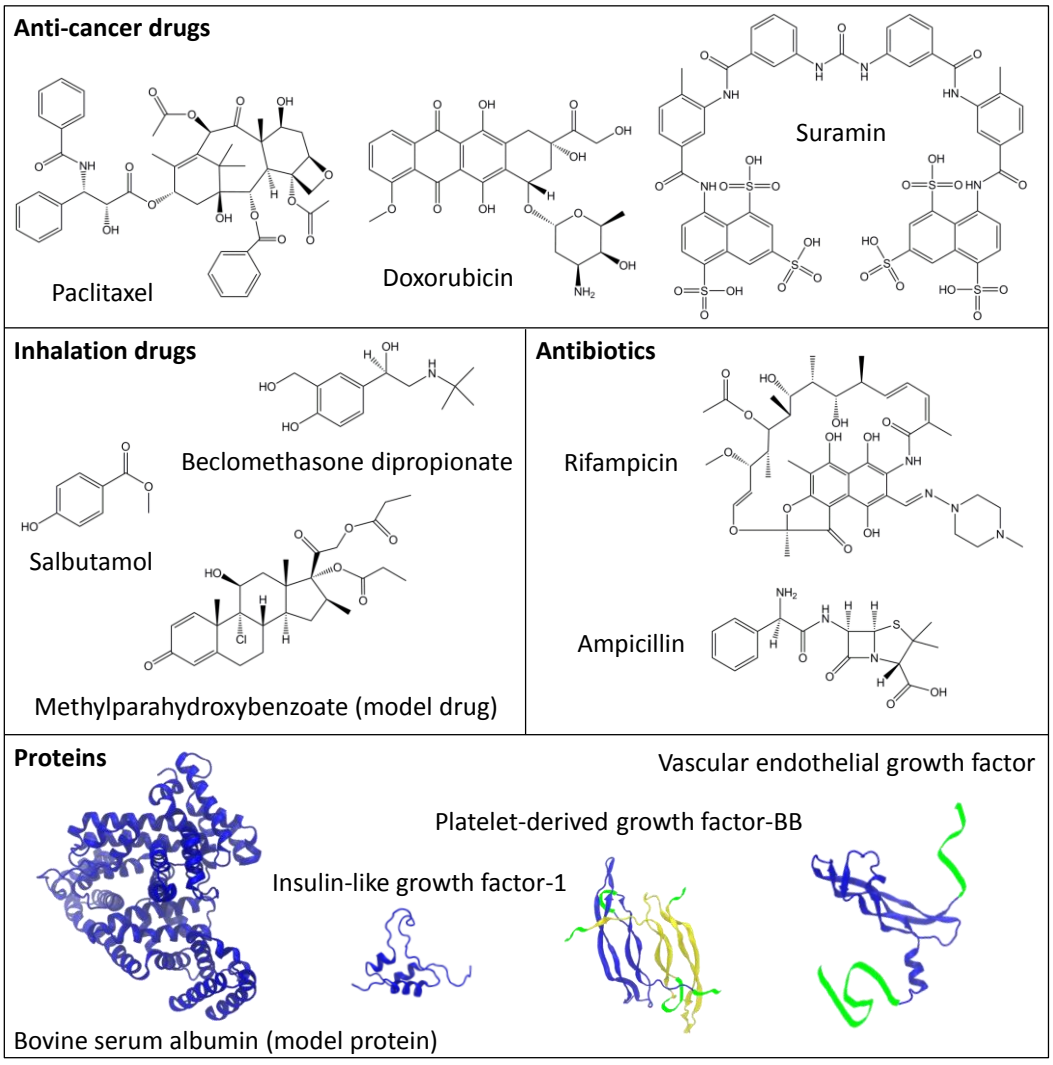

Fig. 6. Structures of some drugs and proteins which have been encapsulated in electrosprayed particles [94].

4.2. Loading and encapsulation

4.2.1. Definitions and methods

Electrospraying is an encapsulation process in which efficiency is measured by the traditional encapsulation efficiency (EE) and loading capacity (LC) parameters commonly used in the field. Encapsulation efficiency represents the weight of biomolecules effectively loaded in particles (w_{Loaded}) with respect to the initial weight of biomolecules available (w_{Total}) (Equation (9)). Loading capacity is the weight of biomolecules effectively loaded in particles (w_{Loaded}) as a fraction of the total weight of particles ($w_{Particles}$) (Equation (10)):

$$\mathrm{EE} = \frac{w_{Loaded}}{w_{Total}} \qquad (9)$$

$$\mathrm{LC} = \frac{w_{Loaded}}{w_{Particles}} \qquad (10)$$

Extraction is the most commonly used process to determine these parameters. Briefly, particles are dissolved in an organic solvent, usually identical to that used to initially solubilize the polymer, followed by the addition of an aqueous solution. The mixture is vortexed to extract the encapsulated biomolecule to the aqueous phase, eventually followed by centrifugation to separate the oil and water phases. The aqueous phase is then collected and analyzed. In some cases, organic solvent is left to evaporate before addition of the aqueous phase [27, 29, 31]. Since most studies encapsulate BSA, the standard assay for concentration determination is the micro-bicinchoninic acid (µ-BCA) protein assay [31, 43, 51], and sometimes the Bradford assay [52]. When small molecules containing chromophores or large quantities of protein are loaded, high-performance liquid chromatography (HPLC) [25, 27, 30-31, 63] and UV spectrophotometer [36] have been used. In all cases, calibration curves (produced by serial dilutions of the biomolecule in question) allow the quantification of encapsulated contents.

From the literature, it appears that most studies only undertake one extraction, with the exception of Nie *et al.*'s study where a total of three extraction cycles were performed for suramin recovery [30]. Doing only one extraction is quite restrictive considering that $E(\%)=100D/(1+D)$, where E is the amount extracted and D is the distribution coefficient. BSA is likely to have a relatively high distribution coefficient into aqueous solutions and may give high extraction values with only one cycle, however for biomolecules that have a lower distribution coefficient, two or three extraction cycles are necessary to maximize recovery. In general terms, two or three smaller extractions are always more efficient than one large one [95].

The choice of solvent for extraction is paramount to success. DCM is widely used for general extractions and extractions of loaded electrosprayed particles. DCM is an excellent choice for extraction: it is immiscible with water and is more dense and volatile, allowing an easy removal by evaporation if required. Its drawback is that being a chlorinated solvent, like chloroform, DCM has a greater tendency to form emulsions than non-chlorinated solvents [95]. This might be an issue for full recovery of biomolecules.

A final important consideration with the extraction process is that it does not represent the amount of biomolecules effectively encapsulated/loaded in particles but comprises also non-encapsulated molecules which may be simply adsorbed on the surface, (which are responsible for the initial burst release often seen with such systems). This is an issue since very high EE

are reported in the literature but there is rarely sufficient description of quantification of adsorbed/encapsulated molecules. Some quantification was attempted in a study from Ding *et al.*, where the particles received an ultrasonic treatment after dispersion in water, followed by freeze-drying. The EE of particles from this batch was reduced over 18%, corresponding to the loss of adsorbed molecules on the surface of particles, readily dissolved in water during the treatment [31]. Some EE/LC numbers are therefore to be considered with caution if measured by the extraction method, as they are not representative of the real amount of encapsulated/loaded molecules; this is a real shortfall in most studies.

Interestingly, the determination of EE and LC is also presented via a "non-entrapped" method proposed by Xu *et al.* [44-45]. Particles were centrifuged at 20,000 g at 15°C for 30 min and the amount of free molecule (BSA in this case) was determined in clear supernatant by UV spectrophotometry at 280 nm using the supernatant of non-loaded particles as a basic correction. LC and EE were calculated according to Equations (11) and (12):

$$LC = \frac{A-B}{A} \times 100 \qquad (11)$$

$$EE = \frac{A-B}{C} \times 100 \qquad (12)$$

where A is the total amount of BSA, B is the free amount of BSA and C is the particles weight. A variant of this technique was used by Arya *et al.* (10,000 g at 12°C for 10 min) [23] and Enayati *et al.* (β-oestradiol, 4300 rpm at room T for 45 min) [40]. This method does not necessarily take into account losses during particle preparation.

4.2.2. Influence of parameters on loading and encapsulation

In traditional encapsulation processes, EE and LC are typically affected by the processing parameters, including particle formation temperature. For example EE in double emulsion procedures is dependent on the balance between solvent evaporation rate and immiscibility between water and particle, rate of polymer precipitation and thus hardening rate of the sphere wall [2]. In electrospraying, similar variables such as the nature of the polymer, protein/polymer weight ratio, along with flow rates for instance, are parameters influencing EE and LC, and will be presented hereafter.

4.2.2.1. Loading capacities

High loading capacities are always desirable for an increased availability of the therapeutic molecule in targeted areas with minimal use of carrier materials. Nevertheless, this can induce possible changes of particle morphology that occur with increased loading, and thus possible alteration of release profiles. In a study from Hong *et al.*, it was proven that an increase in the loading capacity led to a loss of sphericity of microparticles [24] which in turn affected the release profiles. The scaling laws of electrospraying were nevertheless verified with almost no theoretical variation from non-loaded to loaded particles. The authors stipulated that the shrinkage and drying processes were responsible for such variation of morphology. Actual loading capacities in electrospraying have also been shown to be slightly decreased compared to theoretical loadings. For instance a loss of 20% was seen when loading paclitaxel in PCL and PLGA microspheres [27]. Loadings also affect burst release with a higher loading leading to a higher burst release. This was observed for PLGA microparticles when a loading from 10 to 20% of paclitaxel almost doubled the burst release for 15 µm-particles [26], and a loading from 10 to 50% of celecoxib increased the burst release from 39 to 54% [37] for 2-4 µm-particles.

In terms of parameters affecting the loading capacity, an increase in protein/polymer weight ratio dramatically decreased the loading capacity in the case of emulsions of BSA in PLA solution [45], while it increased for solid dispersion of BSA in chitosan solution [44]. In the case of coaxial electrospraying, drug loading could be increased by increasing inner protein aqueous solution flow rate or increasing inner protein concentration [51].

4.2.2.2. Encapsulation efficiencies

Electrospraying is known as a technique which can give high encapsulation efficiencies (EE), and indeed has been shown to reach 100% EE for doxorubicin and rhodamine-loaded PLGA particles [22]. Electrospraying also presents the great benefit that encapsulation of both types of drugs, hydrophilic and hydrophobic, are efficiently obtained compared to traditional methods [22, 36], mainly since there is no need of an emulsion step. In emulsion-based methods, the presence of both aqueous and organic phases may indeed lead to preferential diffusion of the drug to one phase or the other according to their hydrophilicity/hydrophobicity characteristics and thus reducing final EE. This is avoided with electrospraying where emulsions are not required.

EE depends case by case on the combination of drug/solvent/polymer selection, where the hydrophilic nature of these components plays an important role. This may be illustrated by considering the nature of the polymer itself, for example the encapsulation of BSA in a more hydrophobic polymer such as PCL has led to 28% EE compared to 40% for PLGA microparticles electrosprayed in the same conditions [43]. The use of hydrophilic additives should also be considered and it has been shown that Pluronic F-127, a highly hydrophilic copolymer used as a surfactant, increased encapsulations efficiencies from 53.4% to 76.7% by using 5% and 10% of Pluronic respectively in PLGA microparticles loaded with BSA, by enhancing the w/o emulsion stability. It was further stated that the use of a probe sonication to form the emulsion could enhance the EE [43].

An increase in loading generally leads to a decrease in EE, as seen in electrosprayed PLGA films loaded with paclitaxel, where a 5, 10, 15 and 30% loading respectively led to 80, 71.9, 66.4 and 63% encapsulation efficiency [29]. This was attributed to the partition coefficient, referring to the equilibrium solubility of the drug in the polymer against the equilibrium solubility of the drug in the solvent and responsible for diffusion of the drug into the polymer phase. With paclitaxel being more hydrophobic and soluble in organic solvents, increasing the loading could have led to preferential diffusion into the solvent, and thus reduced the encapsulation efficiency [29]. In a study from Xie *et al.*, for similar polymer solutions and spraying conditions, an increase of paclitaxel loading from 8% to 16% slightly decreased EE from 82% to 78% [27] in PLGA microparticles. This was also shown for PLA microparticles encapsulating BSA where EE decreased with increasing BSA/PLA ratio and increased with organic/aqueous phase ratio. This latter may be explained by an increase in viscosity when increasing the organic/aqueous phase ratio, leading to better encapsulation [45]. Furthermore, a strong correlation was found between BSA/PLA weight ratio and organic/aqueous phase ratio with respect to encapsulation efficiencies. Size affects encapsulation efficiencies as well, where smaller particle sizes lower the EE [36].

In the case of coaxial electrospraying, higher EE in both core and shell can be obtained by encapsulating hydrophobic drugs in the core and hydrophilic drugs in the shell [30]. In monoaxial electrospraying, similar EE were found for hydrophobic and hydrophilic drugs (54% BDP and 56% SS, respectively) in PLA nanoparticles, demonstrating the versatility of the technique. Loss of drugs can, however, be an issue in electrospraying, mainly caused by spreading of the particles to the receiving vessel walls and other manufacturing equipment. This was measured as 20% for SS-loaded PLA nanoparticles sprayed in ethanol. When electrospraying in a cross-linking solution however, an increase in the concentration of the cross-linking agent (10% against 5%) led to a significant increase in encapsulation efficiency

of BSA [44]. This was due to an increased intermolecular interaction of the polymer and cross-linking agent when increasing their respective concentrations, inhibiting the loss of BSA into the collection solution and improving EE. When gelation was incomplete, as seen for higher flow rates, more BSA was lost in the collection solution [44].

4.3. Molecule dispersion

Controlled dispersion of the drug within the polymer matrix is of upmost importance for consistent release. It was previously stated that drug concentration in a particle matrix tends to decline as we move outwards from the centre with the increase of the particle diameter as seen in rifampicin-loaded particles [24]. This is explained by the diffusion mechanism of solutes, stating that an increase in the droplet size provides a longer distance and time for diffusion of solutes, leading to a drug gradient within the particle.

An electrosprayed droplet of polymer contains macromolecules which move and diffuse during solvent evaporation, providing the final polymer network. The level of intermolecular entanglement among macromolecules dictates these parameters, affecting the diffusion rate of macromolecules towards the center. When adding small molecules like drugs to this system, they generally diffuse easily towards the droplet center due to the absence of intermolecular action. However the intermolecular entanglement of polymer macromolecules is weakened, leading to a decrease in the diffusion coefficient of solutes expressed by the Stokes-Einstein Equation (13):

$$D = \frac{k_B T}{6\pi\eta R_H} \qquad (13)$$

where k_B is the Boltzman's constant, η the viscosity of solvent, T the temperature, and R_H the hydrodynamic radius of solutes [24]. Therefore by increasing the concentration of small solutes in a polymer droplet composed of big macromolecules, the diffusion coefficient decreases. Above a critical concentration value, the diffusion of solutes becomes slower than solvent evaporation and the small molecules are trapped on the surface of the droplet, leading to a molecule saturated layer of semi-solidified skin [24, 32]. Such a configuration is not ideal for the physical and release properties of particles, since with further evaporation of the droplet, the skin moves towards the droplet center, leading to particle collapse and a final wrinkled morphology, which does not lend itself to sustained and reproducible release properties. This critical concentration value was found to be 30% w/v in the case of rifampicin in a PLGA/chloroform system and led to the loss of particle sphericity and subsequent increased burst release compared to the sustained release from spherical particles obtained with 10% w/v loading of rifampicin [24].

Ideal and homogeneous molecule dispersion, which is preferable for sustained release, is therefore obtained for low loadings, smaller particle size (which limits the drug gradient effect) and a good balance between the diffusion and evaporation mechanisms. If high loadings are needed, it is important to control diffusion and ensure that it does not become lower than evaporation. This can be balanced by using a slow evaporating solvent (such as DMF).

A few techniques have been used to assess the integration of drugs within the polymer matrix of electrosprayed particles, although they do not allow for physical visualization of drugs within the droplets (although confocal laser scanning microscopy may be used to look at fluorescently-labeled drugs). Differential scanning calorimetry (DSC) relies on the fact that if a drug is well dispersed in the polymer matrix, the melting transition of the drug will be suppressed either partially or completely [31]. This theory was used for Taxol®-loaded PCL

particles where only a slight heat flow peak of Taxol® was observed in the physical mixture of PCL and Taxol® [31]. The authors concluded that the drug was well-dispersed within the matrix. The same theory was used for paclitaxel-loaded PLGA and PCL microparticles where no peak at all was seen in the 150-250°C temperature range, while paclitaxel normally has an endothermic peak of melting at 223°C [27]. From this result, the authors stated that the paclitaxel was in an amorphous or disordered-crystalline phase of a molecular dispersion or a solid solution state in the polymer matrix. The same conclusion was made for hydrogel beads encapsulating paclitaxel-loaded PLGA microspheres [25]. This was further seen in electrosprayed PLGA films loaded with the same drug [29]. The authors even annealed their samples for 3 days at 60°C to facilitate a higher diffusion rate for dispersed drug molecules, but still no crystalline peak of paclitaxel was observed for annealed samples, leading to the conclusion that the drug was in a solid solution state within the matrix, as compared to a metastable molecular dispersion [29]. A similar theory was used for BDP and SS-loaded PLA nanoparticles where no melting peak at all was seen for BDP-loaded particles and only a smaller and broader peak was seen in SS-loaded particles [36]. The crystallinity of PLA was changed in the presence of both drugs, namely higher when SS was encapsulated and lower when BDP was encapsulated. This was tentatively explained by the presence of water, since SS was emulsified before electrospraying, thus reducing evaporation rate, allowing for more polymer diffusion and chains re-arrangement, and was thus responsible for the higher value for crystallinity [36]. The crystallinity of all materials (BDP, SS and PLA) in the nanoparticle formulations were decreased although the crystalline intensities were distributed as 80% for BDP and 20% for PLA, or 54% for SS and 46% for PLA. Importantly, no new peaks were seen in the DSC profiles, indicating no strong physical or chemical interactions were present between the drugs and polymer. A similar result was observed for celecoxib-loaded PLGA microparticles, where the melting endotherms of celecoxib shifted down or disappeared according to decreased drug content, suggesting that the drug was molecularly dispersed within the PLGA matrix [37]. The disappearance of the Tamoxifen peak for loaded PAA-Cholesterol nanoparticles suggested the same result [42].

X-ray diffractometry (XRD) may also be used for determining the physical state of a drug within polymeric matrices since characteristics of the peaks mark the degree of crystallization of the drug with the matrix. XRD previously showed that paclitaxel was in an amorphous form in the PLGA matrix, even for up to 30% drug loading, since no peak was seen in the expected range of temperature (200-250°C) when analyzing the polymeric matrix [29].

Analysis of surface chemistry by X-ray photoelectron spectroscopy (XPS) can also give information regarding the distribution of drugs within microparticles, by examining the C, N and O element compositions. This technique has been used to show that paclitaxel was present on the surface layer of PLGA microparticles (with up to 0.8% atomic mass concentration), a phenomena which is argued to be responsible for the initial burst release seen in the *in vitro* release study [27]. XPS showed that the amount of nitrogen increased with increasing paclitaxel contents (0-30% loading) in electrosprayed PLGA films, attesting of the presence of the drug.

Confocal laser scanning microscopy (CLSM) is another way of qualitatively looking at fluorescently labeled biomolecules encapsulated within particles. This method allows for screening of cross-sections of a loaded particle through the entire particle, for further 3D reconstruction. This powerful tool proves to be very useful for visualizing in 3D the biomolecule distribution inside the particles after production, and studying the mechanisms of release from particles. CLSM has been used successfully for other fabrication methods such as spray-drying [96], however it has yet to be extensively utilized for visualization purposes with electrosprayed particles [22], although it would be very valuable, especially in combination with the aforementioned analysis techniques for a more thorough characterization of molecule dispersion.

4.4. Release kinetics

Polymeric microparticles for controlled drug delivery have been extensively studied in the last 50 years and various reviews detail their preparation, the factors affecting the release and the current difficulties faced during processes [1-2, 4, 10, 97]. Most of these reviews encompass microparticles made from traditional fabrication techniques and limited information is available on release kinetics from electrosprayed particles.

In general terms, release occurs through two different mechanisms: passive diffusion and polymer degradation. Ideally a controlled release system would show a zero-order release profile, meaning a constant release rate over time. However the release profile from particles is usually split in two distinct processes:

1. The initial burst release of molecules contained on and in the surface of the particle due to the leaching occurring at the outer wall of the particle as it becomes hydrated [2].
2. The slower and more constant release of molecule from the inner part of the particle.

Release profiles can be affected by physical and chemical factors: the nature of the polymer (molecular weight, blending, crystallinity), the nature of the loaded molecule, its distribution and activity, the morphology of microspheres, their porosity and size distribution [1-2]. In electrospraying, similar parameters are able to tailor release kinetics and they are discussed in the next section. Table 2 illustrates various electrospraying studies with the release profiles and corresponding morphologies.

Table 2. Drug loading and release characteristics of electrosprayed particles loaded with various bioactive molecules. *Adapted from [22-24, 27, 31, 37, 40, 43, 45, 51] with permission. 2006, 2008, 2005, 2011 Elsevier Science Ltd. [22, 24, 27, 31, 37, 45, 51]; 2007, 2009 John Wiley and Sons [23, 43]; 2010 Royal Society [40].*

Ref.	Polymer	Molecule	LC	EE	Size (μm)	Morphology	Cumulative release profiles (%) (y axis)
[45]	PLA	BSA	74-91%	23-81%	0.8-4	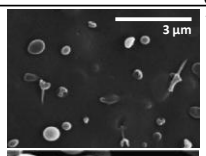	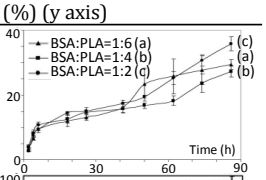
[43]	PLGA 50:50	BSA	-	20-77%	20-22	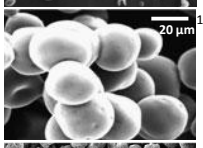	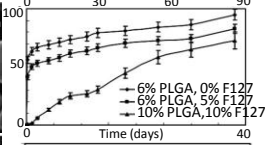
[51]	PLGA 75:25	BSA Lysozyme	0.3-0.8%	-	0.8-10	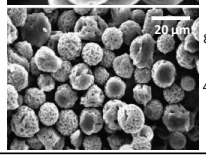	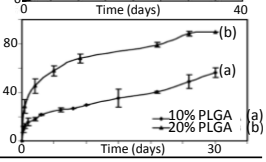
[31]	PCL	Paclitaxel	1-2%	77-98%	7-11	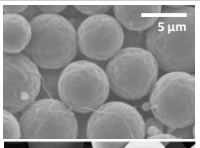	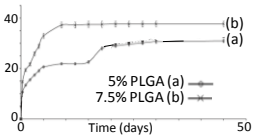
[27]	PLGA 50:50 PCL	Paclitaxel	8-16%	78-84%	11-15	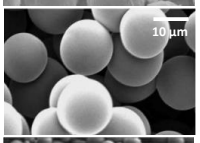	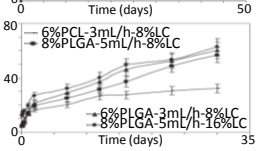
[22]	PVA coated PLGA 50:50	Rhodamine Doxorubicin	0.05%	4-100%	0.6-1.3	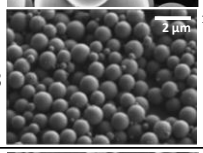	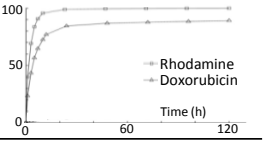
[23]	Chitosan	Ampicillin	50%	80%	0.5	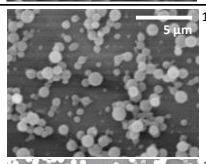	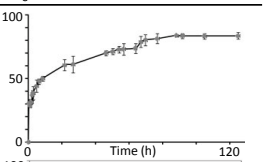
[24]	PLGA 80:20	Rifampicin	10-30%	-	3-7	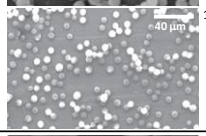	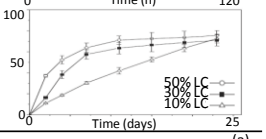
[37]	PLGA 50:50	Celecoxib	10-50%	-	2-4	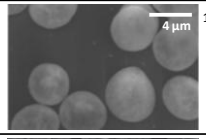	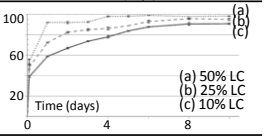
[40]	PCL	β-oestradiol	15%	85-89%	0.3-5	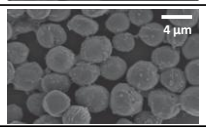	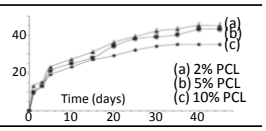

Size

The size of particles which encapsulate bioactive molecules is paramount in tailoring release profiles. A larger surface area to volume ratio (smaller particles) leads to faster release since particles are more easily penetrated by fluids, favoring easier diffusion of drugs and faster degradation of the polymer matrix. However, it is important to emphasize that it is not size itself that controls the release profiles but it has more to do with the polymer/drug/solvent selection and processing parameters that are used in each case, as explained in section 3.2.2. Therefore size is a result of other variables which have an inter-dependent effect and need to be appropriately correlated to truly control release kinetics.

In a study by Enayati *et al.* for instance, β-oestradiol-loaded PCL particles had similar release pattern for mean sizes of 0.34, 0.8 and 4.6 μm, however release was 45, 42 and 36%,

respectively, after 45 days, thus showing a reduced release for increasing particle size [40]. This increase in size was actually due to an increase in polymer content (2, 5 and 10%, respectively), showing that polymer concentration do indeed provide bigger particle sizes but may also provide reduced release rates at the same time. In this study, due to the nature of the polymer (PCL) where degradation is unlikely to have occurred over a seven-week period, the release was due to diffusion of β-oestradiol from the particles, proving that drugs loaded in smaller particles comprising less polymeric bulk material are prone to better diffusion outside the polymeric matrix and thus enhanced release [40]. However, burst release is also more likely to happen from smaller particles. This was observed for paclitaxel-loaded PCL particles where two formulations with similar sizes (9.45 and 9.52 µm) showed a similar release pattern and amount released, while a slight decrease in size to 8.68 µm gave the same release pattern but with a higher burst at the beginning (11% compared to 7% burst within a day). This was again attributed to a higher polymer concentration (5% PCL in DCM for the smaller size and 7.5% for the larger size) which influenced the final size, where larger particles had a denser polymer matrix and thus a reduced rate of diffusion, in turn reducing the initial burst release [31]. When working with smaller concentrations, size is less affected although release profiles can still show great differences. For instance for an increase in chitosan concentration from 1 to 2%, size was slightly higher, but not significantly (7.48 and 8.11 µm, respectively), while a higher burst was observed for the reduced concentration (7 and 2% after 4 days) leading to a final cumulative release of 33% and 21% for the 1% and 2% concentration formulations, respectively. Although an increase in polymer concentration is generally shown to increase size and decrease release rates/burst release at high concentrations, the contrary is seen for loadings. An increase in loading is generally responsible for increased sizes too, but generates faster release rates and burst, especially on the submicron scale [44]. This can be seen for doxorubicin-loaded chitosan nanoparticles for example, where an increase in loading from 0.25 to 1% doxorubicin increased the resultant particle size from 527.3 to 873 nm and led to 40% burst release within 3 hours while only a 20% burst release was observed for the smaller sizes [71]. For microparticles, however, size is less affected by loading although release is affected. For instance, in paclitaxel-loaded PCL particles, when loading was increased from 7.9 to 15.8%, the resultant size was very similar (15.2 and 15.2 µm, respectively) although burst release was 10 and 20% after 1 day, and the final cumulative release reached 57 and 62%, respectively [27].

In the case of emulsions, the organic/aqueous phase factor has little effect on release profiles although size is significantly affected, as a consequence from decreased conductivity with increased organic phase, and thus increased size, as explained in section 3.2.2. This was seen for BSA-loaded PLA particles where at a constant ratio of 1:4 BSA/PLA, but increased organic/aqueous phase ratio ranging from 6.7:1 to 20:1, size increased from 0.8 to 1.9 µm but showed similar release pattern and amount released [45].

Another significant factor affecting release kinetics is the degree of agglomeration of the particles. The burst release process is mainly diffusion-driven while the second process providing a slower release is erosion-driven. It was shown by Almería *et al.* that the burst release stage was greatly affected by particle agglomeration and particle size, whereas the slower release part was much less dependent on particle size [22]. Agglomeration however was shown to affects release kinetics for hydrophilic biomolecules, since sizes of particle clusters result in orders of magnitude larger than individual particles. This aggregation compromises the reproducibility of release profiles and provides less cumulative release than dispersed particles (Rhodamine B from PLGA electrosprayed particles) [22]. Coating techniques may thus be used for preventing aggregation when electrospraying in solution and enables tight control over particle size.

Morphology

Along with size distribution, morphology is another major contributor for controlling drug release behavior and like size, morphology is directed by the polymer/drug/solvent selection and processing parameters [31]. It was indeed shown that wrinkled particles led to a burst release of 50% of cumulative release of BSA form PLGA particles in the first day, which was not seen for spherical particles with the same size distribution (21 µm average diameter, 2 µm SD) [43]. This is a direct consequence of lower polymer concentration used in wrinkled particles (6%) compared to dense and spherical particles made of 10% PLGA. More pores were found in wrinkled particles allowing for molecule adsorption instead of encapsulation. Water penetration is more accessible in porous particles and leads to the rapid diffusion of adsorbed molecules, responsible for the high burst release. In denser particles, the rate of water penetration is reduced, allowing for desirable zero-order release kinetics.

Similarly to polymer concentration, molecular weight (MW) is another important factor for tailoring particles and their release profiles, since both parameters direct the viscosity of solutions. This was illustrated with PLGA capsules containing IGF-1, made of low (5-15 kDa) and high MW (40-75 kDa) [47]. The release profiles were similar, triphasic in nature, but with an initial burst which was more prevalent for the low MW formulation, for same PLGA concentration and IGF-1 loading. The burst was 5.5% compared to 7% and led to a final cumulative release of 10 and 12% for high and low MW formulations, respectively. The morphology of high MW particles was spherical while the low MW particles displayed an irregular morphology. This was a consequence of weaker chain interactions in the low MW PLGA where packing of polymer chains was looser than that of high MW PLGA, which allowed the encapsulated IGF-1 to diffuse through the polymer more easily [47].

The solvent is another means to control particle morphology, due to different evaporation rates that lead to more or less porous structures respectively. This will ultimately condition the release kinetics as well, as seen with PLGA particles containing doxorubicin, electrosprayed from a 2,2,2-trifluoroethanol (TFE) solution and TFE-dimethyl sulfoxide (DMSO) mixture (vapor pressures at room temperature of TFE and DMSO are 0.08 kPa and 10.09 kPa respectively). As expected, PLGA particles electrosprayed from TFE were more porous than the ones from TFE-DMSO, leading to 77% compared to 52% of drug released by diffusion (burst), respectively [22].

Nature of polymer

It is accepted that degradation of polymeric particles initially occurs in amorphous regions, followed by a slower degradation of the crystalline regions of particles [2]. Freiberg *et al.* stated that low crystallinity allows better drug dispersion and increased drug-polymer interactions while the degree of crystallinity is also influenced by the drug loading and the concentration and removal rate of organic solvent [2]. Therefore, the use of polymers with highly crystalline structures such as PCL enables the production of microparticles with uniform and reproducible physical characteristics [59], but might be inadequate for optimal drug dispersion and release characteristics. For instance, in a study from Ding *et al.*, the cumulative release of Taxol® from electrosprayed PCL particles (65k) did not exceed 37% of the total amount of encapsulated Taxol® after 10 days of release (tested up to 50 days), suggesting that a high percentage of drug aggregated after contact with the polymer [31]. In a similar fashion, a study by Xie *et al.* showed that PCL microparticles loaded with 8.1% paclitaxel were able to release only 32% of this load after 30 days of *in vitro* incubation while PLGA microparticles loaded with the same amounts and electrosprayed with the same conditions reached 60% of cumulative release [27]. Regions of high crystallinity and aggregated protein may likely contribute to the incomplete release of the protein [67].

Responsive polymers such as elastin-like polypeptides can also release biomolecules, such as doxorubicin, according to pH variation. However in all cases (pH: 2.5, 5.5 and 7.5), all

systems suffered from burst release were maximum release was achieved after 15 min only, and therefore they did not provide sustained release [33].

Nature of drug

Interactions between loaded molecules and polymers direct the location of molecules within the polymer matrix (either encapsulated in the core or adsorbed on the surface of the particle) and affect the kinetics of release [36]. In the case of coaxial electrospraying for loading of multiple drugs within microcapsules, it was shown that the nature of the drugs and their location within the microcapsules affected the release patterns: loading of hydrophilic drug in the shell and hydrophobic drug in the core provided a sequential release, while the opposite led to the drugs being released in parallel [30].

The physicochemical affinity of the drug with the polymer system has a great influence on release kinetics. For similar size distributions and loadings, dramatic differences can be observed when varying the hydrophilicity/hydrophobicity of the drug encapsulated. For instance when rhodamine B (RHO_B) and rhodamine B octadecyl ester perchlorate (RHO_{BOEP}) were used as hydrophilic and hydrophobic drug surrogates respectively, 98% of RHO_B was released within 1 day, while only 6% of total RHO_{BOEP} was released after 5 days. This was explained by the strong affinity of RHO_{BOEP} with PLGA, preventing any initial burst release (RHO_B and RHO_{BOEP} have octanol/water partition coefficients such that log K_{OW} = 1.48 and 8-9 respectively). When compared with doxorubicin (DOX) (log K_{OW} = 1.85), an intermediate behavior was observed where 60% of the drug was released in the first 24h and further 20% was released after 5 days. This was attributed to the different partition coefficients of the two substances within PLGA [22]. The release of RHO_B will occur rapidly by diffusion of molecules inside the polymer matrix while DOX - having a greater partition coefficient within PLGA - remains entrapped longer in the hydrophobic porous regions of the matrix.

Additives

The use of additives can greatly affect the release kinetics, such as the use of polyethylene glycol (PEG), commonly used in traditional encapsulation processes. Due to its hydrophilicity, PEG increases the degradation rate of the main polymer matrix by rendering the overall polymer network more hydrophilic, increasing swelling and thus accelerating release [98].

In co-axial electrospinning, for instance, an aqueous PDGF solution was encapsulated in a blend of PCL:PEG nanofibers [99]. PEG acted as a porogen and PDGF release reached 100% in 35 days with a relatively linear release profile, while less than 1% of PDGF was released from the PCL nanofibers with no PEG in the shell. The rate of protein release was shown to be controlled by the molecular weight and concentration of PEG [99]. Johnson *et al.* showed that the amount of PEG co-lyophilized with PLGA before encapsulation in discs was the dominating factor in the rate of nerve growth factor (NGF), allowing modulation of the release [100]. Nevertheless, for particle fabrication methods based on emulsions, the efficiency of PEG was mainly observed when the therapeutic molecules were lyophilized with PEG before emulsion. When adding PEG directly in the polymer solution instead, encapsulation efficiencies and/or release amounts have been shown to be reduced. For instance, the encapsulation efficiency of transforming growth factors beta 1 (TGF-β1) in PLGA microspheres was reduced from 83% to 54% for PEG contents of 0 and 5%, respectively, and also showed a decreased cumulative mass of released GFs [101]. In another study intended to incorporate brain-derived neurotrophic factor (BDNF) in microparticles, a blend of PLGA:PEG was compared to a blend of PLGA:PLGA-poly(ε-carbobenzoxy-L-lysine)(PLL)-PEG. The final cumulative release showed a 7-fold increase for the second blend, showing the potential of PEG used in a copolymer compared to a blend [92].

These results may serve as a useful guide for the use of PEG in electrosprayed particles and tailoring of release kinetics.

Loading/EE/in vitro release and processing parameters

In electrospraying, the drug/matrix ratio and organic/aqueous phase ratio affect EE, LC and *in vitro* release in different fashions as shown in a study encapsulating BSA in a PLA matrix [45] and summarized in Table 3. As mentioned before, EE decreased with increasing BSA/PLA ratio and increased with organic/aqueous phase ratio. However opposite results were observed for *in vitro* release where: release was reduced with increasing organic/aqueous phase ratio and was enhanced by the increase in the BSA/PLA ratio. In the same study it was shown that increasing BSA/PLA ratio dramatically decreased the BSA loading [45]. These results show how complex the optimization of parameters can be, especially in the case of emulsions. Nevertheless the study summarized in Table 3 represents only one case and may not be true for every polymer/drug/solvent selection.

High drug contents are generally responsible for faster release rates [44]. For higher drug loadings, initial rate of drug release increases as seen for 30 and 50% loading of rifampicin in PLGA-loaded particles while a 10% loading provided zero-order release profile. It was stated that the drug concentration affects the drug distribution in the particle matrix, with a gradual increasing gradient of concentration present from the centre of the particle towards the surface, which was proportional to the drug concentration [24]. In the case of microcapsules of PLGA containing an aqueous solution of BSA obtained by coaxial electrospraying, a 0.5% loading indeed led to an increased burst release (almost double) as compared to the 0.3% loading, although the release rates were identical once passed the burst release [51]. A similar result was observed for paclitaxel-loaded PLGA microparticles where 10 and 20%-loaded particles showed similar release kinetics, with only a higher initial burst release over the first 2 days for the 20% formulation, followed by identical sustained release kinetics from both formulations for the remaining 28 days [26]. By increasing the drug content in a similar matrix type, a higher amount of porosity is created in the matrix, thus the drug diffuses more easily through though the matrix, generating an increased burst release [37].

Table 3. Influence of organic/aqueous phase ratio and protein/polymer phase ratio on various parameters. Protein was BSA, polymer was PLA 175 kDa. Ratios of organic/aqueous phase ranged from 6.7:1 to 20:1 (v/v). Ratios of protein/polymer ranged from 1:2 to 1:6 (w/w). ↑ = increase, ↓ = decrease. *Particle size was shown to initially increase and then decrease in the studied range [45].

	Viscosity	Electrical conductivity	Particle size	Loading capacity	Encapsulation efficiency	*In vitro* release
↑ Organic/aqueous phase	↑	↓	↑	↑	↑	↓
↑ Protein/polymer phase	↑	Little effect	↑↓*	↓	↓	↑

Matrix use

When loading electrosprayed particles into a matrix such as hydrogels, different release kinetics may be obtained by varying the gelation time, the concentration of the cross-linking agent and particle loading. For example, paclitaxel-loaded PLGA microspheres (12 µm average size) loaded in alginate macrobeads (1.61-1.68 mm average size) provided different release kinetics. Although the authors did not show the release profiles of non entrapped microspheres, most alginate formulations provided zero-order release kinetics of paclitaxel over 60 days reaching over 70% cumulative release for the best formulation (50% microsphere loading, 5 min gelation time and 1% $CaCl_2$) [25]. The small burst release (maximum of 10%) observed for the 50% microsphere-loaded formulations was reduced

when alginate beads were increasingly loaded to 80 and 90% of microspheres. However overall kinetics were also reduced reaching a maximum of 50% and 22% cumulative release after 60 days for 80 and 90% microsphere-loaded formulations respectively. The extent of cross-linking did not show a clear trend, since for the 50%-loaded formulation, extended cross-linking resulted in lower release profiles while the opposite was seen for the 80% formulation and it was not significantly different for the 90% formulation. This indicates that the microsphere loading in the matrix may be a more determinant factor in release kinetics than the extent of cross-linking [25].

4.5. Denaturation

Electrospraying remains a process that employs organic solvents and therefore the possibility of drug degradation and protein denaturation needs to be assessed and compared to traditional encapsulation techniques to prove its superiority. So far, limited studies have addressed this issue, nonetheless they present promising results. The techniques generally employed are sodium dodecyl sulphate-polyacrylamide gel electrophoresis (SDS-PAGE), Fourier transform infrared (FTIR), ultraviolet (UV), and circular dichroism (CD) spectroscopy [43, 51-52, 80].

In the early stages of denaturation assessment by electrospraying, the model protein BSA was directly electrosprayed from an ethanol solution. Structural changes were assessed by UV and CD spectroscopy showing that electrospraying of the protein did not result in significant structural changes of BSA, particularly at higher concentrations (up to 20 mg/mL) [80]. When encapsulating the same protein in PLGA microcapsules, no alteration in the secondary structure of BSA was observed as confirmed by comparing the CD spectra of BSA before and after release from polymeric microparticles [51]. In a study from Xie and Wang, the authors used SDS-PAGE to investigate the protein integrity of BSA released from PLGA (50:50) microparticles after 38 days and characterized the secondary nature of BSA by FTIR and CD spectroscopy. They found that the released BSA was almost identical to native BSA (after 1 day release) and no protein degradation was observed during the 38 days release [43].

Although promising progress has been made, more studies are required to assess a greater variety of molecules (drugs, growth factors, enzymes, DNA) in contact with various organic solvents, and various polymers, since the purity and source of molecule, and the nature of polymer can also influence the stability of loaded molecules. Besides, BSA remains a very stable protein which is unlikely to suffer from denaturation. Typically, protein denaturation is potentially a major problem in encapsulation processes involving organic solvents and it needs to be more thoroughly assessed for the electrospraying technique. So far, when therapeutically relevant proteins such as IGF-1, PDGF and VEGF were loaded in electrosprayed particles, authors discussed the bioactivity of the released proteins by performing cell-proliferation assays rather than using the typical assays for the assessment of protein degradation (SDS-PAGE, CD, etc.). Since in both studies the released proteins were shown to be bioactive, i.e. induced cell proliferation, the authors correlated their results with denaturation, concluding that the electrospraying technique was efficient in protecting the growth factors from denaturation [47-48]. This approach is a nice start to degradation assessment, showing that part of the released proteins was indeed intact; however it remains a qualitative assessment and does not conclude quantitatively on potential protein structural changes.

Traditionally, with emulsion techniques, additives such as surfactants, carrier proteins, sugars, salts, amino acids and polymers are considered to protect the loaded molecules [102]. Hydrophilic additives such as BSA as an excipient [103] and polyethylene glycol (PEG) [100, 104-105] have demonstrated good protection of growth factors in traditional emulsion techniques. However such use has not yet been seen in electrospraying since there is little

focus on denaturation of loaded proteins, where in most studies, loadings, encapsulation efficiencies and *in vitro* release profiles of electrosprayed particles remain the most discussed characteristics of these systems. This approach is not ideal when one considers that denatured proteins will ultimately not fulfill their intended function, despite whether they have proven to be ideally loaded, encapsulated or released. As discussed earlier, bioactivity assessment is an indirect way of assessing denaturation, although it does not provide thorough description of structure changes of proteins. Therefore, although the denaturation of protein drugs seem to be minimal through the electrospraying process, as seen with bioactivity assays, more extensive denaturation studies are required. To this end, the use of appropriate additives for the electrospraying technique may be identified to fight any potential degradation of molecules. To date, only Xie *et al.* have published the use of Pluronic F-127 as an additive to tailor and enhance the protection of BSA in PLGA electrosprayed particles [43].

Another potential disadvantage of electrospraying is the use of electric fields, since they intensify around the highly charged droplets in the course of solvent evaporation. Such high fields may induce conformational changes of the bioactive molecule, leading to denaturation and thus loss of bioactivity. It was indeed proven that electrospinning of collagen out of fluoroalcohols denatured collagen to gelatin due to the presence of high voltage [106]. Nevertheless, this hypothesis is counterbalanced in the literature by the fact that, in electrospraying, the droplet size is on the micro-to nano-scale, allowing for solvent evaporation to occur over milliseconds, which is considered too short to have significant effects on denaturation [16].

4.6. Bioactivity

The bioactivity of electrosprayed molecules was first assessed by electrospraying insulin from an acidic water-ethanol solution. Bioactivity was assessed by comparing the insulin receptor binding properties from electrospray-processed insulin and control insulin. No significant differences were observed and the authors further stated that the electrospraying technique was sufficiently 'gentle' not to hinder the insulin biological activity [16]. Progressing towards the bioactivity of molecules encapsulated within a polymeric matrix, several types of tests involving different cell lines are presented, according to the type of encapsulated molecule: protein, anti-cancer drug, anti-bacterial drug, antibiotic, etc.

The most commonly used model protein encapsulated in electrosprayed particles is BSA. However, BSA's bioactivity after encapsulation is rarely studied. Interestingly, in a study from Xie *et al.*, PLGA microparticles were used to encapsulate BSA, however lysozyme was used as the "model protein" to study the bioactivity of entrapped molecules, although BSA was the focus of all other characterizations in the paper [43]. The concentration of released lysozyme from lysozyme-loaded PLGA microparticles was quantified by characterizing the rate of lysis of *Micrococcus lysodeikticus* cells by lysozyme after one day of incubation with particles. 92% of bioactivity was calculated and it was stipulated to be much higher than with traditional encapsulation methods (30-80%) [43]. In a similar study from the same authors, the same assay was used for PLGA microcapsules made by coaxial electrospraying and lysozyme bioactivity reached this time 94.6% after *in vitro* release [51]. Although promising, both these studies mainly described the encapsulation of BSA (denaturation, encapsulation efficiencies and release) but used lysozyme for depicting bioactivity. This creates a gap in characterization since results may not necessarily directly translate from one molecule to the other: since BSA (a plasma protein) and lysozyme (an enzyme) have different structures and size (66.4 kg/mol and 14.7 kg/mol respectively), thus they may be affected by the electrospraying process in a different way, likely leading to different results.

When encapsulating anti-cancer drugs such as paclitaxel, bioactivity is generally assessed by Coumarin-6 (C6) glioma cells (brain tumor cells) inhibition with cell cycling analysis and

3-(4,5-dimethylthiazol-2-yl)-5-(3-carboxymethoxyphenyl)-2-(4-sulfophenyl)-2H-tetrazolium (MTS) assay [27]. In the study from Xie *et al.*, cell viability was hardly affected by particle concentration but was significantly decreased with increasing exposure time (1 to 5 days), showing a delayed cytotoxic effect of particles, equivalent to Taxol® treatment at day 4 and 5 only [27]. The same cytotoxicity test was used for electrosprayed PLGA films loaded with paclitaxel [29] where a decrease of C6 glioma cell viability compared to unloaded films was clearly seen, while an increase in the loading (5 to 30%) showed only a slight decrease in cell viability (from around 65% to 52% viability) without being statistically significant. In another study from Nie *et al.* where paclitaxel and suramin were coaxially encapsulated in microcapsules, a continued marginal increase in apoptotic activity of C6 glioma cells was shown after 9 days, proving the efficiency of the capsule system to deliver anti-cancer agents in a sustained way. Interestingly, cellular recovery was observed in free drug treated groups, indicative of the limitations of systemic drug administration, providing only short and acute exposure due to low terminal half-life of paclitaxel and suramin [30]. In another study the same authors showed that apoptotic activity was increased with the delivery systems compared to the free Taxol® groups over 9 days. They also found an increased apoptotic activity for their co-delivery system compared to single delivery with the combination 'suramin in the core' and 'paclitaxel in the shell' (S/P) outperforming the opposite formulation (P/S). This could be correlated with *in vitro* release results where the S/P formulation released higher doses of drugs compared to the P/S formulation [63].

A similar result was observed by measuring *in vitro* cellular apoptosis from alginate macrobeads containing electrosprayed PLGA microspheres releasing paclitaxel. Although the Taxol® control group gave high apoptosis of C6 glioma cells at day 2, it decreased at day 4 and 6 while beads formulations were giving increased and significantly higher apoptosis over time, demonstrating the potential of the delivery system to sustain therapeutic levels of paclitaxel [25].

When loading antibiotics to treat antibacterial infections such as ampicillin or ripamficin in electrosprayed particles, bioactivity can be assessed by measuring the zone of inhibition in contact with sensitive bacterial strain such as *E. coli DH5α* in the case of ampicillin. When using such test, the bioactivity of ampicillin released from chitosan particles was proven by a similar inhibition zone for loaded particles and for the same amount of free drug [23]. However a very small inhibition zone was also observed with unloaded particles, which the authors attributed to the inherent antibacterial activity of chitosan. This result may be further investigated to ensure the non-cytotoxicity of unloaded particles before loading of any therapeutic molecule.

For tissue regeneration and mainly angiogenesis, when growth factors such as IGF-1, PDGF and VEGF were loaded in electrosprayed particles, their bioactivity was respectively assessed by a smooth muscle cell (SMC) proliferation assay for IGF-1 [47] and human umbilical vein endothelial (HUVEC) cell and lung fibroblasts (LF) proliferation assays for VEGF and PDGF respectively [48]. The SMC viability was assessed by a (3-(4,5-Dimethylthiazol-2-yl)-2,5-diphenyltetrazolium bromide (MTT) assay and was shown to be significantly increased over a 4 week period with exposure of released IGF-1. The results showed that the bioactivity of IGF-1 was dependent on: the amount of IGF-1 loaded; the amount of PLGA and its molecular weight. Briefly, IGF-1 demonstrated more bioactivity for higher PLGA concentration, higher IGF-1 loadings and lower molecular weight PLGA [47]. The viability of HUVECs and fibroblasts used for determining the bioactivity of PDGF and VEGF was assessed by the PicoGreen dsDNA quantitation kit. The bioactivity of both GFs was shown to be high after two days *in vitro* indicating minimal changes to the proteins during the electrospraying process (around 80-90%). Interestingly, bioactivity decreased to less than 21% after 21 days, which authors attributed to the *in vitro* conditions that were too

harsh for growth factors, prone to oxidation and pH dependent deamidation in the *in vitro* context [48].

When encapsulating therapeutic molecules in polymeric devices, the use of PEG as an additive is shown to affect the release profiles, but also known to protect the bioactivity of encapsulated molecules. PEG has not been used yet in electrosprayed particles, although other polymeric devices have proven its benefits. For instance Morita *et al.* indicated that co-lyophilization of PEG and horseradish peroxidase before exposure to organic solvents increased the retention of bioactivity [104]. Johnson *et al.* confirmed this theory by showing significantly more retention of nerve GF (NGF) when PEG was co-lyophilized before encapsulation in PLGA discs [100]. Co-lyophilization of PEG with therapeutic molecules may thus be considered in electrospraying when the solid dispersion method is used for enhanced bioactivity.

4.7. In vivo performance

Most studies on electrosprayed particles loaded with therapeutic molecules are done within an *in vitro* context. This approach is very important so that parameters can be tailored and optimized in the first instance, before the use of animals to further validate the optimized formulations. However *in vivo* data remains essential for translation of electrosprayed particles loaded with therapeutic molecules to the clinic. Owing to electrospraying, as applied to biological loadings, being in its relative infancy, only limited *in vivo* data is currently available, although these studies do show promising results.

Most *in vivo* studies involve the assessment of tumor treatment by sustained release of anti-cancer agents such as paclitaxel and suramin [25-26, 63]. In the study from Naraharisetti *et al.* for instance, 10 and 20% (w/w) of paclitaxel were loaded in PLGA 50:50 particles by electrospraying from a DCM solution, providing final microparticles of 15.0 µm in diameter within a narrow size distribution of 1.7 µm [26]. C6 glioma cells were inoculated subcutaneously to BALB/c nude mice and loaded particles were injected to the tumor in two doses on day 14 and 28 at 0.5 mg paclitaxel/injection. A control injection of 1 mg of commercial paclitaxel (Taxol®) was injected only at day 14 for comparison. All the groups showed improved tumor suppression over the placebo control and cytotoxicity of the microparticles was evident in the analysis by H&E staining of the tumor tissue when compared with the placebo and commercial Taxol® control. Both *in vitro* release profiles from 10 and 20%-loaded particles showed similar release kinetics, with an initial burst release over the first 2 days before sustained release for the further 28 days, with only the burst being higher for the 20% formulation. Such burst release was shown to be more effective in treating the tumor since the 10% drug-loaded group performed poorly compared to the 20% drug-loaded group and the Taxol® control (10% drug-loaded group had to be sacrificed at 14 days due to excessive tumor volume, and a second injection at 28 days could not therefore be performed) [26].

In a similar study from Ranganath *et al.* (Fig. 7A-C), monodisperse paclitaxel-loaded PLGA microspheres were obtained by electrospraying, with an average size of 11.79±2.79 µm and a smooth, spherical morphology [25]. The loaded microspheres were further loaded in alginate macrobeads (1.61-1.68 mm average size) (Fig. 7A) and presented various release profiles according to gelation time, concentration of the cross-linking agent and microsphere loading (Fig. 7B). Two formulations were selected to be implanted in subcutaneous C6 glioma tumor in mice and both showed smaller tumors in comparison to the blank after 21 days. However, only the formulation with medium cross-linking (M80) was able to demonstrate significantly smaller tumors compared to the free Taxol® group, while the highly cross-linked formulation (H80) gave lower tumor formation but not significantly (Fig. 7C).

Importantly these results were different from the *in vitro* results where H80 released more paclitaxel than M80 and in a slightly more rapid manner [25].

Still within the context of brain tumor treatment, Nie *et al.* prepared electrosprayed core/shell capsules by coaxial electrospraying of PLLA for the core and PLGA 50:50 for the shell (Fig. 7D-G) [63]. They loaded simultaneously both paclitaxel and suramin, with either paclitaxel in the core and suramin in the shell (P/S formulation) which provided a sequential release, or the opposite (S/P formulation), which provided a release in parallel (Fig. 7F). Interestingly, *in vitro* data showed that the highest apoptotic activity was obtained for the S/P formulation over 9 days. However when looking at the *in vivo* results (subcutaneous inoculation of U87 MG-luc2 xenograft in BALB/c nude mice), the P/S formulation was best in inhibiting growth of brain tumors after 21 days (Fig. 7G). The authors deducted that the presence of a higher released dose of suramin at the early stage efficiently prevented the excess growth of tumor cells while a subsequent controlled and sustainable release of paclitaxel could induce the apoptosis of tumor cells continuously [63].

The results from both these studies underline the versatility of the electrospraying technique being able to generate different release profiles according to the processing parameters (in these cases being the drug loading [26], the extent of matrix cross-linking [25] and the location of loaded drugs [63]) and generating different *in vivo* results. Importantly, an initial burst release before the onset of a linear release was shown to be more effective in tumor suppression and provided important feedback for tailoring *in vitro* release profiles, showing that zero-order release kinetics are not always desired for efficient therapeutic effect [26]. The importance of undergoing *in vivo* studies is also shown to be paramount when looking at the study from Ranganath *et al.* and Nie *et al.*, where *in vivo* results may give different results to what would be extrapolated from the *in vitro* data [25, 63].

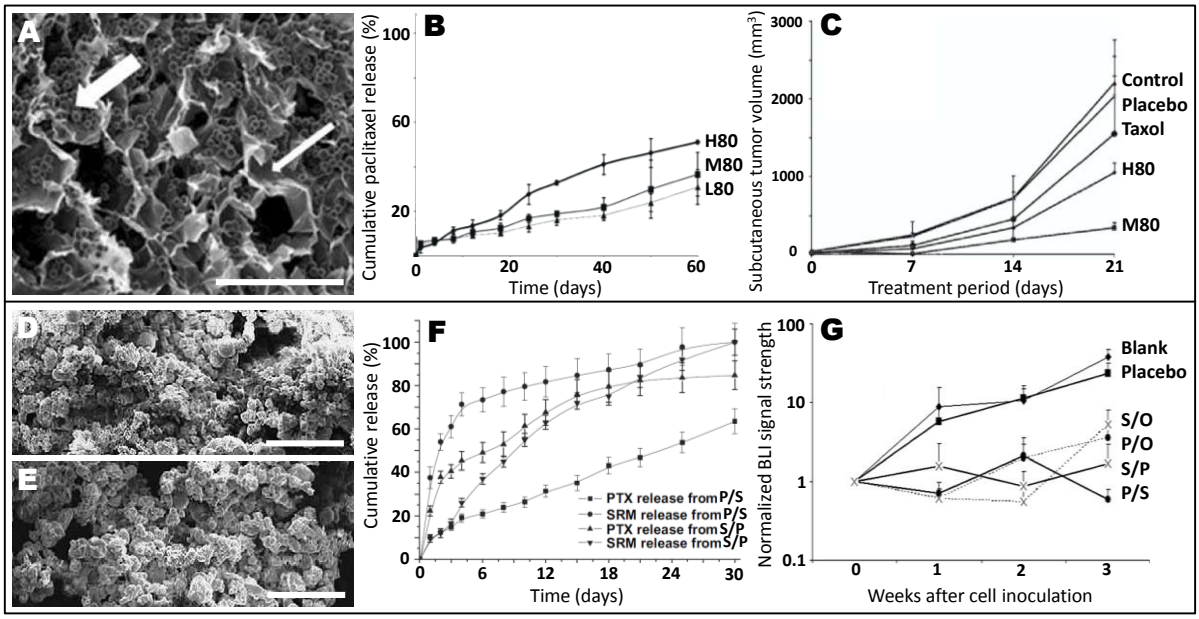

Fig. 7. (A) Representative SEM image of paclitaxel-loaded PLGA microspheres (large arrow) entrapped in an alginate matrix (small arrow). Scale bar is 200 µm. (B) *In vitro* release of paclitaxel from different formulations of microspheres entrapped in the alginate matrix. L80, M80 and H80 correspond to different degrees of cross-linking (low, medium, high) with 1, 5, 15 min gelation time and 0.5, 1, 2% (w/w) of $CaCl_2$ concentration, respectively. (C) *In vivo* subcutaneous C6 tumor volume profiles of mice treated with different groups for 21 days (n=5). The control group had no beads and no drug; the placebo group was implanted with alginate macrobeads but no drug; the Taxol® group received an injection of 180 µg of Taxol® directly in the tumor mass; and animals in the H80 and M80 were implanted with 2

mg of alginate beads loaded with microspheres containing an average amount of 162 μg of paclitaxel per animal [25]. (D-E) Representative SEM images of PLLA/PLGA capsules loaded with (D) P/S formulation (paclitaxel (PTX) in the core and suramin (SRM) in the shell) and (E) S/P formulation (SRM in the shell and PTX in the core). Scale bar is 100 μm. (F) *In vitro* release of PTX and SRM from P/S and S/P formulations. (G) *In vivo* subcutaneous U87 MG-luc2 tumor progression profile over the period of treatment measured as normalized bioluminescence intensity (n=5). The blank group received no injection of drug; the placebo group was implanted with blank particles; the S/O group received particles loaded with only suramin in the core while particles were loaded only with paclitaxel in the P/O group [63]. *Adapted from [25, 63] with permission. 2009 Springer [25]; 2010 Elsevier Science Ltd. [63].*

5. The use of electrosprayed particles in electrospun scaffolds

5.1. Electrospun nanofibers and drug delivery

Amongst the many scaffolds that have been generated to date in the field of tissue engineering (TE), some of the most promising are the scaffolds produced which comprise nanofiber structures [107-108]. The nanoscale could be argued as being the most realistic scale to approach when mimicking the architecture of natural tissues. Nanofiber scaffolds are distinctive compared to scaffolds at the micro- or macro-scale owing to their similarity to natural extracellular matrices, like collagens, which are the major protein components of many tissues including skin, tendon, ligament and bone. Collagen is characterized by a fibrillar structure shown to enhance cell attachment, proliferation and differentiation in tissue culture [108]. For this reason, engineers aim to mimic its structure whilst fabricating engineered tissues to closely resemble the native tissues. In addition, the high surface to volume ratio of nanofiber scaffolds is highly favorable for drug loading, while its high porosity and interconnected pores facilitates nutrient and waste exchange during tissue regeneration. These scaffolds can also be further modified by various 3D surface modification techniques to incorporate other valuable features of the extracellular matrix [108]. Nanofiber scaffolds are studied in various areas of TE: in neural TE, where uniaxially aligned nanofibers can be used to guide the growth of neurons [109], in bone TE, where nanofibers may be mixed with hydroxyapatite (HA) to mimic the bone extracellular matrix which is mainly composed of collagen and HA [109-110], and in cartilage TE, where nanofiber meshes can support cell spreading and growth of chondrocytes [110].

Three main techniques have recently emerged in the production of nanofibers: electrospinning, phase separation and self-assembly. The two first techniques mainly use polymeric materials due to their ease of processability and capacity to provide a large variety of cost-effective materials. All methods can produce nanofibers, even though electrospinning has been shown to generate larger diameter nanofibers on the upper end of the nano-range of natural collagen, rather considered to be submicron [107]. Electrospinning remains the most widely used technique for production of nanofibers, due to numerous advantages when compared to the other techniques: it is simple, cost effective, reproducible and versatile: a wide range of natural and synthetic polymer solutions can be used (collagen, silk fibroin, PCL, PLGA, polyurethane (PU), poly(methyl methacrylate)(PMMA), etc.) and the method allows for control of fiber diameter and alignment [107-108, 110-111] (Examples include 30-120 nm for silk fibroin [112], 250-800 nm for PCL [113-114] and 200-1000 nm for PLGA [115]).

Electrospinning is an electrohydrodynamic variant of electrospraying which uses identical apparatus. Compared to electrospraying, solution electrospinning requires polymer solutions with higher viscosity, which can be obtained by using higher molecular weights or most generally higher polymer concentrations that ensure at least 2.5 entanglements per polymer

chain [78]. The regime used for electrospinning must be in the *semi-dilute highly entangled regime* where ratio $C > 3C_{ov}$ which can be up to $10C_{ov}$ for obtaining uniform fibers, and which depends on the molecular weight distribution of the polymer chains in solution [79].

Nanofibers have been investigated as drug delivery vehicles as well, where drugs could be dissolved or dispersed in the polymer solution before electrospinning [116] or by using coaxial electrospinning wherein a secondary polymer solution containing the biomolecules is electrospun within the core of the forming nanofiber [99, 117]. The tissue-conductive only scaffold then becomes a tissue-inductive scaffold by releasing bioactive agents capable of inducing specific tissue treatment. Nanofiber scaffolds applied to drug delivery have predominantly been focused on the loading of antibiotics and anti-cancer agents [118], and there have been several reports regarding the incorporation of growth factors into these scaffolds [99, 119-123]. More details on electrospinning and drug delivery can be found to review by Sill and von Recum [124].

Although direct incorporation of drugs into nanofibers seems promising, there is presently a lack of characterization of these systems. For instance some studies have been done *in vitro*, while the understanding of scaffold behavior and effectiveness *in vivo* is essential for clinical applicability of these devices [118]. In addition, drawbacks such as low reproducibility do not allow sufficient control over drug distribution and thus insufficient control of the release profiles. This impairs both reproducible pharmacokinetics and pharmacodynamics. Drug aggregation in solution is another issue which can lead to denaturation and non-homogeneous distribution within the scaffold after processing [120, 123]. Importantly, when the scaffold is responsible for load bearing and drug delivery simultaneously, direct incorporation of drug within the nanofibers may have adverse effects on the mechanical properties of the scaffold [125]. This is particularly important for bone applications where bioactive agents such as growth factors must be released when the load-bearing implant can still perform its function [126]. For instance, when NGF was directly incorporated into the electrospinning solution, it resulted in a loss of control of the mesh properties and in a low loading efficiency (about $3x10^{-4}$%), which was attributed to differences in charge densities between the GFs and polymer resulting in a chaotic and instable jet [123]. Based on these factors, it may be concluded that the loading of bioactive agents in nanofibers may not be ideal for controlled drug delivery.

5.2. Electrospun nanofibers and particles for drug delivery

The use of loaded microparticles in nanofiber scaffolds was introduced as a response to the drawback provided by direct encapsulation in nanofibers, where both scaffold properties and delivery requirements were difficult to attain [127]. Separating the drug of interest from the scaffold permits the use of a different material for encapsulation, which allows enhanced properties for the intended function of both the scaffold and drug reservoir. Among many others, the scaffold material requires higher mechanical properties, slower degradation and interconnected structures for cell infiltration, while the microparticles containing the drug need to provide positive interactions with the drug for high loading and enhanced protection from the environment, along with tunable degradation for the tailoring of release profiles. The use of such composites can enhance encapsulation efficiencies but also allows control over drug distribution within the scaffold, by providing different gradients or loading patterns within the scaffold. Importantly, in direct encapsulation in scaffolds, loading is often limited to only one component [30] since bioactive agents can aggregate and denature after contact with each other when multiple loading is attempted within the same scaffold material [128]. However, some applications such as tissue regeneration or cancer therapy require the action of more than one type of drug or protein being delivered in various fashions (linear, pulsatile, delayed, burst) according to a programmed cascade triggered by cells for a specific treatment

[3]. For instance in tissue regeneration, the formation of a mature vascular network is known to involve, among others, VEGF-165 and PDGF, both with distinct temporal actions [129]. By using separate populations of microspheres, independent bio-agents can be loaded, whose release profiles are tuned with the particle characteristics, without altering the scaffold characteristics, thus meeting both the delivery and scaffold requirements.

5.2.1. Loaded particles in electrospun nanofibers

The incorporation of loaded nano/microparticles into electrospun scaffolds can be achieved by using a drug emulsion (Fig. 8A) [130-131] or pre-formed microspheres (Fig. 8B-D) [125, 132] within the electrospinning solution. In the first case, an aqueous solution containing a bioactive agent is mixed with an organic polymer solution, also known as emulsion electrospinning, providing aqueous reservoirs within electrospun nanofibers. Dong *et al.* used this technique to incorporate two distinct populations of nanospheres within fibers, and presented their findings in a short communication (Fig. 8B-C) [131]. They first loaded PVA particles with BSA or epidermal growth factor (EGF) by a single emulsion process. This involved emulsifying the PVA solution containing BSA or EGF, followed by hardening of the formed nanoparticles, before incorporating in a polyurethane (PU) solution and further electrospinning (Fig. 8B). In terms of parameters, increasing the concentration of PVA from 1 wt% to 5 wt% in the PU solution led to the formation of larger PVA particles, with an average diameter increasing from 200 nm to 300 nm. The fibers had an average diameter of 2 µm. The authors managed to show the distinct populations of nanospheres within the fibers by labeling BSA and EGF with fluorescent dyes (Fig. 8C). They commented on the opportunity to control the release of multiple compounds, potentially at distinct rates, but did not provide more details. No information was given pertaining to loading and efficiency capacities, bioactivity of released molecules or release profiles [131].

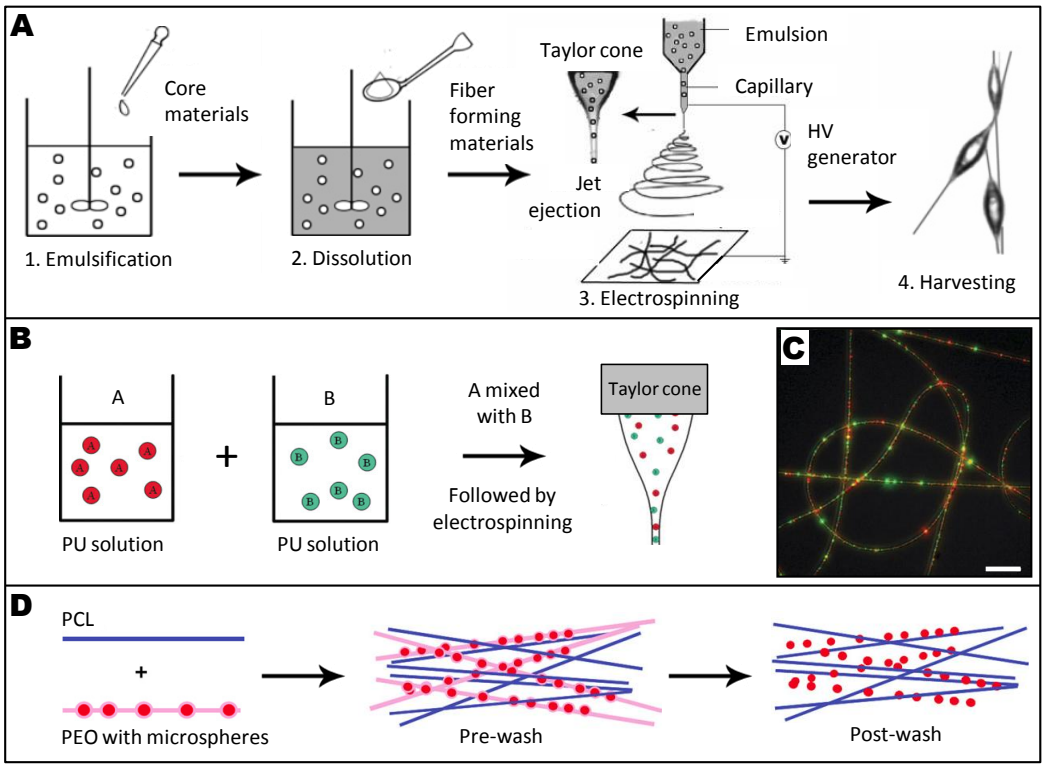

Fig. 8. Incorporation of loaded nano/microparticles into nanofibers by using (A) drug emulsions [130] and (B-D) pre-formed microspheres [125, 131]. (A) Schematic overview over the four major steps of microencapsulation in fibers by emulsion electrospinning [130]. (B)

Schematic illustration of the preparation of polyurethane electrospun fibers containing two distinct populations of nanoparticles. (C) Overlay of fluorescence image of polyurethane fibers containing PVA/EGF-AF488 and PVA/BSA-TR particles when excited with blue light with fluorescence image when excited with green light. Scale bar is 20 μm [131]. (D) Preparation of composite scaffolds through a sacrificial PEO fiber fraction coupled with a stable PCL fiber fraction (Pre-wash). With PEO dissolution (Post-wash), microspheres remained entrapped within the PCL network [125]. *Adapted from [125, 130-131] with permission. 2006 American Chemical Society [130]; 2009 John Wiley and Sons [131]; 2010 Elsevier Science Ltd. [125].*

More consistently, Qi *et al.* formed loaded PLLA nanofibers by adding PLLA in an emulsion of calcium (Ca)-alginate microspheres containing BSA, providing homogeneous beads-in-string structures after electrospinning [130]. Although microspheres had larger diameters than fibers, they were found embedded within the fibers (Fig. 9B). The authors supposed that when the emulsion flew through the capillary, due to the rapid jet elongation, the dispersed phase accumulated in the centre of the liquid along the fluid direction, allowing microspheres to settle into fibers rather than on surfaces. However, an increase in the electrospinning voltage, above 20kV, led to inferior morphology with a decrease in fiber diameter and microspheres transforming into spindles. Although the final cumulative release of microspheres in nanofibers was slightly decreased compared to blank microspheres (less than 10% difference), the microspheres from the composite provided a lower initial burst release as well as a more sustained release over the period of study (120 hours) as seen in Fig. 9C [130]. Although the delivery characteristics of this system were promising, no information was given on the scaffold properties and performance after addition of microspheres.

In a similar study, chitosan nanoparticles encapsulating naproxen and rhodamine B separately were made by ionic gelation and mixed into a PCL electrospinning solution [132]. After electrospinning, nanoparticles were embedded in the fibers and release rates from fibers were slower than bare nanoparticles. Different release kinetics could be obtained by incorporating the raw molecule or incorporating the chitosan nanoparticles containing the molecule in the PCL solution. However, less final cumulative release was observed in the latter case for loading of rhodamine B (18% from nanoparticles in fibers versus 70% from fibers after 70 hours) [132].

In addition to the emulsion method and direct incorporation of particles into the electrospinning solution, an interesting technique was recently proposed, using a co-spinning process of a sacrificial polymer (polyethylene oxide (PEO)) solution containing preformed PLGA microspheres, with a PCL solution [125]. Upon hydration, PEO was removed, leaving the microspheres entrapped between the PCL nanofibers (Fig. 8D). The use of sacrificial fibers in electrospinning was previously shown to increase scaffold porosity and cell infiltration by the same authors [133]. Using this method for incorporating microspheres was aimed at mitigating any changes to the scaffold properties, an issue with direct encapsulation into nanofibers [99]. In order to assess the mechanical properties of scaffolds, polystyrene microspheres (15.7 μm in diameter) were used as a model microsphere (since authors argued that PLGA microspheres would have dissolved in the solvent used for electrospinning) and entrapped either within or between the nanofibers, for mechanical comparison. When microspheres were included in PCL, it was shown that both the stiffness and modulus decreased with increasing microsphere density. However, when the microspheres where entrapped between the fibers, no change in stiffness was observed for any density, and the modulus were equivalent but only for low microsphere densities (0.05 mg of microspheres/mL of solution). In terms of loaded biomolecules, BSA and chondroitin sulphate (CS) were used for encapsulation in PLGA microspheres through a w/o/w double emulsion. Very low encapsulation efficiencies were obtained; 13% and 11% respectively. Release kinetics were independent from one another and comparable to composites

containing only the single populations. A slightly more sustained release profile was observed for CS in the scaffold compared to free microspheres (25 days, maximum release of more than 60% in all cases), while the maximum release was reached after only 5 days for BSA with about 20% for free microspheres and 10% for microspheres within the scaffold (Fig. 9D-F)) [125].

All these studies underline the increasing interest for incorporating particles in electrospun scaffolds, although release profiles are not yet optimal and their effects on cells in both the *in vitro* and *in vivo* environments remain to be addressed, along with the characterization of mechanical properties of scaffolds after incorporation of loaded particles.

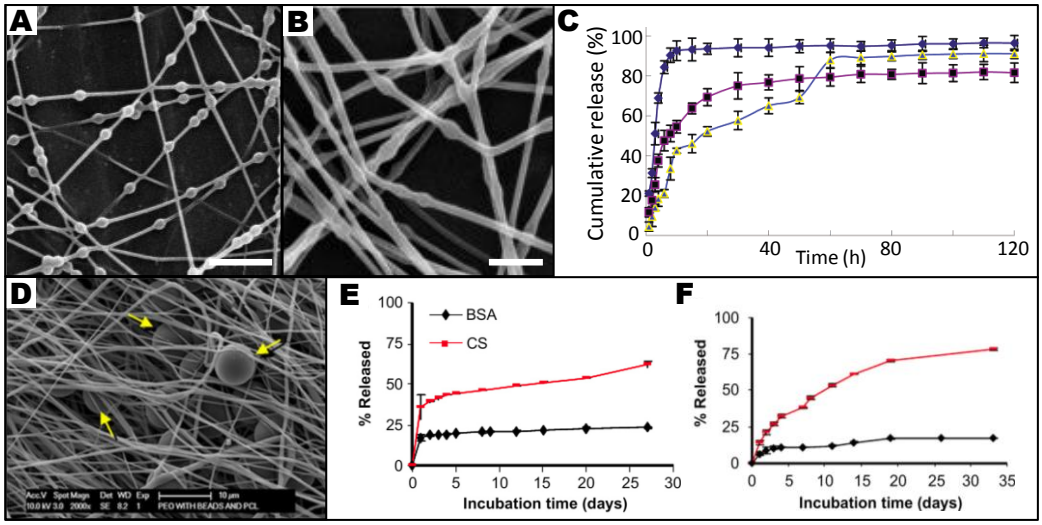

Fig. 9. Morphology and release profiles of loaded nano/microparticles embedded in nanofiber scaffolds by using (A-C) drug emulsions [130] and (D-F) pre-formed microspheres [125]. (A) SEM micrograph of electrospun PLLA fibers containing pre-made polystyrene microspheres. Scale bar is 2.5 µm (B) SEM micrograph of electrospun PLLA fibers containing Ca-alginate microspheres formed by w/o emulsion. Scale bar is 10 µm. (C) Release profiles of BSA from: Ca-alginate microspheres (diamonds); fibers shown in B, made at 15kV (squares); fibers with spindle particles corresponding to electrospinning at 20kV (triangles) [130]. (D) SEM micrograph of composite scaffolds made through a sacrificial PEO fiber fraction containing BSA- and CS-loaded microspheres coupled with a stable PCL fiber fraction. (E) Release of BSA or CS from PLGA microspheres. (K) Release of both BSA and CS from the single composite system containing both BSA and CS microspheres at a 1:1 ratio [125]. *Adapted from [125, 130] with permission. 2006 American Chemical Society [130]; 2010 Elsevier Science Ltd. [125].*

5.2.2. Multiple electrospraying/electrospinning

5.2.2.1. Concept

As explained previously, the electrospinning/electrospraying processes use simple apparatus consisting of syringe pumps, collectors and external voltage supplies, and thus they can be easily manipulated to fit specific requirements (horizontal, vertical, or angled setups). For this reason, these apparatus may be easily used in combination, for the production of composites with an increased number of properties. Early attempts to electrospray whilst electrospinning consisted of side-by-side capillaries and a flat collector moving on an *x-y* stage [134]. Although the scaffolds yielded were 100 µm in thickness after 45 min, the area of stream convergence was so small that non-uniform integration was obtained. The authors attributed this problem to a stream repulsion effect from Coulombic forces, which they limited by locating the nozzles perpendicular to one another and using a rotating mandrel

translating on its axis. Stream repulsion was minimized and the combination of rotation and translation of the mandrel target provided an ideal integration of both components (electrosprayed smooth muscle cells and poly(ester urethane) urea (PEUU) fibers in this case). Using this configuration, 5x5 cm construct sheets ranging from 300 to 500 nm in thickness were created and scaffold thickness could be controlled by adjusting polymer feed rate or fabrication time. The authors concluded that this setup may find other applications in the future as a means to fabricate more uniform composite scaffolds by electrospinning multiple materials or introducing drug-laden microspheres between fibers, a setup which has indeed been used in consecutive years for either multiple electrospinning or simultaneous electrospraying/electrospinning [134].

5.2.2.2. Multiple electrospinning

Compared with single electrospinning, more versatility in properties can be achieved with multiple electrospinning. The drug delivery characteristic can indeed be effectively coupled with desired mechanical properties. This was obtained, for example, by simultaneously electrospinning PLGA fibers loaded with tetracycline hydrochloride (TET), for antibacterial activity, with PEUU, that maintain the required elastomeric properties [135]. The use of a rotating mandrel for collecting these constructs is the best approach in multiple electrospinning. It allows aligned fibers, a configuration highly desirable in tissue engineering, since it mimics some of the fibrous musculoskeletal tissues, like tendons and ligaments. Although fewer studies on multiple electrospraying/electrospinning are available, they also use a rotating mandrel collector and most of these studies face similar issues relating to this mandrel approach.

Fundamentally, the main limitation in aligned fibers obtained by collection onto a rotating mandrel is the high density fiber packing, since fibers are drawn in parallel to one another. This becomes an issue for cellular infiltration, where in most cases, cellular and tissue formation are often limited to the surface of the electrospun construct, impairing the necessary cell growth within the central architecture of the construct [48]. The use of a second electrospinning apparatus was proposed for simultaneous electrospinning of sacrificial fibers that, once they are removed from the scaffold, confer an increased porosity, beneficial for cell infiltration, while maintaining the anisotropy of the scaffold. To this end, PCL and PEO were co-electrospun onto a rotating mandrel, followed by dissolution of PEO into water after production (Fig. 10B) [133]. Importantly, cell infiltration and distribution after three weeks in culture increased in the starting sacrificial fraction when scaffolds were seeded with mesenchymal stem cells [133]. On the other hand, limited cell infiltration was reported when a PCL/collagen blend was co-spun with PEO [136]. Certainly the electrospinning parameters have a great influence in the fiber deposition and fiber characteristics and must be optimized for effective improvement in cell infiltration. Another approach to improve cell infiltration was proposed which involved simultaneously electrospinning microfibers and nanofibers, obtained by melt and solution electrospinning, respectively (Fig. 10A). Microfibers increased the porosity of scaffolds to facilitate cellular infiltration and nanofibers gave an enhanced effect on cell attachment and growth due to the nanoscale features (Fig. 10C-E). The so-produced PLGA composite scaffolds provided significantly higher attachment and spreading of both human epidermal keratinocytes and fibroblasts (Fig. 10F-H) [137].

Another drawback of electrospun fibers from synthetic polymers, which may be overcome by multiple electrospinning, is the lack of biological recognition. For some applications however, such as vascular grafts, a cell-responsive surface is paramount. This has been achieved by simultaneously electrospinning PCL and silk fibroin, for their respective mechanical and cell-conducive properties, onto a rotating mandrel, conferring anisotropic properties as well [138]. More than a simple overlapping of nanofibers, double

electrospinning provided a high integration of both types of fibers and the change of mandrel rotation speed may render the anisotropy tunable. This may be kept in mind when optimizing the electrosprayed/electrospun constructs.

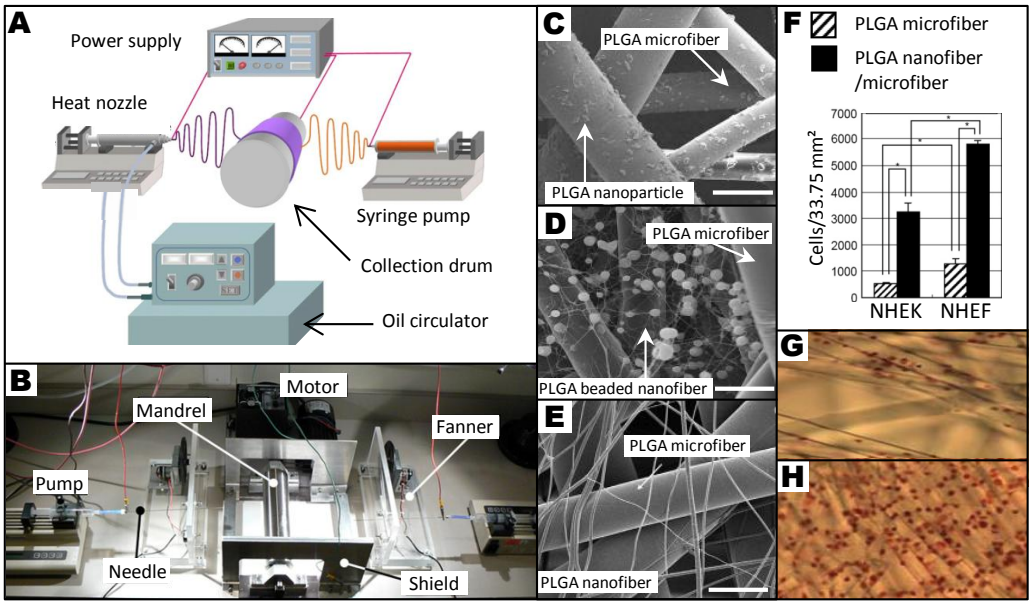

Fig. 10. Multiple electrospinning. Schematic of (A) co-solution/melt electrospinning on a rotating mandrel [137] and (B) photo of co-solution electrospinning apparatus [133]. (C-E) SEM images of three types of nano-/microfiber composite scaffolds: (C) nanoparticle/microfiber scaffold for 1wt% solution of the nano-component, (D) beaded nanofiber/microfiber scaffold for 9wt%, (E) nanofiber/microfiber scaffold for 10 wt%. Scale bar is 20 µm. (F) Cell numbers of human epidermal keratinocytes (NHEK) and human epidermal fibroblasts (NHEF) that adhered to two types of scaffolds after 1h (means±SD, n=4). (G-H) Micrographs of NHEF in (G) PLGA microfiber scaffold and (H) PLGA nano-/microfiber scaffold (10/90) [137]. *Adapted from [133, 137] with permission. 2010, 2008 Elsevier Science Ltd.*

5.2.2.3. Applications of multiple electrospraying/electrospinning

The multiple electrospinning devices have recently proven quite promising in enhancing the typical properties obtained with single electrospinning. In a similar fashion but different scope, the association of electrospinning with electrospraying was proposed to provide a 3D structural construct of nanofibers embedded with electrosprayed particles for varied applications such as drug delivery, coatings or cellularization of the constructs. Such a simultaneous process would allow the composite production in a single step sequence and permit a better integration of particles within the scaffold. Due to the versatility of both processes, several types of scaffolds could be easily and quickly achieved while adding extra properties without affecting the essential properties required for scaffolds.

5.2.2.3.1. Drug delivery

The application of coaxial electrospraying technique in association with electrospinning applied to drug delivery was first reported in 2009 by Wang *et al.* and shown in Fig. 11 [47]. They created a soft tissue-engineered construct (TEC) with anisotropic structure, able to deliver growth factors for the survival of cells which were often subjected to hypoxia and a nutrient starvation microenvironment in the context of TECs [139]. The co-spinning technique enabled simultaneous electrospinning of polyurethaneurea (PUU) nanofibers and electrosprayed PLGA microcapsules of an IGF-1 gelatin solution, obtaining the direct

assembly of a scaffold onto a rotating mandrel collector (Fig. 11A). Results showed that the release profile and bioactivity of IGF-1 were dependent on: the amount of IGF-1 loaded (tested with 50 and 150 µg/mL); the amount of PLGA (tested with 5 and 10 wt%) and the molecular weight (tested with high MW (40-75 kDa) and low MW (5-15 kDa)). The release profile was triphasic with an initial burst release attributed to the imperfect core-shell structure of the microcapsule (Fig. 11E). It was hypothesized that during the travel of the microcapsules toward the collector, the inner part of the shell may have solidified slower than the outer part, allowing the leakage of the aqueous IGF-1 into the shell, becoming trapped there. The increased release occurring after 3 weeks was attributed to the release of accumulated acid from PLGA bulk, creating pores that allowed the encapsulated IGF-1 to quickly diffuse out. Bioactivity was maintained over the 4-week study period and the cell growth on all loaded scaffolds was assessed *in vitro* for a 7-day culture period under normal conditions and under hypoxia/nutrient starvation conditions with a MTT assay (Fig. 11F). The authors stated that the loaded scaffolds were able to significantly enhance cell growth at day 7 in both types of conditions. However, by correlating these results with the release results observed from day 7 to day 21 day, where the IGF-1 release is almost inexistent, it may have been expected that cell survival would decrease after day 7. The authors also performed mechanical studies on the scaffolds and observed that the incorporation of PLGA microspheres did not significantly alter tensile strength, modulus and elongation break at the perpendicular direction, while it did in the alignment direction, which may be a potential concern. However mechanical properties at the perpendicular direction were very weak compared to those at the alignment direction, before and after incorporation of microspheres, which may be why incorporation did not alter significantly the mechanical properties at the perpendicular direction [47].

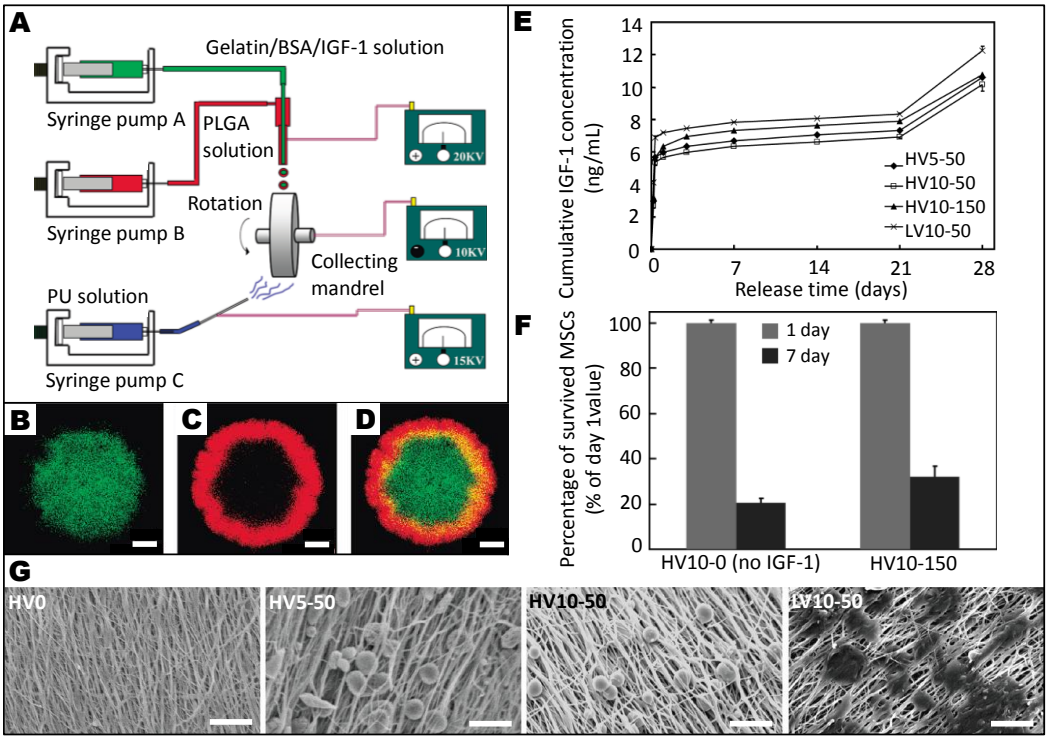

Fig. 11. (A) One-step fabrication of protein loaded microcapsules and nanofiber scaffolds by simultaneous coaxial electrospraying/electrospinning techniques. (B-D) Structure of the fabricated microcapsules. FITC-labeled BSA was added into the protein solution, and rhodamine-B was loaded into the PLGA solution before fabrication. The resulting microcapsule showed: (D) a core-shell structure with (B) protein solution as the core and (C)

PLGA as the shell. Scale bars are 2 µm. (E) IGF-1 release kinetics from scaffolds fabricated with different PLGA concentration and viscosity and IGF-1 loading at 37 °C. (F) Effect of IGF-1 loading on MSC survival under hypoxia/nutrient starvation conditions. MSCs were cultured for 1 day under normal culture conditions (21% O_2, 5% O_2, and 20% fetal bovine serum (FBS)) followed by 6 days under hypoxia/nutrient starvation conditions (5% O_2, 5% CO_2, and 1% FBS). (G) Surface morphologies of scaffolds embedded with loaded microcapsules. Abbreviations: HV: 40-75kDa PLGA, LV: 5-15kDA PLGA, HV0: scaffolds with no microspheres, HV5-50: 5%PLGA-50µg/mL IGF-1, HV10-50: 10%PLGA-50µg/mL IGF-1, HV10-150: 10%PLGA-150µg/mL IGF-1, LV10-50: 10%PLGA-50µg/mL IGF-1. *Adapted from [47] with permission. 2009 American Chemical Society.*

5.2.2.3.2. Other applications

Coating

A clear advantage in simultaneous electrospraying and electrospinning can be found when the application is coating of nanofibers. This is achieved by electrospraying of hydrogels as well as non-polymeric particles, such as metal oxide nanoparticles, ceramics, or even cells. Using a simultaneous device for coating was first of all shown to be more effective as compared to electrospinning and electrospraying in sequence. In a comparative study, Jaworek *et al.* assessed the merits of simultaneous electrospraying during the electrospinning process against electrospraying onto the same rotating drum after electrospinning was completed and electrospraying onto the electrospun mat removed from the drum and placed onto a heated table [140]. Metal oxide nanoparticles such as TiO_2, MgO and Al_2O_3 (20-100 nm size) were deposited on poly(vinyl chloride) (PVC), polysulfone (PSU) or nylon nanofibers of a maximum diameter of 500 nm. The authors observed that the simultaneous process produced particle coating with lower density, but particles were distributed more uniformly between fiber layers, an advantage for homogenous coating. Post-spinning deposition allowed production of denser layers, but the particles were mainly deposited on the mat surface, with only minor penetration into the mat while the post-spraying as a separate process gave denser coating. However, in this latter case, the coated surface was limited to the base of the spray plume that required scanning deposition onto the mat in order to cover larger areas [140].

Bone tissue engineering

The simultaneous process was used for several studies requiring coating of fibers, due to a need for homogeneous coating. For instance in bone tissue engineering, electrospun nanofibers can mimic the composite nature of bone but lack the osteoconductive property, which may be counterbalanced by using a blend of hydroxyapatite (HA), the mineral component of bone. However, blending HA with the nanofiber material may mask the osteoinductive property of HA since the particles are completely embedded inside the polymer fibers. Therefore, an electrosprayed coating of HA on nanofibers was proposed to create a better environment for growth and mineralization of bone cells. A poly(L-lactic acid)-co-polycaprolactone (PLACL)/gelatin blend was spun along with a HA methanol solution on a rotating mandrel and the resulting properties were compared with direct blending of HA in the polymer solution [141]. The electrospun fibers presenting electrosprayed HA particles showed better cell proliferation, enhanced mineralization and alkaline phosphatase activity (ALP). This was due to the exposure of HA to the cells which gave them the necessary cues to start to lay down bone matrix, but it also enhanced/roughened surface topography which is preferential for cell adhesion. Mechanical properties were also superior to the blend, collectively proving that electrospraying of HA in combination with electrospinning of nanofibers produced suitable osteoconductive scaffolds for bone tissue regeneration [141]. The same authors also used this process to coat electrospun gelatin only with HA, followed by cross-linking with 50% glutaraldehyde solutions, whose cytotoxic effect was negated by washing and drying of the scaffolds. Results

were compared with electrospun HA/Gelatin nanofibers of different HA/Gelatin ratios. Electrospray-coated nanofibers had a higher pore size and porosity than blended nanofibers, as well as larger fiber diameters. Similarly to the previous study, proliferation and ALP activity were significantly higher for electrospray-coated nanofibers at 5, 10 and 15 days of culture, again due to the complete exposure of HA on the surface of nanofibers. Cross-linking was found to confer better stability and mechanical properties than for non-cross-linked scaffolds with a tensile strength of 2.7 MPa and a strain at break of 41.5% which are close to suitable values for guided bone tissue regeneration [142].

Cell infiltration and vascularization

Co-spinning has also been employed for coating electrospun PCL/collagen microfibers with electrosprayed Heprasil™, a synthetic hydrogel comprising chemically modified hyaluronic acid (HyA) and heparin as an attractive template for cells [136]. By comparing only microfibers with nanofibers, better cell infiltration was shown for microfibers. Technical considerations included the size of the mandrel used during the co-spinning process with 0.8, 1.4 and 1.7 cm diameter leading to a 20, 30 and 70% Heprasil collection efficiency respectively. As expected, larger mandrels were able to capture the hydrogel droplets more efficiently and 1.7 cm was further used to limit losses. Heprasil was loaded with AlexaFluor488-labeled BSA, allowing visualization of the random dispersion of Heprasil regions within the composite. Cell infiltration in Heprasil-coated PCL/collagen microfibers was significantly higher than uncoated fibers, reaching more than 200 µm compared to 50 µm respectively, after 10 day culture with human foetal osteoblasts. The authors stated that the inclusion of Heprasil regions within the mesh created a reduction in the volume density of fibers and created compartments of hydrogel for cells to further infiltrate [136].

A prospective advantage of co-deposition of hydrogel is also the loading of bioactive molecules into the composite. Indeed the same authors further used their device to load angiogenic factors (VEGF and PDGF), in order to recapitulate the vascular system essential in all tissue-engineered constructs [48], which is often hard to achieve (Fig. 12B-F). They loaded the growth factors in the Heprasil hydrogel mix which was further electrosprayed simultaneously with electrospinning of the PCL/collagen blend microfibers, obtaining 200 ng/cm² of growth factors for a 32 cm² area of PCL/collagen-Heprasil co-deposition (Fig. 12B). The use of a co-culture assay of human umbilical vein endothelial (HUVEC) cells and lung fibroblasts (LF) with sequential seeding of LF followed by HUVEC permitted the infiltration of cells in the mesh with a HUVEC:LF ratio 1:5 being the most satisfactory, while seeding alone of HUVEC or higher HUVEC:LF ratios did not yield favorable results. Cells also exhibited more physiological morphologies as compared to conventional tissue culture plastic, reflecting a more physiological cellular state that ultimately influence cellular function and behavior. In terms of release profiles, a burst release followed by sustained release was observed for both GFs with approximately 48% and 30% of the total loaded VEGF and PDGF, respectively, being released after 5 weeks (Fig. 12D), while bioactivity of both GFs constantly decreased from around 80-90% bioactivity after two days *in vitro* to 1-20% after 21 days, which authors explained by VEGF in particular being susceptible to pH dependent deamidation and oxidation *in vitro* (Fig. 12E). Importantly cell penetration after 14 days of co-culture was shown to be similar for the GF-loaded group and the positive control (constructs were only cultured in endothelial media (EBM-20) supplemented with VEGF and PDGF) and was significantly higher than the pre-load group (Direct GF incorporation prior to cell seeding, equivalent to bolus injection), reaching approximately 190, 210 and 85 µm of infiltration depth in average, respectively (Fig. 12C,F). In conclusion, the PCL/collagen-Heprasil loaded hybrid scaffolds were shown to be able to recapitulate the primitive capillary network required for vascularized TECs, by initiating a capillary network not only on the surface but also throughout the scaffolds. However, the previous release profiles and bioactivity results suggest that this system may be effective only in the first days of cell

culture, rather than providing a continuous effectiveness over several weeks of culture. The morphogenic and chemotactic actions provided by this initial kick-start may be responsible for initial migration of cells in the constructs, triggering subsequent formation of endothelial network [48].

Electrospraying of cells

Electrospraying has also been employed to produce cellularized constructs by simultaneous electrospraying of smooth muscle cells (SMCs) and electrospinning of PEUU nanofibers [134]. Such co-processing allowed the integration of cells into the smallest pores of the electrospun scaffold as it was constructed, providing a large numbers of cells which infiltrated throughout the bulk after a few days of perfusion culture, which had spread within the scaffold. Importantly, there was no significant decrease in cell viability and electrosprayed SMCs spread and proliferated at a similar rate than the control unprocessed SMCs while cells *sprayed* from a bottle without voltage did not. The *sprayed* cell suspensions were supplemented with 3 wt% bovine skin gelatin for increasing viscosity and maximizing viability by protecting cells from mechanical and chemical stresses, since the physical forces of the pressurized spray in combination with the exposure of cells to processing solvents initially caused a significant reduction in SMC viability. Mechanical integrity was disrupted because of gelation within the fiber network. Because viability and proliferation of *electrosprayed* cells were not affected, they were electrosprayed with media alone, maintaining the mechanical properties of the construct. These results underline the advantage of *electrospraying* over simple *spraying* and are consistent with literature stating that cells can survive exposure to high voltage [134]. Importantly, the SMC-integrated PEUU composites presented lower tensile strengths and higher breaking strains, which were explained by the cells disrupting the PEUU fiber network and replacing elastic PEUU volume with cellular volume. The authors still concluded that the measured properties were still more than sufficient for the SMC-integrated PEUU composites to serve as a support structure for soft tissue growth and mechanical training.

Following these encouraging results, the same authors extended their process to the fabrication of small-diameter tubular conduits that possess mechanical properties similar to native blood vessels, after only a few days in culture (Fig. 12A) [143]. A 4.7 mm diameter mandrel was used in place of the previously employed 19 mm for sheets [134]. Interestingly they decreased the TTC distance from 5.0 to 4.5 cm and lowered the mandrel negative charge from -10 to -3 kV to obtain reproducible and defect free small-diameter tubular constructs. SMC integration was uniform radially and circumferentially within the conduits after initial static culture, while conduits were strong and flexible with mechanical properties that mimicked those of native arteries. Cultures of such cell-based scaffolds are recommended to be performed in spinner flasks or perfusion rather than static, since in both cases they led to much higher viable cells and enhanced spreading within the electrospun fibers [134, 143].

In 2008, mention of simultaneous electrospraying of chondrocytes and electrospinning of PCL was made in a review by Wu *et al*. [70]. They stated that confocal microscopy was used to visualize the living cells embedded in the fibers after being cultured in the cell media for a set time not mentioned. They also stated that the experimental results revealed that 80% of the cells were still viable after the electrohydrodynamic process, while no more information than this was provided (no description of materials or methods).

Although the futility of the last study, electrospraying of cells with simultaneous electrospinning of a polymer matrix remains an efficient and rapid method for the production of tissue-engineered constructs. However, this is by no means a trivial and straight forward procedure and issues of sterility and time required to produce thicker scaffolds may potentially limit this application [133].

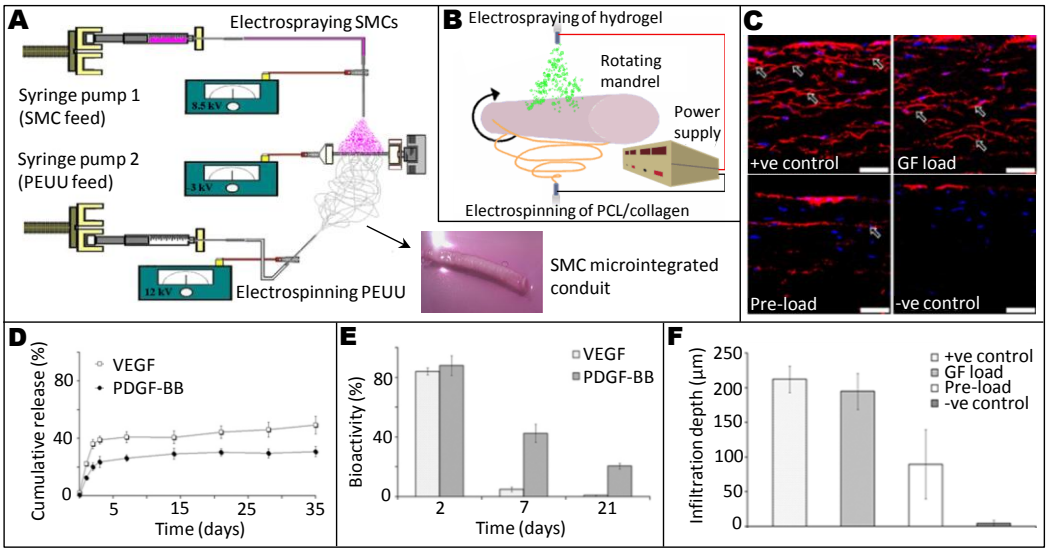

Fig. 12. (A) Schematic of the microintegration process of SMCs into PEUU fibers for small-diameter blood vessel construct fabrication. A perpendicular nozzle configuration was utilized for electrospinning PEUU (6wt% in HFIP at 1.5mL/h) and electrospraying SMCs ($7.5x10^{-6}$ SMCs/mL in medium at 0.1mL/min) onto a rotating small-diameter mandrel (4.7 mm, 250 rpm) transversing on a linear stage (1.6 mm/s). The macroscale appearance of SMC microintegrated PEUU tubular constructs are illustrated after removal from the mandrel (bottom right hand corner) [143]. (B-F) 3D vascularization of GF-releasing hybrid scaffold of PCL/collagen fibers and HyA hydrogel [48]. (B) Schematic of the co-electrospraying/electrospinning setup used for production of meshes, allowing simultaneous deposition of PCL/collagen fibers and HyA hydrogel. (C) Cellular infiltration measured by vWF section staining (Co-culture of HUVEC cells and LF) and endothelial network formation in meshes cultured in media supplemented with VEGF/PDGF (+ve control), meshed loaded with VEGF/PDGF in the Heprasil component during fabrication (200 ng/cm^2 each) (GF load), meshes loaded shortly prior to seeding (200 ng/cm^2 each) (Pre-load) and meshes lacking VEGF/PDGF (-ve control). Scale bars are 50 µm. (D) Release of VEGF and PDGF from meshes studied *in vitro* via ELISA. (E) Bioactivity of the incorporated VEGF and PDGF by cell proliferation assessment. Percentage bioactivity was obtained through comparison with equal amount of fresh VEGF and PDGF as 100% values. *Adapted from [48, 143] with permission. 2007, 2010 Elsevier Science Ltd.*

6. Conclusions

The controlled and targeted delivery of therapeutic molecules is tantamount to the success of many medical treatments. With the development of superior treatment options for cancer, asthma and hormonal therapies there is a concomitant demand to encapsulate and release the active molecules in a safe, reproducible and effective manner.

The technique of electrospraying has emerged as a promising technology to produce particles with entrapped therapeutic molecules which may be released as the particle degrades. The size and morphology of the particles produced are of paramount importance to enable batch-to-batch reproducibility and appropriate efficacy of the system. We have reviewed the many variables and interplays of the processing parameters which affect the production of microparticles and have highlighted the shortfalls associated with many current technologies. Importantly we have also highlighted the need to thoroughly assess and publish the encapsulation efficiencies, bioactivity and denaturation of the encapsulated biomolecules, both *in vitro* and *in vivo*. Only when all of these considerations are properly tackled can a delivery system for the use in targeted biomolecule delivery - for example in tissue engineering, be properly realized and translated to the clinic.

Acknowledgments

Thanks to Dr. Tristan Croll from the Tissue Repair and Regeneration program for molecule designing, Jaime Nakahara for proof-reading and to the Biomaterials and Tissue Morphology Group, Tissue Repair and Regeneration program, Regenerative Medicine group, IHBI and the Australian Research Council (DP0989000) for financial support.

References

[1] Sokolsky-Papkov M, Agashi K, Olaye A, Shakesheff K, Domb AJ. Polymer carriers for drug delivery in tissue engineering. Adv Drug Deliv Rev. 2007;59:187-206.
[2] Freiberg S, Zhu X. Polymer microspheres for controlled drug release. Int J Pharm. 2004;282:1-18.
[3] Chen F-M, Zhang M, Wu Z-F. Toward delivery of multiple growth factors in tissue engineering. Biomaterials. 2010;31:6279-308.
[4] Freitas S, Merkle HP, Gander B. Microencapsulation by solvent extraction/evaporation: reviewing the state of the art of microsphere preparation process technology. J Control Release. 2005;102:313-32.
[5] Li HF, Zhang HM, Guo XL. Preparation of Micro-/Nano- Nonspherical Polymer Particles. Prog Chem. 2011;23:1196-210.
[6] Chan H-K, Kwok PCL. Production methods for nanodrug particles using the bottom-up approach. Adv Drug Deliv Rev. 2011;63:406-16.
[7] Peltonen L, Valo H, Kolakovic R, Laaksonen T, Hirvonen J. Electrospraying, spray drying and related techniques for production and formulation of drug nanoparticles. Expert Opin Drug Deliv. 2010;7:705-19.
[8] Lassalle V, Ferreira ML. PLA nano- and microparticles for drug delivery: An overview of the methods of preparation. Macromol Biosci. 2007;7:767-83.
[9] Place ES, Evans ND, Stevens MM. Complexity in biomaterials for tissue engineering. Nat Mater. 2009;8:457-70.
[10] Ye M, Kim S, Park K. Issues in long-term protein delivery using biodegradable microparticles. J Control Release. 2010;146:241-60.
[11] Jaworek A, Sobczyk AT. Electrospraying route to nanotechnology: An overview. J Electrost. 2008;66:197-219.
[12] Jaworek A. Electrostatic micro- and nanoencapsulation and electroemulsification: A brief review. J Microencapsul. 2008;25:443-68.
[13] Ciach T. Application of electro-hydro-dynamic atomization in drug delivery. J Drug Deliv Sci Technol. 2007;17:367-75.
[14] Hartman RPA, Brunner DJ, Camelot DMA, Marijnissen JCM, Scarlett B. Jet break-up in electrohydrodynamic atomization in the cone-jet mode. J Aerosol Sci. 2000;31:65-95.
[15] Brandenberger H, Nussli D, Piech V, Widmer F. Monodisperse particle production: A method to prevent drop coalescence using electrostatic forces. J Electrost. 1999;45:227-38.
[16] Gomez A, Bingham D, Juan Ld, Tang K. Production of protein nanoparticles by electrospray drying. J Aerosol Sci. 1998;29:561-74.
[17] Yue H, Wei W, Yue Z, Lv P, Wang L, Ma G, et al. Particle size affects the cellular response in macrophages. Eur J Pharm Sci. 2010;41:650-7.
[18] Xie YB, Castracane J. High-Voltage, Electric Field-Driven Micro/Nanofabrication for Polymeric Drug Delivery Systems Electrostatic Techniques and Biomedical Application. IEEE Eng Med Biol Mag. 2009;28:23-30.
[19] Amsden BG, Goosen MFA. An examination of factors affecting the size, distribution and release characteristics of polymer microbeads made using electrostatics. J Control Release. 1997;43:183-96.
[20] Chakraborty S, Liao IC, Adler A, Leong KW. Electrohydrodynamics: A facile technique to fabricate drug delivery systems. Adv Drug Deliv Rev. 2009;61:1043-54.
[21] Almeria B, Deng WW, Fahmy TM, Gomez A. Controlling the morphology of electrospray-generated PLGA microparticles for drug delivery. J Colloid Interface Sci. 2010;343:125-33.

[22] Almería B, Fahmy TM, Gomez A. A multiplexed electrospray process for single-step synthesis of stabilized polymer particles for drug delivery. J Control Release. 2011;154:203-10.
[23] Arya N, Chakraborty S, Dube N, Katti DS. Electrospraying: A Facile Technique for Synthesis of Chitosan-Based Micro/Nanospheres for Drug Delivery Applications. J Biomed Mater Res B Appl Biomater. 2009;88B:17-31.
[24] Hong YL, Li YY, Yin YZ, Li DM, Zou GT. Electrohydrodynamic atomization of quasi-monodisperse drug-loaded spherical/wrinkled microparticles. J Aerosol Sci. 2008;39:525-36.
[25] Ranganath SH, Kee I, Krantz WB, Chow PKH, Wang CH. Hydrogel Matrix Entrapping PLGA-Paclitaxel Microspheres: Drug Delivery with Near Zero-Order Release and Implantability Advantages for Malignant Brain Tumour Chemotherapy. Pharm Res. 2009;26:2101-14.
[26] Naraharisetti PK, Ong BYS, Xie JW, Lee TKY, Wang CH, Sahinidis NV. In vivo performance of implantable biodegradable preparations delivering Paclitaxel and Etanidazole for the treatment of glioma. Biomaterials. 2007;28:886-94.
[27] Xie J, Marijnissen JCM, Wang C-H. Microparticles developed by electrohydrodynamic atomization for the local delivery of anticancer drug to treat C6 glioma in vitro. Biomaterials. 2006;27:3321-32.
[28] Xie JW, Lim LK, Phua YY, Hua JS, Wang CH. Electrohydrodynamic atomization for biodegradable polymeric particle production. J Colloid Interface Sci. 2006;302:103-12.
[29] Xie JW, Tan JC, Wang CH. Biodegradable films developed by electrospray deposition for sustained drug delivery. J Pharm Sci. 2008;97:3109-22.
[30] Nie H, Dong Z, Arifin DY, Hu Y, Wang C-H. Core/shell microspheres via coaxial electrohydrodynamic atomization for sequential and parallel release of drugs. J Biomed Mater Res Part A. 2010;95A:709-16.
[31] Ding L, Lee T, Wang CH. Fabrication of monodispersed Taxol-loaded particles using electrohydrodynamic atomization. J Control Release. 2005;102:395-413.
[32] Ciach T. Microencapsulation of drugs by electro-hydro-dynamic atomization. Int J Pharm. 2006;324:51-5.
[33] Wu YQ, MacKay JA, McDaniel JR, Chilkoti A, Clark RL. Fabrication of Elastin-Like polypeptide Nanoparticles for Drug Delivery by Electrospraying. Biomacromolecules. 2009;10:19-24.
[34] Xie JW, Tan RS, Wang CH. Biodegradable microparticles and fiber fabrics for sustained delivery of cisplatin to treat C6 glioma in vitro. J Biomed Mater Res Part A. 2008;85A:897-908.
[35] Ijsebaert JC, Geerse KB, Marijnissen JCM, Lammers JWJ, Zanen P. Electro-hydrodynamic atomization of drug solutions for inhalation purposes. J Appl Physiol. 2001;91:2735-41.
[36] Valo H, Peltonen L, Vehvilainen S, Karjalainen M, Kostiainen R, Laaksonen T, et al. Electrospray Encapsulation of Hydrophilic and Hydrophobic Drugs in Poly(L-lactic acid) Nanoparticles. Small. 2009;5:1791-8.
[37] Bohr A, Kristensen J, Stride E, Dyas M, Edirisinghe M. Preparation of microspheres containing low solubility drug compound by electrohydrodynamic spraying. Int J Pharm. 2011;412:59-67.
[38] Midhun BT, Shalumon KT, Manzoor K, Jayakumar R, Nair SV, Deepthy M. Preparation of Budesonide-Loaded Polycaprolactone Nanobeads by Electrospraying for Controlled Drug Release. J Biomater Sci-Polym Ed. 2011;22:2431-44.
[39] Yu D-G, Williams GR, Yang J-H, Wang X, Yang J-M, Li X-Y. Solid lipid nanoparticles self-assembled from electrosprayed polymer-based microparticles. J Mater Chem. 2011;21:15957-61.

[40] Enayati M, Ahmad Z, Stride E, Edirisinghe M. Size mapping of electric field-assisted production of polycaprolactone particles. J R Soc Interface. 2010;7:S393-S402.
[41] Trotta M, Cavalli R, Trotta C, Bussano R, Costa L. Electrospray technique for solid lipid-based particle production. Drug Dev Ind Pharm. 2010;36:431-8.
[42] Cavalli R, Bisazza A, Bussano R, Trotta M, Civra A, Lembo D, et al. Poly(amidoamine)-Cholesterol Conjugate Nanoparticles Obtained by Electrospraying as Novel Tamoxifen Delivery System. J Drug Deliv. 2011;2011:587604.
[43] Xie JW, Wang CH. Encapsulation of proteins in biodegradable polymeric microparticles using electrospray in the Taylor Cone-Jet mode. Biotechnol Bioeng. 2007;97:1278-90.
[44] Xu YX, Hanna MA. Electrosprayed bovine serum albumin-loaded tripolyphosphate cross-linked chitosan capsules: Synthesis and characterization. J Microencapsul. 2007;24:143-51.
[45] Xu YX, Hanna MA. Electrospray encapsulation of water-soluble protein with polylactide - Effects of formulations on morphology, encapsulation efficiency and release profile of particles. Int J Pharm. 2006;320:30-6.
[46] Xu YX, Skotak M, Hanna M. Electrospray encapsulation of water-soluble protein with polylactide. I. Effects of formulations and process on morphology and particle size. J Microencapsul. 2006;23:69-78.
[47] Wang F, Li ZQ, Tamama K, Sen CK, Guan JJ. Fabrication and Characterization of Prosurvival Growth Factor Releasing, Anisotropic Scaffolds for Enhanced Mesenchymal Stem Cell Survival/Growth and Orientation. Biomacromolecules. 2009;10:2609-18.
[48] Ekaputra AK, Prestwich GD, Cool SM, Hutmacher DW. The three-dimensional vascularization of growth factor-releasing hybrid scaffold of poly (ε -caprolactone)/collagen fibers and hyaluronic acid hydrogel. Biomaterials. 2011;32:8108-17.
[49] Rayleigh. XX. On the equilibrium of liquid conducting masses charged with electricity. Philos Mag Series 5. 1882;14:184-6.
[50] Rezvanpour A, Attia ABE, Wang CH. Enhancement of Particle Collection Efficiency in Electrohydrodynamic Atomization Process for Pharmaceutical Particle Fabrication. Ind Eng Chem Res. 2010;49:12620-31.
[51] Xie JW, Ng WJ, Lee LY, Wang CH. Encapsulation of protein drugs in biodegradable microparticles by co-axial electrospray. J Colloid Interface Sci. 2008;317:469-76.
[52] Pareta R, Edirisinghe MJ. A novel method for the preparation of biodegradable microspheres for protein drug delivery. J R Soc Interface. 2006;3:573-82.
[53] Ahmad Z, Zhang HB, Farook U, Edirisinghe M, Stride E, Colombo P. Generation of multilayered structures for biomedical applications using a novel tri-needle coaxial device and electrohydrodynamic flow. J R Soc Interface. 2008;5:1255-61.
[54] Cahill KS, Chi JH, Day A, Claus EB. Prevalence, Complications, and Hospital Charges Associated With Use of Bone-Morphogenetic Proteins in Spinal Fusion Procedures. JAMA. 2009;302:58-66.
[55] Chen RR, Mooney DJ. Polymeric growth factor delivery strategies for tissue engineering. Pharm Res. 2003;20:1103-12.
[56] Hwang YK, Jeong U, Cho EC. Production of uniform-sized polymer core-shell microcapsules by coaxial electrospraying. Langmuir. 2008;24:2446-51.
[57] Park S, Hwang S, Lee J. pH-responsive hydrogels from moldable composite microparticles prepared by coaxial electro-spray drying. Chem Eng J. 2011;169:348-57.
[58] Kim W, Kim SS. Multishell Encapsulation Using a Triple Coaxial Electrospray System. Anal Chem. 2010;82:4644-7.
[59] Bock N, Woodruff MA, Hutmacher DW, Dargaville TR. Electrospraying, a Reproducible Method for Production of Polymeric Microspheres for Biomedical Applications. Polymers. 2010;3:131-49.

[60] Cohen S, Yoshioka T, Lucarelli M, Hwang LH, Langer R. Controlled Delivery Systems for Proteins Based on Poly(Lactic Glycolic Acid) Microspheres Pharm Res. 1991;8:713-20.
[61] Zhu GZ, Mallery SR, Schwendeman SP. Stabilization of proteins encapsulated in injectable poly (lactide-co-glycolide). Nat Biotechnol. 2000;18:52-7.
[62] Li L, Schwendeman SP. Mapping neutral microclimate pH in PLGA microspheres. J Control Release. 2005;101:163-73.
[63] Nie HM, Fu YL, Wang CH. Paclitaxel and suramin-loaded core/shell microspheres in the treatment of brain tumors. Biomaterials. 2010;31:8732-40.
[64] Woodruff MA, Hutmacher DW. The return of a forgotten polymer--Polycaprolactone in the 21st century. Prog Polym Sci. 2010;35:1217-56.
[65] Cipitria A, Skelton A, Dargaville TR, Dalton PD, Hutmacher DW. Design, fabrication and characterization of PCL electrospun scaffolds-a review. J Mater Chem. 2011;21:9419-53.
[66] Sinha VR, Bansal K, Kaushik R, Kumria R, Trehan A. Poly-epsilon-caprolactone microspheres and nanospheres: an overview. Int J Pharm. 2004;278:1-23.
[67] Seyednejad H, Ghassemi AH, van Nostrum CF, Vermonden T, Hennink WE. Functional aliphatic polyesters for biomedical and pharmaceutical applications. J Control Release. 2011;152:168-76.
[68] Wu Y, Liao IC, Kennedy SJ, Du J, Wang J, Leong KW, et al. Electrosprayed core-shell microspheres for protein delivery. Chem Commun. 2010;46:4743-5.
[69] Anumolu R, Gustafson JA, Magda JJ, Cappello J, Ghandehari H, Pease LF. Fabrication of Highly Uniform Nanoparticles from Recombinant Silk-Elastin-like Protein Polymers for Therapeutic Agent Delivery. ACS Nano. 2011;5:5374-82.
[70] Wu YQ, Clark RL. Electrohydrodynamic atomization: a versatile process for preparing materials for biomedical applications. J Biomater Sci-Polym Ed. 2008;19:573-601.
[71] Songsurang K, Praphairaksit N, Siraleartmukul K, Muangsin N. Electrospray Fabrication of Doxorubicin-Chitosan-Tripolyphosphate Nanoparticles for Delivery of Doxorubicin. Arch Pharm Res. 2011;34:583-92.
[72] Kim SY, Lee H, Cho S, Park JW, Park J, Hwane J. Size Control of Chitosan Capsules Containing Insulin for Oral Drug Delivery via a Combined Process of Ionic Gelation with Electrohydrodynamic Atomization. Ind Eng Chem Res. 2011;50:13762-70.
[73] Park CH, Lee J. Electrosprayed Polymer Particles: Effect of the Solvent Properties. J Appl Polym Sci. 2009;114:430-7.
[74] Wu YQ, Kennedy SJ, Clark RL. Polymeric Particle Formation Through Electrospraying at Low Atmospheric Pressure. J Biomed Mater Res B Appl Biomater. 2009;90B:381-7.
[75] Chang MW, Stride E, Edirisinghe M. Controlling the thickness of hollow polymeric microspheres prepared by electrohydrodynamic atomization. J R Soc Interface. 2010;7:S451-S60.
[76] Meng FZ, Jiang Y, Sun ZH, Yin YZ, Li YY. Electrohydrodynamic Liquid Atomization of Biodegradable Polymer Microparticles: Effect of Electrohydrodynamic Liquid Atomization Variables on Microparticles. J Appl Polym Sci. 2009;113:526-34.
[77] Xue LW, Mao LX, Cai Q, Yang XP, Jin RG. Preparation of amino acid ester substituted polyphosphazene microparticles via electrohydrodynamic atomization. Polym Adv Technol. 2011;22:2009-16.
[78] Shenoy SL, Bates WD, Frisch HL, Wnek GE. Role of chain entanglements on fiber formation during electrospinning of polymer solutions: good solvent, non-specific polymer-polymer interaction limit. Polymer. 2005;46:3372-84.
[79] Gupta P, Elkins C, Long TE, Wilkes GL. Electrospinning of linear homopolymers of poly(methyl methacrylate): exploring relationships between fiber formation, viscosity, molecular weight and concentration in a good solvent. Polymer. 2005;46:4799-810.

[80] Pareta R, Brindley A, Edirisinghe MJ, Jayasinghe SN, Luklinska ZB. Electrohydrodynamic atomization of protein (bovine serum albumin). J Mater Sci-Mater Med. 2005;16:919-25.
[81] GananCalvo AM, Davila J, Barrero A. Current and droplet size in the electrospraying of liquids. Scaling laws. J Aerosol Sci. 1997;28:249-75.
[82] Ramakrishna S. An introduction to electrospinning and nanofibers: World Scientific; 2005.
[83] Zhang SL, Kawakami K. One-step preparation of chitosan solid nanoparticles by electrospray deposition. Int J Pharm. 2010;397:211-7.
[84] Yao J, Lim LK, Xie JW, Hua JS, Wang CH. Characterization of electrospraying process for polymeric particle fabrication. J Aerosol Sci. 2008;39:987-1002.
[85] Iserson KV. The origins of the gauge system for medical equipment. JEM. 1987;5:45-8.
[86] Hao XF, Lu XF, Li ZY, Zhao YY, Shang TC, Yang QB, et al. Effects of the electrospray ionization parameters on the formation and morphology of colloidal microspheres of polyacrylonitrile. J Appl Polym Sci. 2006;102:2889-93.
[87] Enayati M, Farook U, Edirisinghe M, Stride E. Electrohydrodynamic preparation of polymeric drug-carrier particles: Mapping of the process. Int J Pharm. 2011;404:110-5.
[88] Delamora JF, Loscertales IG. The current emitted by highly conducting Taylor cones. J Fluid Mech. 1994;260:155-84.
[89] Kinam P. Albumin: A versatile carrier for drug delivery. J Control Release. 2012;157:3.
[90] Yoo JY, Kim M, Lee J. Electrospraying of micro/nano particles for protein drug delivery. Polym-Korea. 2007;31:215-20.
[91] Jaklenec A, Hinckfuss A, Bilgen B, Ciombor DM, Aaron R, Mathiowitz E. Sequential release of bioactive IGF-I and TGF-beta(1) from PLGA microsphere-based scaffolds. Biomaterials. 2008;29:1518-25.
[92] Bertram JP, Rauch MF, Chang K, Lavik EB. Using Polymer Chemistry to Modulate the Delivery of Neurotrophic Factors from Degradable Microspheres: Delivery of BDNF. Pharm Res. 2010;27:82-91.
[93] Babensee JE, McIntire LV, Mikos AG. Growth factor delivery for tissue engineering. Pharm Res. 2000;17:497-504.
[94] Humphrey W, Dalke A, Schulten K. VMD: Visual molecular dynamics. J Mol Graph Model. 1996;14:33-8.
[95] Harwood LM, Moody CJ. Experimental Organic Chemistry Principles and Practice: Blackwell Science; 1989.
[96] Zaky A, Elbakry A, Ehmer A, Breunig M, Goepferich A. The mechanism of protein release from triglyceride microspheres. J Control Release. 2010;147:202-10.
[97] Mundargi RC, Babu VR, Rangaswamy V, Patel P, Aminabhavi TM. Nano/micro technologies for delivering macromolecular therapeutics using poly(D,L-lactide-co-glycolide) and its derivatives. J Control Release. 2008;125:193-209.
[98] King TW, Patrick CW. Development and in vitro characterization of vascular endothelial growth factor (VEGF)-loaded poly(DL-lactic-co-glycolic acid)/poly(ethylene glycol) microspheres using a solid encapsulation/single emulsion/solvent extraction technique. J Biomed Mater Res. 2000;51:383-90.
[99] Liao I, Chew S, Leong K. Aligned core–shell nanofibers delivering bioactive proteins. Nanomedicine. 2006;1:465-71.
[100] Johnson PJ, Skornia SL, Stabenfetdt SE, Willits RK. Maintaining bioactivity of NGF for controlled release from PLGA using PEG. J Biomed Mater Res Part A. 2008;86A:420-7.
[101] Lu L, Stamatas GN, Mikos AG. Controlled release of transforming growth factor beta 1 from biodegradable polymer microparticles. J Biomed Mater Res. 2000;50:440-51.

[102] Bilati U, Allemann E, Doelker E. Strategic approaches for overcoming peptide and protein instability within biodegradable nano- and microparticles. Eur J Pharm Biopharm. 2005;59:375-88.
[103] Yang YY, Chung TS, Bai XL, Chan WK. Effect of preparation conditions on morphology and release profiles of biodegradable polymeric microspheres containing protein fabricated by double-emulsion method. Chem Eng J. 2000;55:2223-36.
[104] Morita T, Sakamura Y, Horikiri Y, Suzuki T, Yoshino H. Protein encapsulation into biodegradable microspheres by a novel S/O/W emulsion method using poly(ethylene glycol) as a protein micronization adjuvant. J Control Release. 2000;69:435-44.
[105] Mann BK, Schmedlen RH, West JL. Tethered-TGF-beta increases extracellular matrix production of vascular smooth muscle cells. Biomaterials. 2001;22:439-44.
[106] Zeugolis DI, Khew ST, Yew ESY, Ekaputra AK, Tong YW, Yung L-YL, et al. Electro-spinning of pure collagen nano-fibres - Just an expensive way to make gelatin? Biomaterials. 2008;29:2293-305.
[107] Smith LA, Ma PX. Nano-fibrous scaffolds for tissue engineering. Colloids Surf B Biointerfaces. 2004;39:125-31.
[108] Smith LA, Liu XH, Ma PX. Tissue engineering with nano-fibrous scaffolds. Soft Matter. 2008;4:2144-9.
[109] Xie JW, Li XR, Xia YN. Putting Electrospun Nanofibers to Work for Biomedical Research. Macromol Rapid Commun. 2008;29:1775-92.
[110] Venugopal J, Low S, Choon AT, Ramakrishna S. Interaction of cells and nanofiber scaffolds in tissue engineering. J Biomed Mater Res B Appl Biomater. 2008;84B:34-48.
[111] Pham QP, Sharma U, Mikos AG. Electrospinning of polymeric nanofibers for tissue engineering applications: A review. Tissue Eng. 2006;12:1197-211.
[112] Min BM, Lee G, Kim SH, Nam YS, Lee TS, Park WH. Electrospinning of silk fibroin nanofibers and its effect on the adhesion and spreading of normal human keratinocytes and fibroblasts in vitro. Biomaterials. 2004;25:1289-97.
[113] Shin M, Ishii O, Sueda T, Vacanti JP. Contractile cardiac grafts using a novel nanofibrous mesh. Biomaterials. 2004;25:3717-23.
[114] Piskin E, Isoglu IA, Bolgen N, Vargel I, Griffiths S, Cavusoglu T, et al. In vivo performance of simvastatin-loaded electrospun spiral-wound polycaprolactone scaffolds in reconstruction of cranial bone defects in the rat model. J Biomed Mater Res Part A. 2009;90A:1137-51.
[115] Zhao L, He CG, Gao YJ, Cen L, Cui L, Cao YL. Preparation and cytocompatibility of PLGA scaffolds with controllable fiber morphology and diameter using electrospinning method. J Biomed Mater Res B Appl Biomater. 2008;87B:26-34.
[116] Sanders EH, Kloefkorn R, Bowlin GL, Simpson DG, Wnek GE. Two-phase electrospinning from a single electrified jet: Microencapsulation of aqueous reservoirs in poly(ethylene-co-vinyl acetate) fibers. Macromolecules. 2003;36:3803-5.
[117] Jiang H, Hu Y, Li Y, Zhao P, Zhu K, Chen W. A facile technique to prepare biodegradable coaxial electrospun nanofibers for controlled release of bioactive agents. J Control Release. 2005;108:237-43.
[118] Hadjiargyrou M, Chiu JB. Enhanced composite electrospun nanofiber scaffolds for use in drug delivery. Expert Opin Drug Deliv. 2008;5:1093-106.
[119] Nie H, Soh BW, Fu YC, Wang CH. Three-dimensional fibrous PLGA/HAp composite scaffold for BMP-2 delivery. Biotechnol Bioeng. 2008;99:223-34.
[120] Li CM, Vepari C, Jin HJ, Kim HJ, Kaplan DL. Electrospun silk-BMP-2 scaffolds for bone tissue engineering. Biomaterials. 2006;27:3115-24.
[121] Fu YC, Nie H, Ho ML, Wang CK, Wang CH. Optimized bone regeneration based on sustained release from three-dimensional fibrous PLGA/HAp composite scaffolds loaded with BMP-2. Biotechnol Bioeng. 2008;99:996-1006.

[122] Choi JS, Leong KW, Yoo HS. In vivo wound healing of diabetic ulcers using electrospun nanofibers immobilized with human epidermal growth factor (EGF). Biomaterials. 2008;29:587-96.
[123] Chew SY, Wen J, Yim EKF, Leong KW. Sustained Release of Proteins from Electrospun Biodegradable Fibers. Biomacromolecules. 2005;6:2017-24.
[124] Sill TJ, von Recum HA. Electrospinning: Applications in drug delivery and tissue engineering. Biomaterials. 2008;29:1989-2006.
[125] Ionescu LC, Lee GC, Sennett BJ, Burdick JA, Mauck RL. An anisotropic nanofiber/microsphere composite with controlled release of biomolecules for fibrous tissue engineering. Biomaterials. 2010;31:4113-20.
[126] Porter JR, Ruckh TT, Popat KC. Bone Tissue Engineering: A Review in Bone Biomimetics and Drug Delivery Strategies. Biotechnol Prog. 2009;25:1539-60.
[127] Chen FM, Chen R, Wang XJ, Sun HH, Wu ZF. In vitro cellular responses to scaffolds containing two microencapulated growth factors. Biomaterials. 2009;30:5215-24.
[128] Biondi M, Ungaro F, Quaglia F, Netti PA. Controlled drug delivery in tissue engineering. Adv Drug Deliv Rev. 2008;60:229-42.
[129] Richardson TP, Peters MC, Ennett AB, Mooney DJ. Polymeric system for dual growth factor delivery. Nat Biotechnol. 2001;19:1029-34.
[130] Qi HX, Hu P, Xu J, Wang AJ. Encapsulation of drug reservoirs in fibers by emulsion electrospinning: Morphology characterization and preliminary release assessment. Biomacromolecules. 2006;7:2327-30.
[131] Dong B, Smith ME, Wnek GE. Encapsulation of Multiple Biological Compounds Within a Single Electrospun Fiber. Small. 2009;5:1508-12.
[132] Wang YZ, Qiao WL, Wang BC, Zhang YQ, Shao PY, Yin TY. Electrospun composite nanofibers containing nanoparticles for the programmable release of dual drugs. Polym J. 2011;43:478-83.
[133] Baker BM, Gee AO, Metter RB, Nathan AS, Marklein RA, Burdick JA, et al. The potential to improve cell infiltration in composite fiber-aligned electrospun scaffolds by the selective removal of sacrificial fibers. Biomaterials. 2008;29:2348-58.
[134] Stankus JJ, Guan J, Fujimoto K, Wagner WR. Microintegrating smooth muscle cells into a biodegradable, elastomeric fiber matrix. Biomaterials. 2006;27:735-44.
[135] Hong Y, Fujimoto K, Hashizume R, Guan J, Stankus JJ, Tobita K, et al. Generating elastic, biodegradable polyurethane/poly(lactide-co-glycolide) fibrous sheets with controlled antibiotic release via two-stream electrospinning. Biomacromolecules. 2008;9:1200-7.
[136] Ekaputra AK, Prestwich GD, Cool SM, Hutmacher DW. Combining electrospun scaffolds with electrosprayed hydrogels leads to three-dimensional cellularization of hybrid constructs. Biomacromolecules. 2008;9:2097-103.
[137] Kim SJ, Jang DH, Park WH, Min BM. Fabrication and characterization of 3-dimensional PLGA nanofiber/microfiber composite scaffolds. Polymer. 2010;51:1320-7.
[138] Bonani W, Maniglio D, Motta A, Tan W, Migliaresi C. Biohybrid nanofiber constructs with anisotropic biomechanical properties. J Biomed Mater Res B Appl Biomater. 2011;96B:276-86.
[139] Malda J, Klein TJ, Upton Z. The roles of hypoxia in the In vitro engineering of tissues. Tissue Eng. 2007;13:2153-62.
[140] Jaworek A, Krupa A, Lackowski M, Sobczyk AT, Czech T, Ramakrishna S, et al. Nanocomposite fabric formation by electrospinning and electrospraying technologies. J Electrost. 2009;67:435-8.
[141] Gupta D, Venugopal J, Mitra S, Giri Dev VR, Ramakrishna S. Nanostructured biocomposite substrates by electrospinning and electrospraying for the mineralization of osteoblasts. Biomaterials. 2009;30:2085-94.

[142] Francis L, Venugopal J, Prabhakaran MP, Thavasi V, Marsano E, Ramakrishna S. Simultaneous electrospin-electrosprayed biocomposite nanofibrous scaffolds for bone tissue regeneration. Acta Biomater. 2010;6:4100-9.
[143] Stankus JJ, Soletti L, Fujimoto K, Hong Y, Vorp DA, Wagner WR. Fabrication of cell microintegrated blood vessel constructs through electrohydrodynamic atomization. Biomaterials. 2007;28:2738-46.